1987

In Vivo and In Vitro Effects of Hydralazine on Cellular Growth, Differentiation and Chromatin Structure

Allen John Fasbender

In Vivo and In Vitro Effects of Hydralazine on Cellular Growth, Differentiation and Chromatin Structure

by Allen John Fasbender

A thesis submitted
in partial fulfillment of the requirements for
the degree Master of Science
Major in Chemistry
South Dakota State University
1987

In Vivo and In Vitro Effects of Hydralazine on Cellular Growth, Differentiation and Chromatin Structure

This thesis is approved as a creditable and independent investigation by a candidate for the degree, Master of Science, and is acceptable for meeting the thesis requirements for this degree. Acceptance of this thesis does not imply that the conclusions reached by the candidate are necessarily the conclusions of the major department.

Dr. Donald P. Evenson
Thesis Advisor

Date

Dr. David C. Hilderbrand
Head, Chemistry Dept.

Date

Acknowledgements

The author wishes to express sincere appreciation to Dr. Donald Evenson for his supervision and guidance throughout this research.

The author also thanks Rebecca Baer and Lorna Jost for their assistance with various aspects of the research project and for their assistance in preparing this thesis and the manuscript. Thank you also to Paula Bennett and Kennedy Gauger who typed the text and prepared all graphs and tables.

I would like also to thank the professors of the Chemistry Department of South Dakota State University, in particular, Dr. David Hilderbrand, Dr. John Grove, Dr. Ivan Palmer, and Dr. Harry Hecht for their encouragement and advice regarding future career goals.

TABLE OF CONTENTS

cont.

Contents

TABLE OF FIGURES

cont.,

cont.,

cont.

LIST OF TABLES

cont.

INTRODUCTION

Hydralazine has been used medicinally as an antihypertensive since 1952. Within two years after its introduction to clinical medicine, an unusual set of symptoms was noted in a significant portion of patients. This set of symptoms resembled those symptoms observed in idiopathic systemic lupus erythematosus. The fundamental problem underlying this drug-related systemic lupus erythematosus is autoimmune in nature. Hydralazine produces a characteristic profile of anti-nuclear antibodies that is unique from that present in idiopathic systemic lupus erythematosus. Other drugs such as procainamide and isoniazid have also been associated with drug-related systemic lupus erythematosus. Interestingly, these drugs differ in the antinuclear antibodies with which they are associated. The reason for the formation of these antinuclear antibodies is unknown. It is generally agreed that hydralazine is interacting with normal nuclear material, in particular, DNA, RNA and histones, and in some way eliciting an immune response. This response to hydralazine is a dose-related phenomena and shows a prevalence for slow acetylators; acetylation is the predominant metabolic route for hydralazine elimination.

The objective of this research was to determine the relationship between hydralazine concentration and cell growth and differentiation both _in vivo_ and _in vitro_. Hydralazine-induced alterations of chromatin structure of both histone containing somatic cells and protamine containing sperm cells were analyzed in an attempt to study mechanisms of these alterations that may provide clues as to why

hydralazine treated patients develop antibodies against DNA/chromatin with lupus-like symptoms.

Flow cytometric techniques are available that facilitate simultaneous quantitation of cellular DNA and RNA. This can be applied to the study of cell cycle population kinetics. It is possible to determine the percentage of cells in G_0, G_1, S, and G_2M phases of the cell cycle. Knowing the biochemical events that take place during the phases of the cell cycle, insight may be gained about where and how hydralazine is acting. In addition, susceptibility to acid-induced DNA denaturation as measured by flow cytometry has been used to assess the effects of chemicals on chromatin structure.

Human lymphocytes provided a cell type that could be maintained in tissue culture for study. This cell type allowed for study of the effect of hydralazine on both resting and actively dividing cells.

Spontaneously hypertensive rats provided an *in vivo* model for the study of the long term effects of hydralazine on lymphocytes. Also, the effect on testicular cell growth and differentiation was assessed.

Friend leukemia cells provided a model to study growth and viability changes following exposure to varying concentrations of hydralazine. A stathmokinetic experiment was performed to assess the terminal point of drug action, in other words, to determine at what point in the cell cycle hydralazine exerted its effect.

Finally, Chinese hamster ovary cells, a well defined monolayer

cell line, was used to assess the ability of mammalian cells to recover from exposure to a dose of hydralazine that inhibited growth and affected viability.

REVIEW OF THE LITERATURE

I. Hydralazine

A number of drugs have been implicated in causing a clinical illness similar to systemic lupus erythematosus (1,2). Hydralazine is second only to procainamide in inducing this problem (3). Drugs that have a definite association with this problem include hydralazine, procainamide, and isoniazid (4). There are other drugs that have been implicated in this problem although incidences are infrequent and there is less proof of a definite association.

Drug-related systemic lupus erythematosus is an autoimmune phenomena. There is a very specific pattern of antinuclear antibodies produced in lupus erythematosus. The pattern differs from idiopathic systemic lupus erythematosus and is unique for the drug inducing the condition (5). Hydralazine is thought to interact chemically with nuclear material, modifying it so that it triggers an immunologic response. It has been known for a long time that modified nuclear material can be highly immunogenic.

Many of the compounds are aromatic amines or hydrazines which are potential substrates for the polymorphic acetylation pathway of drug metabolism by humans (6). These compounds undergo N-acetylation which is an important early step in their elimination from the body (7). People with a low capacity for N-acetylation, such

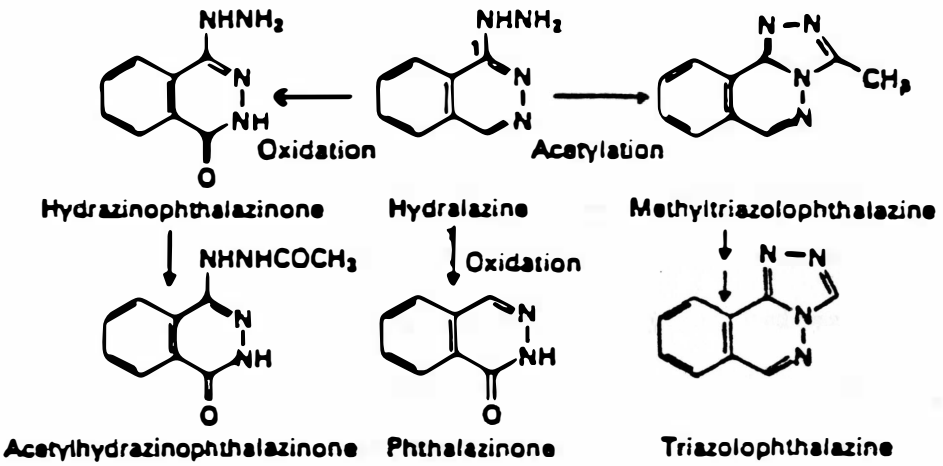

Figure 1. Major metabolic pathway of hydralazine in man (8).

as phenotypic slow acetylators, are more likely to develop drug-induced lupus or some manifestations of this disorder than are rapid acetylators (8).

Hydralazine is 1-hydrazinophthalazine, a monosubstituted hydrazine, that is quickly and extensively metabolized (9) (Figure 1). Approximately 75% of the dose appears in the first urine collection with less than 2% appearing as unchanged drug. Hydralazine undergoes benzylic oxidation to hydrazinophthalazinone which can be acetylated to acetylhydrazinophthalazinone. Hydralazine can be acetylated to methyltriazolophthalazine, and can be oxidized to phthalazinone (10). In addition, experiments have shown that in patients treated with hydralazine 100 mg orally twice a day, plasma levels of hydrazine average 1.5 mcg/ml in slow acetylators versus 0.75 mcg/ml in rapid acetylators (10). The authors felt that the very low levels and the lack of significant effect of acetylator phenotype, in comparison with similar studies done on isoniazid, suggest that hydrazine is probably not responsible for the autoimmune symptoms of lupus (10). This issue is not fully resolved at present.

A number of theories have been proposed in an attempt to define the relationship between hydralazine and the autoimmune symptoms of lupus. Hydralazine has been associated with several clinical effects, but the relationship between these effects and the toxic symptoms of hydralazine are not known. These effects include the following. Hydralazine is capable of causing clinically significant depletion of pyridoxine by binding to and increasing the urinary loss

of pyridoxine (11). Hydralazine also reacts with ionic iron and its chronic use apparently can and does induce some degree of iron deficiency anemia (11,12). Hydralazine lowers serum cholesterol levels also, an effect that is quite similar to that induced by disodium calcium EDTA and penicillamine. All three compounds produce a similar set of symptoms. Hydralazine is thought to bind to a transition metal that is presumably functioning as a coenzyme in the biochemical pathways of cholesterol metabolism (11). The relationship of the above deficiencies to the lupus syndrome is unclear.

The main focus of research has been on the interactions of hydralazine with the immune system. It is believed that antinuclear antibodies must be present for lupus to develop. In addition, patients with active hydralazine-related lupus have circulating antibodies to hydralazine (11).

Denatured DNA and nucleohistone are major targets of autoreactivity in hydralazine related lupus (13). The proposed mechanisms include: 1) the drug may bind to a macromolecule, and serve as a specificity-determining hapten for antibodies that then cross-react with nuclear antigens, 2) drug may bind to a usually nonantigenic molecule of nuclear origin and render it immunogenic, with the major specificity determinants being those of the nuclear macromolecule itself, 3) drug may cause cell damage and release of contents in a form that is immunogenic, 4) drug may combine with selected cell surface receptors and stimulate B cells that are normally silent, or 5) drug may eliminate populations of suppressor cells, leaving

unregulated B cells free to produce autoreactive products (13). In both idiopathic and drug-related lupus, the basic question is whether the primary process results from an unusual presentation of antigen or from an abnormality of the immune system. It has not been determined whether the mechanism is different between idiopathic and drug-related lupus. The frequency of antinuclear autoreactivity and the lupus syndrome among patients given some types of drugs is much higher than the frequency of idiopathic systemic lupus would predict. For this reason a great deal of focus has been placed on the possibility that hydralazine may act by selectively modifying nuclear macromolecules, making them antigenic to the immune system.

Patients with idiopathic systemic lupus erythematosus form antibodies to both native and denatured DNA and double-strand RNA as well as to histones, histone-DNA complexes, several ribonucleoproteins, and surface structures of several cell types (14). In patients with drug-related lupus, anti-ribonucleoprotein antibodies are formed early and antidenatured DNA and antihistone-DNA antibodies predominate later (13). Anti-native DNA is infrequent if it does occur at all. In normal animals, nucleic acids and histones are poor immunogens. If administered with a suitable protein carrier, denatured DNA and synthetic polynucleotides (including helical forms such as double-strand RNA or RNA-DNA hybrids) can induce antibody formation. With the same carriers native DNA has not been shown to be immunogenic (13). Chemically modified DNA with an appropriate carrier is strongly immunogenic with the modified structure usually determining the major

specificity (15). Histones are regularly immunogenic when they are presented as histone-RNA complexes (13).

In helical double strand DNA, all purine and pyrimidine bases are directed toward the center of the helix and are unavailable for reaction with antibody. The major antigenic sites in native DNA, therefore, are likely to involve the sugar-phosphate backbone (13). The shape of the DNA helix is important for the latter specificity and native DNA is immunochemically distinguishable from double-strand RNA or RNA-DNA hybrid helices (16). Antibodies to these backbone determinants occur in idiopathic lupus but not in drug-related lupus. The collapsed coil of single-strand denatured DNA contains significant amounts of intrastrand base-pairing and may present loops of sugar-phosphate backbone toward its surface, either as single-chain or helical structures (17). In addition, many purine and pyrimidine bases are now exposed and available to react with antibodies. These form the determinants for antibodies that react only with denatured DNA (15). These antibodies which are specific for the bases or for short base sequences in a stacked array occur in both idiopathic and drug-related lupus (15).

The fundamental subunit of chromatin is the nucleosome (18). This consists of a particle in which a 146-base pair length of helical DNA is wrapped around an octamer of histones H2a, H2b, H3 and H4. In addition, an amount of DNA, up to 60 base pairs, links adjacent nucleosomes in a chain and is associated with H1 or H5 histone (13). The amino terminal portions of the histones have high concentrations

of positively charged amino acids, particularly lysine (19). These portions are accessible at the nucleosome surface to antibodies, the globular central regions of the molecules being less accessible (20). Antibodies to the native nucleosome structure occur in some autoimmune sera. Nucleosomes have been characterized specifically as the nuclear antigens showing cross-reactivity with some rheumatoid factors and anti-cell surface autoantibodies (21). Trypsin cleavage of the amino-terminal regions of the histones eliminates the reactive-site while leaving the rest of the nucleosome intact, thus these antibodies appear to be specific for conformations of the amino terminal histone regions that occur at the surface of native nucleosomes (22). Idiopathic lupus sera and sera from patients with drug-related lupus both contain antibodies that react with varying specificities for isolated histones or histone-DNA complexes.

Several forms of ribonucleoprotein occur in both nuclear and cytoplasmic compartments of eukaryotic cells. These particles contain a chain of RNA along with several polypeptides (13). Some may be segments of newly transcribed RNA rapidly associated with protein after transcription (24). With RNA of characteristic size and sequence some may be involved in mRNA processing steps such as splicing. Such ribonucleoprotein particles contain the reactive sites of Sm and RNP antigens for antinuclear antibodies of idiopathic lupus and for antibodies to cytoplasmic antigens as well (25). The binding sites on the ribonucleoprotein have not been defined.

An understanding of drug-related lupus requires a plausible

mechanism for the formation of antibodies to purine and pyrimidine determinants of denatured DNA, histone determinants in nucleohistone complexes, and unidentified determinants of ribonucleoproteins (13).

Antibodies to hydralazine, as well as to nuclear antigens occur in sera of patients with lupus induced by this drug (25,26). The question has been asked whether these are cross-reacting populations. On the basis of chemical structure and previously known binding of purines by cross-reactive or multispecific antibodies, some cross-reaction between hydralazine and purines may be considered possible (15, 27). Antiadenylate antibodies have shown some cross reaction with hydralazine (27). In one experimental system, a small population of antibodies induced in rabbits by a hydralazine-heterologous protein conjugate was found to cross-react with DNA (28). Both native and denatured DNA were reactive, since hydralazine inhibited the reaction of both forms, some of the bases may have been exposed in this sample of native DNA (28). If not, the cross-reaction would have to involve the highly negatively charged backbone determinants, which is unlikely. The cross-reactive population was not induced when autologous protein was the carrier even though a strong antihydralazine response occurred (13). No similar cross-reactivity was found in another study in which hydralazine in adjuvant was injected into guinea pigs (29). No antinuclear antibodies have been induced by procainamide-protein conjugates even when strong antiprocainamide reactions occurred (30). Isoniazid induces antinuclear antibodies, probably antinucleohistone, but does not induce antiDNA

antibodies (31). In view of these findings and the difficulty in accounting for both antiDNA and antihistone specificity on the basis of cross-reactivity with these and other lupus-inducing drugs, it seems unlikely that this mechanism is involved (13).

A number of studies have shown that hydralazine can bind to DNA or nucleoprotein and alter their physical properties (32,33). The bound drug or a metabolite of the drug could render some portion of the macromolecule immunogenic or could help form a recognition site directly, acting as a carrier rather than as a hapten. As a parallel example, the azobenzenearsonate group which is not immunogenic by itself, can be a specificity-determining hapten when bound to protein or, when linked only to tyrosine, can serve as a carrier for haptens of low or high molecular weight (34). Modified bases of nucleic acids may also serve both carrier recognition and specificity-determining hapten functions. One of the earliest examples of this was the ability of hydroxymethylcytosine, present in T-even bacteriophages to induce antibody formation in rabbits (35). Other examples of altered DNA used for immunization include ultraviolet-irradiated DNA, photo-oxidized DNA and carcinogen-modified DNA (36,37). In all of these cases the modified base products determined specificity of most of the antibody, but small amounts of antibody to the normal bases were formed also. These antibody populations were distinct so that cross reactivity did not have to be involved. The question has been asked, can this also be the case for DNA modified by the drugs of interest for drug-induced lupus? Immunization of rabbits with procainamide-

modified DNA gave rise to both antiprocainamide and antidenatured DNA antibodies but procainamide-induced lupus may occur in the absence of antibodies to the drug (34). In these cases, either a noncross-reactive metabolite is the active agent or a purely carrier role of the drug would have to be responsible if this hypothesis is to be supported. In the case of hydralazine-induced responses, this mechanism would predict that the antihydralazine and antidenatured DNA or anti-nucleohistone antibodies are distinct populations (13).

The interaction of hydralazine with cell surfaces has been studied also. If a drug like hydralazine becomes associated with cell surfaces in the body and triggers a cell-mediated cytotoxic response, the end result will be cellular destruction. This cellular destruction, with the release of intracellular contents (such as DNA), could provoke immune responses against a variety of autologous antigens (38,39). It is apparent, however, that cellular destruction alone cannot be sufficient to account for the triggering of lupus, because the cell-mediated cytotoxicity mechanism destroys cells as part of its normal operation without triggering such profound autoimmune consequences (40). It has been concluded that while cell-mediated cytotoxicity is a plausible candidate for involvement in the triggering of lupus, there must be other predisposing conditions which remain to be defined (38). In summary, the role of hydralazine in inducing drug-related lupus remains to be clarified.

II. Method of approach to the problem.

The problem being addressed is the toxic response to

hydralazine and the related production of autoantibodies.

There are two questions being asked; first, does hydralazine cause an alteration of cell growth and differentiation in vivo and in vitro? Second, does hydralazine induce alterations in chromatin structure of either histone containing somatic cells or protamine containing sperm cells?

The proposed method of approach to the problem consists of a series of in vitro and in vivo experiments using several model systems.

The in vitro experiments utilized human lymphocytes, Friend leukemia cells, and Chinese hamster ovary cells. Lymphocytes were studied in both the quiescent state and when actively growing and dividing after mitogen stimulation. Cell cycle population kinetics were studied to determine if hydralazine affected number or percent of cells in various phases of the cell cycle. Susceptibility to acid-induced DNA denaturation of lymphocytes in the resting state and in the actively dividing state was used to assess changes in the chromatin structure. Friend leukemia cells were studied for the effects of hydralazine on growth and viability and how these two were related. In addition, a stathmokinetic experiment aimed at determining the terminal point of drug action was performed using log phase growth Friend leukemia cells. This gave information on where in the cell cycle hydralazine was exerting its effects, and this in turn, might give insight to the mechanism of toxicity.

Chinese hamster ovary cells, a monolayer cell line, were used

to study the ability of cells to recover after being exposed to an inhibitory dose of hydralazine (81).

Finally, spontaneously hypertensive rats were used as a model to study the long term effects of hydralazine on DNA and RNA content of lymphocytes and also on the growth and differentiation of testicular cells. These animals provided an in vivo model system to look at the effects of long term exposure to hydralazine.

Cellular staining with the metachromatic dye acridine orange and measurement of individual cells by flow cytometry was the basis for the analysis of above model systems.

III. Quantitative cell-cycle analysis (cytokinetics).

Cytokinetics is the analysis of the cell-cycle behavior of cell populations. A single DNA distribution contains detailed information about the growth kinetics of an asynchronously growing cell population (42). A DNA distribution typical of an asynchronous, homogeneous cell population is shown (Figure 2A). It shows several distinct landmarks. There is a large peak at unit relative DNA content that represents G_1 phase cells whereas the smaller peak at twice this DNA content is due to G_2M phase cells, and the continuum between is due to S phase cells. These DNA distributions are unchanging or slowly changing with time. For this reason, a population of cells can be studied using flow cytometry to detect influences that a chemical like hydralazine may have on the phase duration and phase population distribution.

DNA distribution sequences are also sensitive indicators of

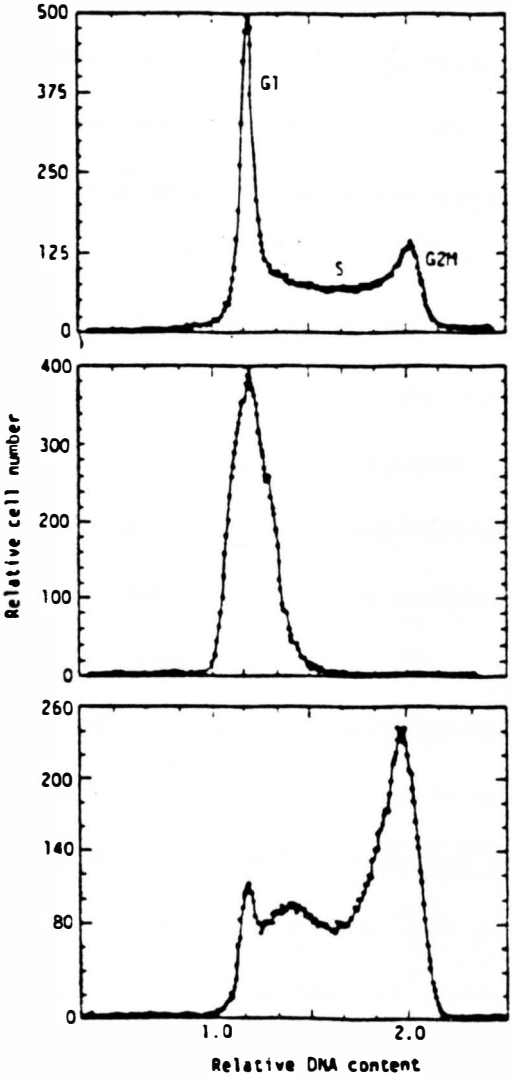

Figure 2A. Flow cytometry measured DNA distribution typical of an asynchronous, homogeneous cell population. This distribution is for an exponentially growing Chinese hamster ovary (CHO) - line cell population (42).

Figure 2B. The DNA distribution for a CHO-line cell population synchronized in late G_1 and early S phase. Note that the landmark features mentioned in Figure 2A are missing (42).

Figure 2C. The DNA distribution for the CHO-line cell population of Figure 2B taken at a later time. The population has desynchronized sufficiently so that the G_1 and G_2M landmarks are visible but not enough so that the population has become asynchronous as in Figure 2A (42).

synchrony in cycling cells, changing in response to changes in the distribution of cells around the cycle (42). The "landmark" features that are characteristic of an asynchronous population may disappear, to be replaced with more complex features that change with time, as seen in Figures 2B and 2C (42). Often, the new features may move from lower to higher DNA content and back to lower DNA content as the synchrony is propagated around the cell cycle from the G_1 to the G_2M phase and, following division, back to the G_1 phase (42). At other times, cells accumulate at a particular DNA content in response to a phase-specific block. DNA-distribution sequences may thus be used to study the dynamics of cell cycle traverse, or to study the response of a cell population to a perturbing agent or condition (42).

The quantitative interpretation of single DNA distributions from asynchronous populations and DNA-distribution sequences from synchronous populations requires a model of cell cycle traverse, an understanding of how DNA content relates to the cell cycle, and an understanding of how measurement variability affects the DNA distribution.

The cell cycle concept is the basis for the interpretation of DNA distribution (21). According to this model, the cell cycle consists of four phases designated G_1, S, G_2 and M. A cell enters the G_1 phase upon division and remains there until the onset of DNA synthesis. The cell is in S phase until it has doubled its DNA content and then enters the G_2 phase. The mitotic or M phase follows and is marked by condensation of chromatin into chromosomes and terminates

when the cell divides into two G_1 cells (42). The G_2 and M phases usually are not differentiated in most flow cytometry studies as both phases contain the same DNA content. The phases are combined into a single G_2M phase. There is also a G_0 phase in which cells have temporarily left the cycle and are not progressing toward division. Heterogeneity in the cell cycle can also be induced by perturbing agents (42).

The factors that affect measured DNA distributions include the extent of biologic, cytochemical, and instrumental variability, the maturity distribution of cells, the rate of DNA synthesis, phase durations and associated dispersion, and cell-population heterogeneity (42). RNA and protein distribution is similarly affected by the above and can be used along with DNA distribution to further characterize effects on the cell cycle.

IV. Fluorescence and the acridine orange staining procedure.

The Cytofluorograf II flow cytometer (Ortho Diagnostics, Inc., Westwood, MA) was used to detect and measure fluorescence of acridine orange stained cells in our research project. When a beam of light strikes a polymer-dye complex such as a polynucleotide-acridine orange complex, the energy absorbed can be given up in a number of ways. The emission of radiation by a molecule, ion, or atom due to the return of an electron to its ground electronic state following its excitation by the absorbtion of electromagnetic radiation is called fluorescence (41). Absorption of radiation in the ultraviolet-visible range always involves an electronic transition and may also involve changes in

rotational and vibrational energy levels. Fluorescence may also involve an electronic transition with the wavelength of the emitted light being in the ultraviolet-visible portion of the electromagnetic spectrum. The absorbtion process results in electrons being excited to a series of excited vibrational levels in the excited electronic state (41). In theory, fluorescence could occur from each of these excited vibrational levels. The spectra observed indicate that the transitions occur only from the ground vibrational level of the excited electronic state and not the higher excited vibrational levels because these vibrational levels have a lifetime on the order of 10^{-10} seconds whereas the lifetime of the excited state in molecular fluorescence is 10^{-8} to 10^{-6} seconds (41). The electrons decay to the first excited electronic state before the process of fluorescence begins. The electronic transitions normally observed in molecular fluorescence are from the first excited electronic state to the ground electronic state. The molecular structure of the compound of interest has a marked effect on the fluorescent quantum yield and emission intensity. The most intense fluorescent intensities are observed for molecules containing double bonds or conjugated systems.

Acridine dyes, especially acridine orange, are widely used as fluorescent stains for nucleic acids in plant or animal cells since the 1940's (43). Acridine orange is 3,6-dimethylamino acridine (Figure 3). The aminoacridines are known antibacterials and known mutagens. Their structure and mode of interaction with nucleic acids resembles other biologically active chemicals like polycyclic hydro-

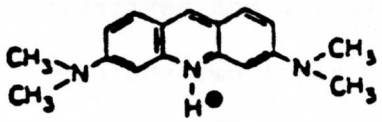

Figure 3. Chemical structure of acridine orange cation (43).

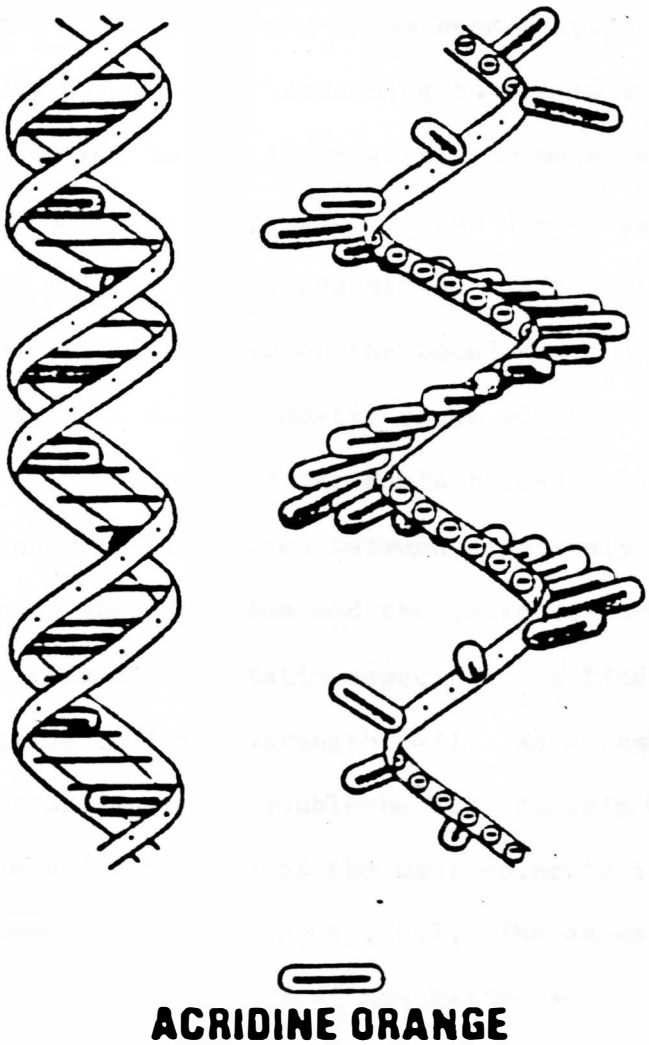

Figure 4. Schematic representation of the intercalation of AO into a double-helical nucleic acid (left) and of the electrostatic interactions between AO and single-stranded nucleic acids (right) (43).

carbons, some nucleic acid derivatives and certain dyes like toluidine blue and ethidium bromide. There are two types of binding sites in nucleic acids, differing in their affinity to acridine dyes. On the basis of studies on optical properties, viscosity, sedimentation, x-ray diffraction, equilibrium dialysis, and thermal denaturation-renaturation, an intercalation model has been proposed as representing the strong binding sites (43). According to the intercalating model, the planar molecule of the dye intercalates between two adjacent nucleotide base pairs, with the plane of the dye perpendicular to the axis of the helix (Figure 4). These strong binding sites have a high binding energy of 6-10 Kcal/mole of the bound dye (46). The binding involves interaction of flat, aromatic rings of the dye with nucleotide bases, mostly via Van der Waals forces (46). The binding also involves electrostatic forces between negatively charged phosphate groups on nucleic acids and the cationic form of the dye. It is because of this electrostatic aspect of the binding that the binding is sensitive to ionic strength (47). As a result of the dye binding, the contour length of double-helical nucleic acid increases due to untwisting and extension of the macromolecule in order to accomodate the dye between base pairs (45, 48). The extent of the possible untwisting and extending of the helix, as a result of dye intercalation, is restricted in superhelical forms of nucleic acids, consequently, superhelicity imposes a limitation on the number of binding sites (49). The maximal number of binding sites in double strand DNA is about one sixth the number of DNA phosphates.

Therefore, at saturation the dye intercalates between approximately every third base pair (45, 48). Since binding by intercalation involves spatial separation of dye molecules from one another, thus excluding dye-dye interactions, the light absorption and emission spectra are close to those of the monomer form of the dye (51, 52).

The second type of dye binding is referred to as weak binding. The binding energy is low, being several orders of magnitude less than the strong binding. The interactions are between negatively charged phosphate and positively charged dye molecules. This binding, being electrostatic in nature, is very sensitive to ionic strength (47). Weak binding is external, and the planes of the acridine rings are more disordered with respect to planes of the nucleotide base rings than in strong binding. In weak binding the number of binding sites approaches the number of the phosphates in the backbone of nucleic acid, a 1:1 molar ratio (43). When the dye to phosphate ratio is high enough, the dye binds to neighboring phosphates. The dye molecules then stack upon each other or aggregate and interact between themselves (54, 55). This interaction results in a loss of some of the energy absorbed by the dye, and the emission spectrum is shifted to lower energy photons of longer wavelength, resulting in red fluorescence as compared to green fluorescence which results from the monomeric form of the dye. This binding process is cooperative in that binding to sites next to sites already occupied by the dye is increased, due to the tendency of the dye to stack. Thus, binding occurs preferentially at sites neighboring the occupied ones (43).

The stacking tendency of single-strand nucleic acids is higher than of the double-strand nucleic acids (53, 56).

The difference between strong and weak binding interactions make it possible to recognize binding of acridine orange to double-strand versus single-strand nucleic acids and thus acridine orange can be used as a fluorescent probe to study the conformation of nucleic acids. At a specific dye concentration and dye to nucleic acid phosphate molar ratio, the dye may intercalate into double-strand nucleic acid and also stack while interacting electrostatically with the phosphate of single-strand nucleic acids (43). The first type of binding is characterized by green fluorescence with maximum emission at 530 nm, the stacking type binding is characterized by red fluorescence with maximum emission at 640 nm (43, 55). Both intercalation and electrostatic binding show different sensitivity to ionic strength, it is therefore possible to find an optimal condition under which the dye binds to single- and double-strand nucleic acid with the same efficiency. Under these conditions the fluorescent intensities at 530 and 640 nm are linearly correlated with the proportions of double- and single-strand nucleic acid, respectively (55).

Acridine orange is a nonspecific cationic dye that interacts with not only nucleic acids, but also binds electrostatically with the anionic residues of molecules such as proteins, polysaccharides, and glycosaminoglycans. Therefore, acridine orange may stain in a nonspecific manner. The electrostatic interactions between the cationic dye and the anionic residues of other molecules needs to be

suppressed while leaving the binding to nucleic acids reactive. One approach is to use low concentrations of acridine orange and at a low molar ratio of acridine orange per binding site because the dye will preferentially stain nucleic acids because of the high affinity of acridine orange for intercalating sites in nucleic acids (45, 48). The drawbacks to this approach are that one must measure the quantity of DNA and double-strand RNA that is available for the dye in each sample cell type to maintain the low acridine orange to DNA phosphate molar ratio. Also, at this low molar ratio, acridine orange binds by intercalation and there is little binding and stacking on single-strand nucleic acids and so the differential staining of double-strand versus single-strand nucleic acids is lost (43). Another approach has been to stain with acridine orange in the presence of cations (57, 58). Under conditions where inorganic cations are in large excess, like 5 mM Mg^{+2} or 0.1-0.2 M Na^{+}, and thus competing with acridine orange ($1.0-2.0 \times 10^{-5}$M) for anionic sites, the electrostatic interactions between the dye and these sites are greatly impeded (46). Intercalation is affected to a lesser extent since the electrostatic component in this type of dye binding is relatively small. In addition, because binding to single-strand nucleic acids and subsequent dye stacking is a cooperative process, in which the electrostatic component in dye stacking is minimal, the metachromatic stainability of single-strand nucleic acids is expected to be relatively resistant to the presence of other cations (46). Thus, the excess of cations increases the specificity of staining of nucleic acids by suppressing

interactions of acridine orange with various anionic residues and allows differential stainability of double-strand versus single-strand nucleic acids since intercalation and stacking are favored (43).

In order to use acridine orange for quantitative estimates of cellular constituents it is usually necessary that a cell be made permeable to the reagents. There are several methods outlined in the literature for inducing cell permeability. In this research, cells were treated with detergent at low pH to induce cell permeability and stain nucleic acids with acridine orange (59, 60). The cells exposed to detergent in the presence of serum proteins do not lyse but become permeable to dyes. At low pH, nucleic acids are insoluble and do not leak out of cells.

Our staining protocol consisted of an acridine orange staining procedure as follows (58). Cells in suspension were exposed to a solution containing 0.1% Triton X-100 (0.08 N HCl, 0.15 M NaCl, at pH 1.4) for 30 seconds, followed by staining with acridine orange solution (containing 10^{-3} M Na_2 EDTA, 0.15 M NaCl, 0.2 M Na_2HPO_4/0.1 M citric acid buffer adjusted to pH 6.0 and 6 mcg/ml or 8 mcg/ml acridine orange). The usual acridine orange concentration was 6 mcg/ml.

Native nuclear DNA is double strand and binds acridine orange or similar dyes by intercalation. Native RNA, on the other hand, has a mixed conformation, meaning a large part is also double helical and thus binds acridine orange by intercalation (61). To obtain differential staining of DNA versus RNA, it is necessary to selectively

denature any double-strand RNA, ensuring that all RNA is single-strand while DNA remains double-strand. It has been found that cell treatment with EDTA, while it denatures almost all double-strand RNA, does not affect DNA. In addition, it has been found that acridine orange itself at concentrations used for cell staining (1-2 X 10^{-5}M) induces slow denaturation of RNA (58). Cell treatment with chelating agents, followed by acridine orange staining, results in a situation in which all cellular RNA is single-strand and may interact with the dye electrostatically with subsequent dye stacking resulting in red fluorescence while native DNA remains unaltered and binds acridine orange by intercalation with resulting green fluorescence (58).

The optimum dye concentration for differential staining of double- versus single-strand nucleic acids is that at which nearly all intercalation sites are saturated. In solutions of varying ionic strength, the optimal concentration of acridine orange varies; our solution contained 0.15 M Na^+. In this concentration of sodium, the optimal concentration of acridine orange is 1-2 x 10^{-5}M (58).

Most nuclear DNA is masked by acid-soluble proteins, mostly histones. The unmasked fraction available for interaction with cationic probes varies with different cell types. It is often advantageous to stain all nuclear DNA rather than only the unmasked fraction, thereby achieving a more constant measure of DNA per cell. This eliminates the differences in chromatin composition and conformation. This research was concerned with the total nuclear DNA per cell. The Triton-X solution provided the acidic environment needed to dislodge

these proteins. The staining process was done near 0°C to inhibit denaturation of DNA (43). Acid treatment increased by two to three-fold the stainability of cellular DNA with DNA specific dyes. Following this treatment the cells were stained with the acridine orange solution. This procedure produces the best resolution in analysis of cell cycle kinetics (43). The coefficient of variation may be considered a parameter reflecting specificity of DNA staining and typically ranges from 2.5-3.0% (43). This staining procedure was used to prepare the cells for analysis in the flow cytometer.

V. Acid-induced denaturation of DNA in situ, of somatic cells

Profound changes occur in both the gross and molecular structure of nuclear chromatin during the cell cycle, as well as during cell transition to quiescence or differentiation (65). A technique is available to study chromatin changes based on differences in sensitivity of DNA, in situ, to denaturation (66, 67). This technique can be used to study the effect of hydralazine, in varying concentrations, on chromatin stability. The factors responsible for these variations in in situ DNA sensitivity to denaturation are poorly understood. It is thought that histones and perhaps other nuclear proteins contribute to the stability of DNA in situ, by providing local counterions, and that their post-synthetic modifications alter DNA stability (65).

The technique used to study DNA denaturability in intact somatic cells is based on subjecting RNase-treated cells to heat or acid and subsequent staining with acridine orange. Our experiments used

acid as the method to induce denaturation. After partial denaturation of DNA by the acid, acridine orange stains the nondenatured DNA sections in green (maximum fluorescence at 530 nm), whereas the dye interactions with the denatured (single-strand) DNA sections result in red luminescence (most likely phosphorescence) with maximum emission at 640 nm (65). The relative proportions, therefore, of red and green luminescence represent portions of the denatured and native DNA, respectively.

In most cell types, the sensitivity of DNA to denaturation correlates with the degree of chromatin condensation. The most sensitive to denaturation is DNA in mitotic cells as well as in quiescient cells characterized by condensed chromatin.

A parameter called α_t is used to quantitate the effects of this denaturation process. α_t is defined as red fluorescence/red + green fluorescence and is a measure of the extent of denaturation of DNA, in situ (66, 67).

Cells to be used for acid-induced denaturation studies may be fixed and stored at -20°C for several months previous to the actual procedure. A maximum of 10^7 cells in 1 ml of Hanks Balanced Salt Solution (HBSS, containing no phenol red) are rapidly admixed in 10 ml of fixative (80% ethanol, or 1:1 mixture of 70% ethanol and acetone) at 0-4°C. Cell clumping is minimized if the cell suspension is admixed rapidly.

The staining procedure involves centrifuging the fixed cells and resuspending in 1 ml of HBSS. RNase A is added at 1-2 x 10^3 units

and incubated at 37°C for 1 hour. A 0.2 ml aliquot of this cell suspension is admixed with 0.5 ml of a 0.2 M KCl/0.2 M HCl solution adjusted to a pH of approximately 1.4. After 30 seconds 2 ml of 6 or 8 mcg/ml acridine orange in 0.2 M Na_2HPO_4/0.1 M citric acid buffer (pH 2.6) is added. The cell suspension is now ready to be transferred to the flow cytometer for measurement.

The above procedure was utilized to study the effects of varying concentrations of hydralazine on chromatin structure in both lymphocytes and Friend leukemia cells.

VI. Flow cytometry, an overview.

Flow cytometry is a process in which individual cells, or other biological particles are made to pass in single file, in a fluid stream, by a sensor or sensors which measure physical or chemical characteristics of the cells or particles (68). It is a process of recent origin that is being applied to the study of a wide variety of biological and medical problems. Most of the present interest in, and applications of, flow cytometers has to do with the utility of the apparatus for the definition and quantification of heterogeneity in cell populations. The following physical and chemical characteristics of cells or other biological particles have been studied with flow cytometry. These include cell size, shape, granularity of the cytoplasm, pigment content, protein content, DNA content and base ratio, chromatin structure, RNA content, rate of macromolecule synthesis, DNA repair, enzyme kinetics, intracellular pH, presence of antigens, and electron potential of organelles (68). Flow cytometry,

therefore, has potential for use in a great variety of cellular physical and chemical parameters.

The fundamental concept of flow cytometry is that cells or biological particles are made to flow at high speed through a sensing region where optical or electrical signals indicative of important biologic properties are generated. The signals generated are analyzed and accumulated for quantitative evaluation. The cells are generally stained with fluorescent dyes, although absorbing dyes are sometimes used, and no staining is necessary for light-scatter measurements or electrical sizing (69). Typical measurements are electronic cell volume, total or multicolor fluorescence from stains bound to cell constituents or from endogenous intracellular components, light scatter from cells which is related to diffractive, reflective and refractive properties of external and internal cell features, axial light loss or extinction, which is the reduction in light intensity caused by a cell passing through the excitation beam, nuclear and cytoplasmic diameter based on fluorescence signal contours or signal time duration measurements, and fluorescence polarization (69). Simultaneous processing of signals from each cell provides a direct way to determine functional, biochemical, and cytological relationships between cells. In addition, a process known as cell sorting permits the physical separation of cells from heterogeneous populations for identifying measured properties with morphology and the concentration of subclasses for functional or biochemical determination (69).

The single file flow of cells necessary for flow cytometry is produced by introducing the sample or "core" fluid containing the cells through a narrow tube intended to be coaxial with a wider tube through which a cell-free "sheath" fluid is flowing (Figure 5). Flow velocity is adjusted so that flow is laminar, confining the core fluid to the central region of the stream (65). Downstream from the injection site of the sample the diameter of the capillary tube is gradually reduced by tapering. The cell suspension is driven under pressure through a disposable filter into a tube connecting to the flow cell, where it is injected into a laminar and concentrically flowing sheath fluid. This technique is called hydrodynamic focusing and produces laminar flow conditions with virtually no mixing between sample fluid and sheath. The sheath fluid in our studies consisted of 1 ml of Triton X-100 (polyethylene glycol p-isooctylphenyl ether) diluted to 1600 ml with double distilled water.

Cells can be optically measured as they emerge in a liquid jet from a flow nozzle and intersect an excitation source. Sensor signals are processed electronically on a cell-by-cell basis in a variety of ways and they are either displayed as frequency distribution histograms using a multichannel pulse-height analyzer or stored in a computer for subsequent analysis and display (70). The cells must be illuminated in order to make measurements of them and fluorescence emission and scattered light have to be collected and directed to a detector. The observation point, sometimes called the interrogation point, is the point where the illumination beam intersects the stream

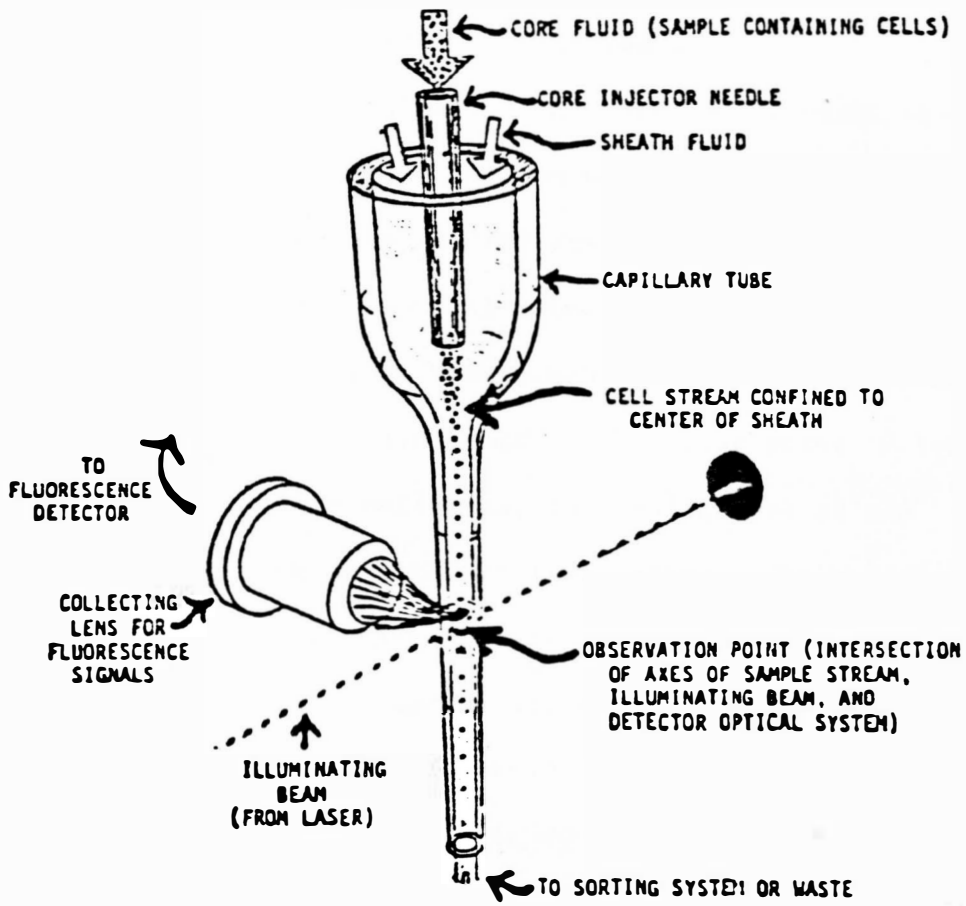

Figure 5. Schematic of a typical flow cell at the interrogation point (68).

of cells and must be somewhere in the field of view of the collection optics. Laser source flow cytometers always use what is called an orthagonal geometry, in which the direction of sample flow, the illuminating laser beam, and the optical axis of the fluorescence collection lens are mutually perpendicular (65). Our research utilized a Cytofluorograf II Model 30-L flow cytometer produced by Ortho Diagnostics. This instrument was equipped with a 100 mW Lexel argon ion laser which was used as a source of illumination.

A laser source has several advantages over an arc-lamp source. Collecting the light and putting it into an observation region of a flow cytometer takes considerable effort, just in terms of selecting lenses. Also, filters or other optical elements must be utilized to define the excitation and emission wavelength regions which will be used. It is easier to direct laser beams to a precise point of focus than it is to control arc lamp emissions, and realignment of the optics is not needed as much as with arc lamp optics. The use of a laser allows the bypass of two-thirds of the optical filter problems, as one can dispense with the excitation filter and the dichroic that are used with the arc lamp and be concerned only with the filter used for the detector (68). The monochromaticity of laser light usually allows the specifications on this filter to be relaxed also. Lasers also provide greater brightness than arc lamps. Argon lasers are the most popular lasers used in flow cytometry. They are most frequently tuned to emit light at 488 nm, a wavelength useful for excitation of dyes like fluorescein, propidium iodide, ethidium bromide, acridine

orange, pyronin Y, various rhodamine and cyanine dyes and anthracycline drugs such as adriamycin. This research utilized the fluorescent dye acridine orange in all experiments and an argon-ion laser tuned to emit light at 488 nm.

The interrogation point is located within the flow chamber. Flow chambers transport the suspended cells at high speed, well separated from each other, and on very uniform trajectories through the sensing region by making use of the fluid mechanical principles of hydrodynamic focusing and laminar flow. The flow chamber also allows for proper entry of the exciting light, collection of fluorescence emission and scattered light and if the flow cytometer is equipped with a cell sorter it provides for jet and droplet formation. The flow cell in the Cytofluorograf Model 30-L is constructed with flat sections of quartz glass and has a specially shaped sample injection nozzle and entry funnel to ensure stable laminar flow of the sample suspension and the concentric sheath. After being interrogated by the laser beam, the flow stream exits the glass flow cell. The cells pass through the beam, one by one, blocking light (axial light loss), scattering light from the beam, or emitting fluorescence as a result of the bound fluorochrome or autofluorescence. Axial light loss is detected by a PIN photodiode which produces a signal proportional to the change in light as a cell passes by the beam. Scattered light falls on a sensor (designated fiber optic) and is conducted to a photomultiplier tube, producing a separate signal. The two signals are related to cell size, refractive index of the cell, and granularity

(67). Fluorescence emissions resulting from argon-ion laser excitation of bound fluorochromes are detected by two fiber optic elements (long and short wavelength fluorescence) (Figure 6). Short wavelength fluorescence corresponding to green fluorescence is an indicator of double-strand DNA content (71). Long wavelength fluorescence, corresponding to red fluorescence, is an indicator of single-strand nucleic acid content. These are the parameters we were concerned with in this research project. These fluorescences falling on the fiber optic elements produce signals proportional to the amount of fluorochrome bound to the cell (71).

The fluorescence emissions and scattered light collected by the fiber optic elements are conducted to photomultiplier tubes. Signals from the photomultiplier tubes are amplified by their respective preamplifiers and then routed to the signal processor. Similarly, signals from the PIN photodiode (axial light loss) are amplified and then routed to the signal processor (71). There are three photomultiplier tubes and one PIN photodiode in the Cytofluorograf II Model 30-L. At the signal processor any two of the four detector signals can be analyzed and displayed at one time. Selection of the desired detector signals is accomplished by means of X and Y axis selection switches. Our Cytofluorograf is interfaced to a Data General Model 2150 Computer System. All four detectors are coupled to the computer so multidimensional analysis is possible. The signal processor has provisions for measuring any one of three characteristics of each input signal pulse height, pulse area and pulse

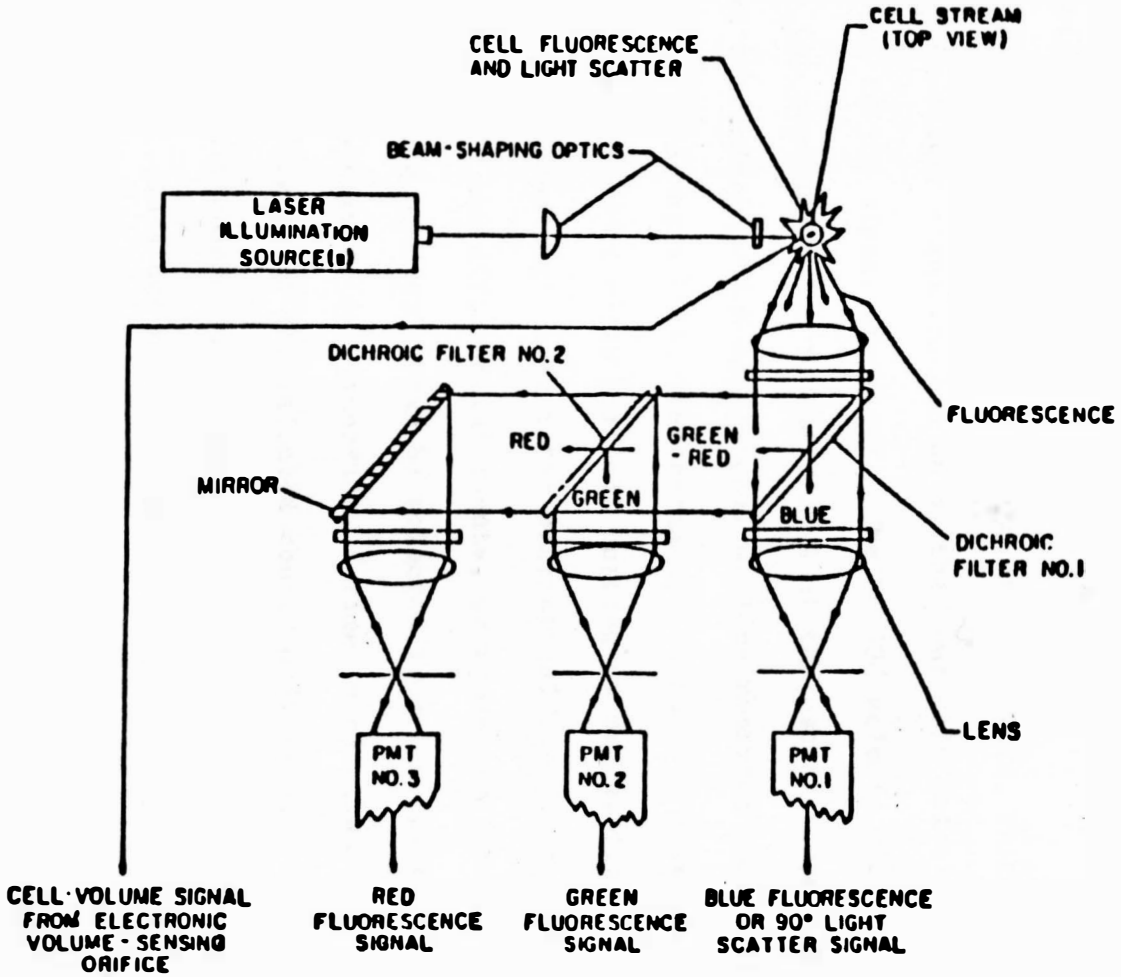

Figure 6. Schematic diagram of optics on a flow cytometer (70).

width (67). First, the detector signals to be used for the X- and Y-axis is determined and then the mode of analysis to be used on each of these signals is decided upon.

As the signals emerge from the preamplifiers, which buffer and amplify the light signal picked up by the four main detectors, they enter the FC 300 signal processor. The FC 300 selects signals individually for viewing on the X- and Y-axis of the oscilloscope, it also selects the mode in which each signal will be measured such as pulse height, width or area (71). Furthermore, it can also select one or two subpopulations of cells for cell sorting or enumeration (differential counting), select the statistical precision or data sample size for the differential counts, or enumerate total cells analyzed. The mode of display can be selected from the following: X-axis or Y-axis signals as a function of time, a cytogram of the total count, or a cytogram of the selected counts only (71).

The Multichannel Distribution Analyzer Model 2103 acquires, stores, and displays one or two single-parameter histograms or two-parameter cytograms on a built in storage oscilloscope.

The cell sorter FC 400 consists of cell sorter controls, two plug-in printed circuit boards, a cell-sorting flow cell assembly, a collection assembly, a deflection assembly and a vacuum system. This unit permits physical separation of subpopulations of cells detected by the laser/optic systems and selected by the FC 300 signal processor. Optical signals are detected, processed, delayed, and combined as required to produce electrical pulses, which charge the

liquid stream positively or negatively at the time the droplet containing the desired cell is forming (71). Droplets broken off while the stream is charged retain that charge. Further downstream the droplets pass through an electric field between two charged plates, the charged droplets are then deflected appropriately into separate containers while the uncharged droplets continue on their original course and are either discharged into a waste container or into a third container.

The computer interfaced to the Cytofluorograf is a Data General Model 2150 which is a data acquisition and processor/cell sorter controller that can fully analyze data as it sorts cell subpopulations into separate collection vessels. Data from the Cytofluorograf is acquired, stored, analyzed, and displayed by the Model 2150 Computer system. The system will accept up to four input parameters per cell with the option of accepting an additional four parameters per cell (77). The standard optical parameters that are measured include: forward and right angle, long and short wavelength fluorescence, narrow forward-angle scatter, right-angle scatter and axial light loss. Each of these parameters can be measured in terms of pulse height, pulse area, and pulse width. The Model 2150 system can create correlated two-dimensional histograms from any two parameters. Also multiple linear regions of interest are definable for one-dimensional histograms. The versatility of this system is enhanced by its ability to perform simultaneous acquisition, data processing, storage, and cell sorting. Multiple user-specified

elliptical and rectilinear regions of interest are definable for two-dimensional histograms. Regions of interest generated on the displays allow calculation of cell counts, means, standard deviations, and coefficients of variation (77). One and two-dimensional histogram displays obtainable with the Model 2150 are presented below (Figure 7, 8). Two dimensional histograms are called cytograms. In addition, an isometric display is shown (Figure 9). By means of a joystick control, it is possible to select a specific area or region of a cytogram to be analyzed, one can then use the keyboard to rotate a two-dimensional histogram display so it can be observed isometrically (77). The system includes a system processor and an acquisition processor. The primary function of the system processor is to store the acquired data from the acquisition processor and to permit this data to be analyzed. User programs developed on the video terminal keyboard are stored in disk memory and then executed via the processors. These programs can be selected and run repeatedly on different samples, or can be modified by the operator or following normal Cytofluorograf operation.

The above provides an overview of our Cytofluorograf Model 30-L interfaced to an Ortho Model 2150 Computer. The discussion is intended to present the principles of a flow cytometer and how this system was used in the study of hydralazine's effects on mammalian cell cycle kinetics.

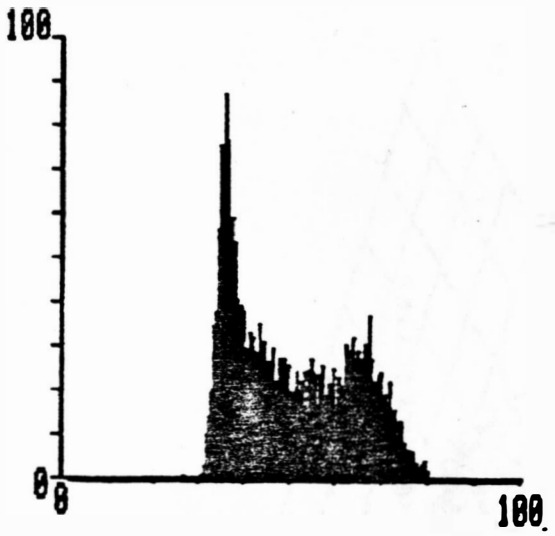

Figure 7. A one dimensional frequency histogram of green fluorescence of acridine orange stained Friend leukemia cells in log-phase growth.

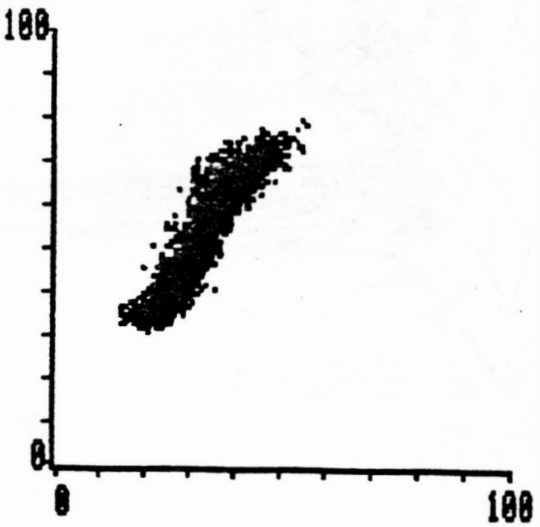

Figure 8. A two dimensional cytogram of green fluorescence (y) versus red fluorescence (x) of acridine orange stained Friend leukemia cells in log-phase growth.

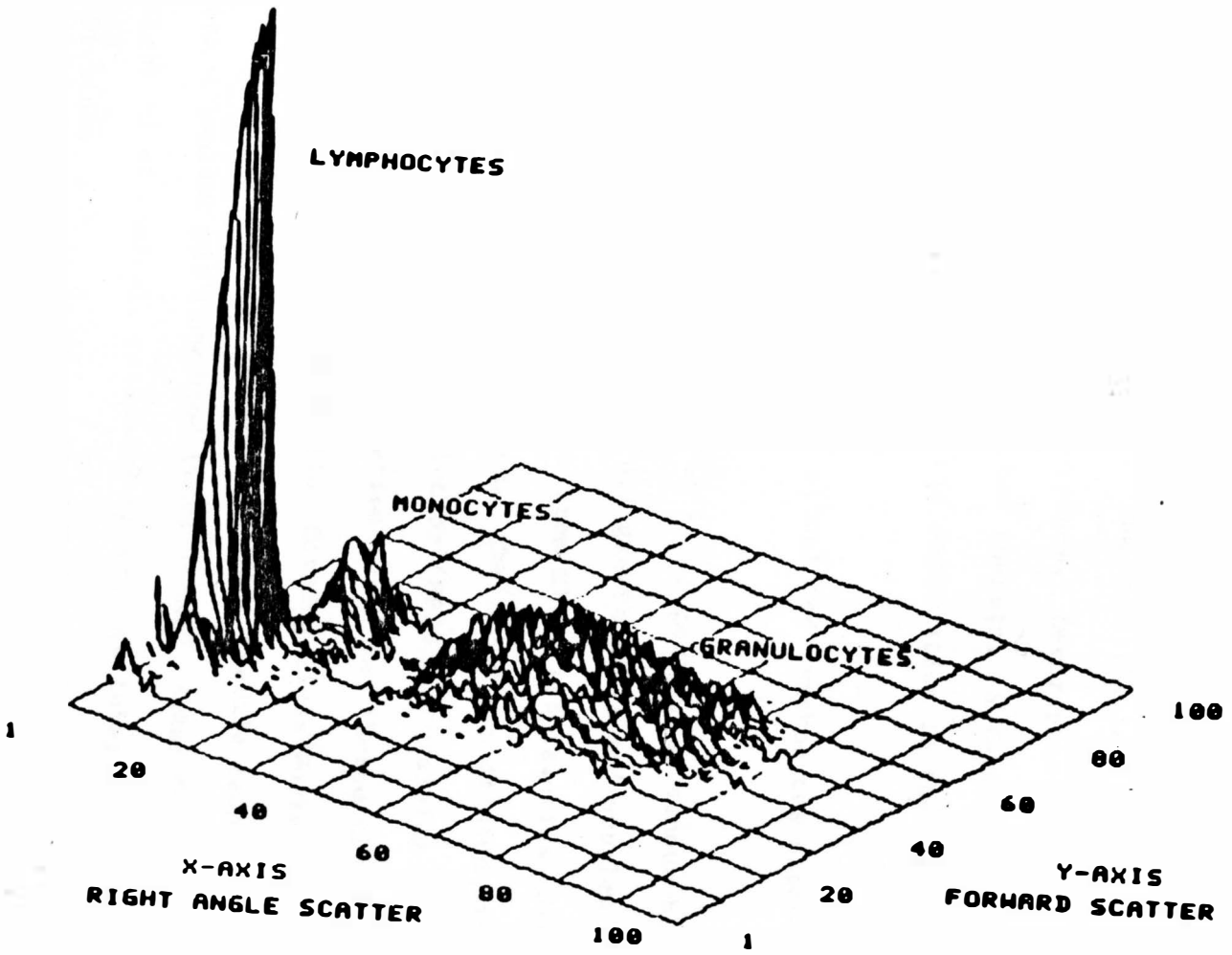

Figure 9. An isometric display (70).

MATERIALS AND METHODS SECTION

This section contains a description of all experiments conducted in this research project. The experiments are presented in outline form for organization purposes. Descriptions of special methods and materials are described therein. Reference is made back to the appropriate section to avoid duplication in the text.

I. Human Lymphocyte Experiments

A. Phytohemagglutinin (PHA) stimulated lymphocytes exposed to hydralazine.

This experiment utilized 40 ml of peripheral venous blood from a healthy laboratory volunteer. All growth media and supplements used in tissue culture experiments were from Gibco Laboratories (Grand Island, NY) unless otherwise stated. The blood was diluted with two volumes of Hanks Balanced Salt Solution (HBSS), containing magnesium, calcium, and phenol red. The dilution was mixed thoroughly in a tissue culture flask (Corning #25110, Corning Glass Works, Corning, NY). All manipulations were performed using sterile technique and utilizing a laminar air flow hood (SterilGARD®, Baker Co., Sanford, ME). Eight 15 ml conical, graduated centrifuge tubes (Falcon #2095 Becton Dickinson & Co., Oxnard, CA) were prepared by adding 5 ml of Lymphoprep® (Nyegaard & Co., Oslo, Norway) to each. Approximately 11 ml of the blood dilution was carefully layered over the Lymphoprep®, using care not to disturb the interface between the two liquid phases. These tubes were centrifuged at 400 x g for 20 minutes. The red blood cells settled to the bottom of the tube. Above the red blood cells

was the Lymphoprep® and serum phase, a buffy white interface of white blood cells (WB cells) and an upper phase consisting primarily of HBSS (59). The HBSS was aspirated to about 1 cm above the WBC layer. The WB cells were removed by aspiration from each of the eight centrifuge tubes and placed in separate conical tissue culture tubes (Falcon #3033). The WB cells were washed with 10 ml of HBSS by centrifugation at 225 x g for 5 minutes. The pellets were resuspended and the cells pooled in a test tube. The supernatant solution was saved and centrifuged again at 325 x g for 8-10 minutes. The resulting suspended cells were added to those previously collected. These cells were diluted and washed once more with HBSS. The supernatant from the second washing was discarded. A cell count was performed using a hemocytometer. An appropriate amount of media and 3 mcg/ml of phytohemagglutinin (PHA) (Purified Phytohaemagglutinin by Wellcome Research Laboratories, Beckenham, England) were added to the WB cells in a single tissue culture flask (Corning #25100) and thoroughly mixed. This suspension was divided up into 14 individual cultures. The cultures contained 1 x 10^6 cells/ml in 1.5 ml total volume. The cultures were incubated for 72 hours in 24-well cell culture plates (Corning #25820). The incubation atmosphere was maintained at 37°C and 5% CO_2 in a humidified environment. Media consisted of RPMI 1640 with 25 mM HEPES buffer supplemented with heat inactivated fetal bovine serum to 16% final concentration. The media contained 2 mM L-glutamine along with 80 U/ml of penicillin and 80 mcg/ml streptomycin. At 72 hours, a serial dilution of hydralazine (Sigma Chemical Co.,

St. Louis, MO), in media, was prepared and added to the cultures. These dilutions were filter sterilized using a 0.22 micron filter (Millex-GS by Millipore Corp., Bedford, MA). Final culture concentrations of hydralazine included 0, 2.5, 5.0, 10.0, 20.0, 40.0 and 80.0 mcg/ml.

At 24 and 48 hours after addition of hydralazine (total culture life of 96 and 120 hours, respectively), aliquots of the cultured WB cells were stained using the acridine orange staining protocol and analyzed by flow cytometry.

The acridine orange staining procedure consisted of admixing a 0.2 ml aliquot of cell suspension (containing a maximum of 3×10^5 cells) with 0.4 ml of a solution containing 0.1% Triton X-100 (Sigma Chemical Co., St. Louis, MO), 0.08 N HCl, 0.15 M NaCl, at a pH of 1.4. After 30 seconds at 4°C, 1.2 ml of a solution containing 6 mcg/ml of acridine orange (Polysciences Inc., Warrington, PA), 10^{-3} M diNaEDTA, 0.15 M NaCl, in 0.2 M Na_2HPO_4/0.1 M citric acid buffer at pH 6.0 was added. After staining, the cells were analyzed by flow cytometry. This experiment was set up in duplicate, and the entire experiment was repeated once, also in duplicate.

B. Lymphocytes exposed to hydralazine, then stimulated with PHA.

The experiment utilized 40 ml of peripheral venous blood obtained from a healthy laboratory volunteer. The WBC cells were isolated as described in Section IA (59). All cultures were set up in duplicate. The total culture volume was 2.0 ml and contained 1×10^6 cells/ml, using media as previously described. A serial dilution of

hydralazine was prepared, again, using a 0.22 micron filter to sterilize the solution. The final culture concentrations of hydralazine were 0, 2.5, 5.0, 10.0, 20.0, 40.0 and 80.0 mcg/ml. The cultures were incubated under the same conditions described in Section IA for 24 hours in 16 x 125 mm tissue culture tubes (Falcon #3033) placed at a 45° angle in the incubator. After 24 hours the cultures were centrifuged at 225 x g for 5 minutes. A pasteur pipette was used to disperse any cell aggregates before centrifugation. Supernatants were aspirated and cells were resuspended in 2 ml of media as previously described, and centrifuged again to wash the cells free of excess hydralazine. The supernatant was aspirated and the cells resuspended in media and counted with a hemocytometer. Cultures were set up, in duplicate, and adjusted to contain 1.4×10^6 cells in a total of 2.0 ml of fresh media. PHA was added to the cultures at a concentration of 3 mcg/ml. The cultures were then incubated for 96 hours at a 45° angle in tubes as described above. Aliquots from these cell cultures were stained using the acridine orange procedure as described in Section IA, and analyzed by flow cytometry.

This experiment was set up in duplicate and repeated as previously described.

C. Effects of hydralazine on susceptibility of DNA to acid-induced denaturation in situ.

In this experiment, 80 ml of peripheral venous blood was collected from a healthy laboratory volunteer. The blood was diluted and the WB cells isolated as described in Section IA, except that the

HBSS used contained no phenol red. Twenty-eight cultures were set up and hydralazine dilutions were prepared as previously described. Final culture concentrations were 2.5 x 10^6 cells in a total volume of 3.0 ml each. The cultures were divided up into 4 series of hydralazine concentrations including 0, 2.5, 5.0, 10.0, 20.0, 40.0 and 80.0 mcg/ml. The cultures were incubated for 24 hours at 37°C in an atmosphere of 5% CO_2 in tissue culture flasks (Corning #25100). After 24 hours, the cultures were centrifuged at 225 x g for 5 minutes. The supernatants were aspirated off and the pellets resuspended in 1 ml HBSS. The cells were fixed as follows. Cells were rapidly admixed by adding 1 ml of cell suspension (not to exceed 10^7 cells/ml) to 10 ml of fixative (1:1 mixture of 70% ethanol and acetone) at 4°C in glass tubes. Cells may be kept in this fixed state for several months at -20°C without any changes (59, 66).

At the time of analysis, the glass tubes were centrifuged at 225 x g for 5 minutes, the cold ethanol/acetone aspirated off to near dryness and the pellets resuspended in 1 ml of HBSS. This suspension was then incubated with 1-2 x 10^3 units of RNase A (Worthington Biomedical Corp., Freehold, NJ) for 1 hour at 37°C. After one hour, a 0.2 ml aliquot of cell suspension (still in HBSS with RNase) was transferred to a small culture tube, 0.5 ml of KCl-HCl buffer was added (1:1 mixture of 0.2 M KCl and 0.2 M HCl at pH of 1.4). After 30 seconds, 2 ml of a solution containing acridine orange (6 mcg/ml) in 0.2 M Na_2HPO_4/0.1 M citric acid buffer at pH 2.6 was added (59). This staining procedure prepared the cells for analysis by flow cytometry.

D. Effects of hydralazine on PHA stimulation of lymphocytes from a control patient and a patient with idiopathic systemic lupus erythematosus (SLE).

Peripheral venous blood was obtained from a healthy laboratory volunteer and a patient with long-term idiopathic systemic lupus erythematosus (SLE). These 20 ml blood samples were processed in parallel and the WB cells were isolated according to the procedure described in Section IA. A cell count was obtained and 12 cultures were set up in tissue culture tubes (Falcon #3033). There were 6 cultures from each patient's blood. One culture from each was stained using the acridine orange procedure described in Section IA and analyzed by flow cytometry the day of collection. The remaining 10 cultures were set up to contain 2 ml total volume, 3 mcg/ml PHA and 1×10^6 cells/ml. All dilutions were made in a 25 cm^2 tissue culture flask (Corning #25100) before dividing up into individual cultures. The cultures were incubated at a 45° angle at 37°C in 5% CO_2 atmosphere. Each succeeding 24 hours, one culture from each individual was stained with acridine orange and analyzed by flow cytometry for DNA and RNA content. After 72 hours, hydralazine was added to the remaining six cultures in dosages of 0, 5 and 40 mcg/ml. At the completion of the experiment we had flow cytometric measurements of PHA stimulated lymphocytes at time 0, 24, 48 and 72 hours. At 96 hours we had instrument measurements of red and green fluorescence of 96 hour old PHA stimulated lymphocytes stained with acridine orange that during the last 24 hours had been exposed to 0, 5 and 40 mcg/ml

hydralazine concentrations. These measurements were obtained on both control patient and lupus patient for a side by side comparison.

In preparation for analysis, the cultures were spun down at 225 x g for 5 minutes, the supernatant aspirated, and the pellet resuspended in HBSS. Aliquots were then stained using the acridine orange procedure described in Section IA.

E. Effect of hydralazine on cell viability of human lymphocytes.

WB cells were separated from 40 ml of venous blood using the method described in Section IA. Fourteen cultures were set up, in media previously described in Section IA, to contain 1 x 10^6 cells/ml with total culture volumes of 2 ml each. A serial dilution of hydralazine was prepared and added 0, 2.5, 5.0, 10.0, 20.0, 40.0 and 80.0 mcg/ml final concentration. These cultures were incubated at 37°C in 5% CO_2 for 24 hours, at which time the cells were gently dispersed with a pipette and centrifuged at 225 x g for 5 minutes. The supernatant was removed by aspiration and the cells were washed twice with HBSS. Cell counts were obtained and new cultures were set up to contain 1.4 x 10^6 cells in a total volume of 2 ml of media. The cultures were stimulated with 3 mcg/ml of PHA. Aliquots were taken at 24 and 96 hours for viability studies. Viability was assessed by trypan blue dye exclusion. Cell suspensions were admixed with 0.4% trypan blue in a 5:1 ratio. These were allowed to stand for more than 5 minutes but less than 15 minutes. Total cell count and count of unstained cells (viable) were obtained by hemocytometer and percent viability was calculated.

II. Rat Lymphocyte and Sperm Experiments

A. Effects of long-term hydralazine exposure on lymphocytes of spontaneously hypertensive rats (SHR).

Sixty male SHR were acquired from Taconic Farms (Germantown, NY), at 8 weeks of age. The animals were randomly separated into twelve groups of five animals each. The animals were housed in separate cages and allowed free access to deionized water and Rodent Blox (Wayne Pet Food Division, Chicago, IL), for a period of four weeks. At the end of this period the animals were weighed. The rats were twelve to fourteen weeks old when the hydralazine administration began.

The eleven groups were divided into the following dosage groups: 0, 0.013, 0.04, 0.12, 0.36, 1.1, 3.3, 10, 30, 60 and 90 mg of hydralazine/kg body weight per day. These dosages allowed for serial dilution of hydralazine in the drinking water. It was desirable for the range of dosages to span those prescribed for humans in clinical situations and well into the toxic range. The animals' average daily water consumptions during the four week equilibration time was observed. Animals consumed 35-45 ml daily and averaged 280-300 grams in weight at the start of the hydralazine administration. Hydralazine was freshly prepared in the drinking water daily. In an attempt to reduce hydration differences between the animals, the hydralazine concentrations in the stock solutions were such that each animal received the specified hydralazine amount and all animals received the same volume of solution in terms of ml/kg daily. It took several weeks to

titrate the ml/kg volume so the animals would consume their daily dose. It was desirable to keep the animals at or near the average volume consumed free choice. The animals averaged 25-35 ml daily volume per animal throughout the 12 week experimental period. The upper dosage groups 60 and 90 mg/kg/day were responsible for the total daily volume being adjusted downward. The animals were started out at about 30-35 ml daily but because of the upper dosage groups' refusal to drink all their water, the quantity had to be adjusted several times throughout the experiment. At about the seventh week, four to five randomly dispersed animals developed some urogenital bleeding that was scant to moderate. These rats were tagged for later reference. Weights were checked every 3-4 weeks during this 12 week experimental period. The temperature was held at 20°C $\pm$ 2°C and a 12 hour light-dark cycle was maintained throughout the experiment.

At the end of the 12 week period, the animals were anesthetized with ether, weighed, and blood was withdrawn by cardiac puncture. About 10 ml of blood was obtained from each rat. The WB cells were isolated using the same procedure as described in Section IA. The isolated cells were stained using the acridine orange procedure outlined in Section IA, the only difference being the acridine orange staining solution contained 8 mcg/ml of acridine orange as opposed to 6 mcg/ml used on all preceding experiments. These cell samples were analyzed by flow cytometry that same day.

B. Effects of hydralazine on testicular cell differentiation and sperm chromatin structure.

The testes from the SHR were surgically removed and weighed. One whole testis was wrapped in cellophane and frozen at -20°C initially and -95°C later for storage. The tunica was removed and a section of the other testis was removed and minced with a curved scissors in HBSS to form a cellular suspension that was filtered through a 53-um nylon mesh (Tetko, Inc., New York, NY). These cells were then stained using the acridine orange procedure outlined in Section IA, and measured by flow cytometry within one hour after sample preparation.

The frozen testes were later thawed and homogenized with 2 ml of double distilled water for 20 seconds using a Virtis Model 45 Homogenizer set at a power setting of 55. Then 3 ml of double distilled water was added to the homogenate and the total volume recorded. These homogenates were sonicated for 60 seconds at a power setting of 50 using a Biosonik IV Sonicator (VWR Scientific, San Francisco, CA) to disrupt tissue debris, sperm tails and spermatogenic cells sensitive to sonication, leaving only the sonication-resistant sperm heads. This suspension was diluted and total volume recorded. Sperm head counts were made using a hemocytometer and light microscope and total sperm head count per gram of testis was calculated (84, 86).

Both caudal epididymi were removed from each animal. One was sliced with a razor blade, then minced and transferred to a tissue culture tube, tissue fragments were allowed to settle and the suspended cells were filtered through a 153 micrometer nylon mesh (Tetko, Inc.). The filtrate was frozen at -95°C in TNE buffer (0.15 M

NaCl, 0.01 M Tris-HCl, 1 mM diNaEDTA, pH 7.4) containing 10% glycerol. For flow cytometric analysis samples were thawed at 37°C in a water bath and a 2 ml aliquot withdrawn and sonicated using a Biosonik IV at a power setting of 50 for 30 seconds, allowed to cool for 30 seconds, and sonicated for 30 more seconds (83, 85). These cell suspensions were diluted with TNE buffer as needed to obtain adequate flow rates and were stained using the acridine orange staining procedure outlined in Section IA and measured by flow cytometry.

III. Friend Leukemia Cells

A. Growth and viability study of Friend leukemia cells (FL cells) exposed to hydralazine.

Stock cultures of FL cells suspended in tissue culture media supplemented with 20% fetal calf serum and 10% dimethyl sulfoxide were stored in liquid nitrogen. The vial containing the cells was removed from the liquid nitrogen and thawed quickly in a 37°C water bath. Ten milliliters of 37°C growth media, as described in Section IA was added. This suspension was centrifuged at 225 x g for 5 minutes and the supernatant aspirated to remove the dimethyl sulfoxide. The pellet was resuspended in 5 ml growth media and incubated at 37°C in 5% CO_2 atmosphere. These cells were passed 1 volume cell suspension to 3 volumes growth media daily for 3 days prior to the experiment to insure cells were in log phase asychronous growth. The cultures were set up to contain 5 ml of cell suspension at a cell concentration of 4×10^5 cells/ml. Hydralazine was added in concentrations of 0, 2.5, 5, 10, 20, 40, 80, 160 and 320 mcg/ml. After 20 hours of exposure,

the cells were observed for viability by trypan blue dye exclusion. A 0.5 ml cell suspension aliquot was stained with 0.1 ml trypan blue and stained samples were counted by use of a hemocytometer and light microscopy (83, 84).

In addition, "Full Bright" fluorescent polystyrene beads (Coulter Corp., Hialeah, FL) were diluted 1:5 with HBSS. Aliquots of each culture were stained using the acridine orange procedure plus each sample received 20 microliters of the fluorescent bead dilution containing 1.2×10^6 beads/ml. These samples were analyzed by flow cytometry. The FL cell concentration was determined by relating fluorescent bead events to FL cell events and basing it on the count of beads/ml in the stained sample. The beads/ml count was determined by hemocytometer and light microscopy.

B. Stathmokinetic experiment to determine terminal point of hydralazine action on logarithmically growing FL cells.

FL cells were passed 1:3 daily for 3 consecutive days until cells were at approximately 8×10^5 cells/ml in a total volume of 360 ml of media as described in Section IA. Vinblastine (Sigma Chemical Co., St. Louis, MO) was added at 0.5 mcg/ml to induce a block in M phase. The cell suspension was divided into four 90 ml cultures. One hour after vinblastine addition, hydralazine was added at 0, 20, 40 and 80 mcg/ml concentrations. Aliquots for acridine orange staining and flow cytometer were taken at 0, 1, 2, 3, 4, 5, 6, 7, 9 and 10 hours post-vinblastine. In addition, 8 ml aliquots were withdrawn at these same time intervals for use in acid-induced denaturation experiments

using the procedure described in Section IC (65, 67, 83, 84, 86).

IV. Chinese Hamster Ovary Cells

A. Viability of Chinese hamster ovary (CHO) cells after twenty hour exposure to hydralazine.

Vials of CHO cells frozen in 10% dimethylsulfoxide were removed from liquid nitrogen and placed in a 37°C water bath. Cell suspensions were centrifuged at 200 x g for 5 minutes and the supernatant containing 10% dimethyl sulfoxide poured off the resulting pellet. The pellet was then resuspended in 10 ml of F-12 (HAM) Nutrient media supplemented with heat-inactivated fetal bovine serum to 16% final concentration, 2 mM L-glutamine, 80 U/ml penicillin and 80 mcg/ml streptomycin. The culture was routinely passed twice weekly by splitting at a ratio of about 1:20. For survival studies on cycling cells, known numbers of exponentially growing cells were seeded in plastic plates (Falcon #3046) containing conditioned media (media in which log phase cells were grown for 6 to 12 hours). The cells were seeded in concentrations of 10^4, 10^3, and 10^2 cells/well in triplicate for each drug concentration. After 2-4 hours to allow for cell attachment, the drug solution was added directly to the culture media in concentrations of 0, 2.5, 5, 10, 20, 40, 80 and 160 mcg/ml. After a 20 hour exposure, the cells were washed twice with HBSS and refed with fresh media. Following cell growth for 7 days, the cultures were washed twice with HBSS, fixed with Carnoys fixative (3 parts methanol:1 part glacial acetic acid) for 15 minutes, and stained with a 0.1% crystal violet solution in 0.1 M citric acid.

Cells that were able to form colonies composed of at least 50 cells were scored for survivability (83, 84). Survival studies on non-cycling cells were performed as above with the following exceptions. Non-cycling cells (in confluency for about 48 hours) were treated with various concentrations of drug for 20 hours, washed with HBSS, trypsinized with 0.4% Trypsin-EDTA (Gibco Laboratories, Grand Island, NY) and replated in conditioned media. CHO cells grow as a monolayer culture and the Trypsin-EDTA is needed to loosen the attachment of the cells from the culture flask. The conditioned media was left in for about 20 hours during which time the cells attached to the culture vessel. At the end of 20 hours, the conditioned media was replaced with fresh media and the cells cultured for 7 days, stained as above (83, 84), and the colonies counted manually (81, 82).

RESULTS

I. Friend leukemia cell experiments

This experiment assessed the effect of hydralazine on the growth and viability of log phase growth FL cells exposed to hydralazine for 20 hours. Survivability of log phase FL cells exposed to hydralazine was analyzed by counting cell concentrations using FCM and cell viability (through the use of trypan blue dye exclusion) by light microscopy. Figure 10 shows the effects of hydralazine on FL cell growth. Cell count was plotted as a percentage of control versus hydralazine dosage. The critical dose for inhibition of cell growth lies between 20 and 40 mcg/ml. The data are presented in Table 1. Figure 11 is a plot of percent viability versus hydralazine dosage after twenty hours of exposure. Notice that viability remained high, approximately 90% for dosages up to 160 mcg/ml. Thus, cell growth is inhibited prior to loss of cell viability. The data are presented in Table 2.

A stathmokinetic experiment was designed to determine where in the cell cycle hydralazine was exerting its inhibitory effects. This type of experiment utilizes vinblastine, which causes an M phase block in the cell cycle. One hour after vinblastine addition, hydralazine was added to the cultures and samples taken every hour for flow cytometric analysis.

The results of the acridine orange staining procedure can be seen in Figures 12, 13, 14 and 15. The control (Figure 12) shows a time-dependent increase in the percent G_2M cells. The 20 mcg/ml dose

(Figure 13) shows a similar pattern, however the 40 mcg/ml dose (Figure 14) tends to show somewhat less of a buildup in G_2M cells suggesting a slowing down of progression through the cell cycle. At 80 mcg/ml (Figure 15) it appears the cells have been halted in their progression through the cell cycle. Data are presented in Tables 3, 4, 5 and 6. A portion of these samples was fixed in ethanol/acetone for later acid-induced denaturation of DNA experiments.

Mitotic cells differ in their susceptibility to acid-induced denaturation of DNA in situ (89). Therefore, upon acid-induced denaturation as described in Section IC of Materials and Methods, staining with acridine orange and analysis by flow cytometry, the mitotic cells can be readily determined. Figure 16 shows the red fluorescence versus green fluorescence cytogram of the raw data from FCM analysis. The population in area 1 represents the mitotic cells.

Figure 17 shows the percent mitotic cells, determined by computer assistance from data represented in Table 7 in each culture at various time points after vinblastine addition. The control curve is nearly linear as would be expected for log phase growth cells. Exposure to 20 mcg/ml and 40 mcg/ml vinblastine caused a delayed entry into mitosis (slowing of the cell cycle rate indicated by a decrease in the rate of mitotic cell accumulation) while 80 mcg/ml caused almost total inhibition (a slope of near zero value). The shift in slope for the 20, 40 and 80 mcg/ml curves occur at approximately 1.5 - 2.0 hours (approximately the length of the G_2 period) after addition of hydralazine, strongly suggesting that the "terminal point

of action" is at the S-G_2 transition. Thus, hydralazine apparently has little or no significant effect on cells progressing through G_2 phase.

The ratio of double-strand to single-strand DNA (after the acid-induced denaturation procedure) represented by the " $_t$" index was assessed by computer assistance of data derived from FCM analysis. The standard deviation of $_t$ was also obtained for the mitotic cell population and plotted versus time after vinblastine addition (Figure 18, Table 8). There was no effect of the various hydralazine concentrations.

II. Chinese hamster ovary cell experiments.

The survivability of log phase and stationary (G_0) phase Chinese hamster ovary (CHO) cells was assessed after twenty hours of exposure to hydralazine. Hydralazine exposure at concentrations of 0-20 mcg/ml had no effect on the survivability (ability to form colonies) of log phase CHO cells (Figure 19, Table 9). At concentrations greater than 20 mcg/ml, the percent colony formation began to decrease and at 160 mcg/ml was only 25% of control. The same experiment was also performed on stationary (G_0) CHO cells. Preliminary data suggested hydralaine in concentrations of 0-160 mcg/ml had no effect on the survivability of stationary phase CHO cells. This experiment was only done once and the validity of the results were questionable, consequently the experiment will be repeated and the preliminary results withheld from this report. We anticipate that log phase CHO cells will show a greater sensitivity to

the inhibitory effects of hydralazine than stationary phase (G_0) CHO cells.

III. Human lymphocyte experiments.

Peripheral blood lymphocytes were isolated from a healthy volunteer and stimulated with PHA for 72 hours at which time the cultures were exposed to varying concentrations of hydralazine. Cell cycle population kinetics were analyzed at 24 and 48 hours after hydralazine addition to determine if hydralazine caused any effect on cell progression through the cell cycle. The following results were observed after 24 hours of hydralazine exposure. Cell cycle population kinetics calculations reveal a 10% decrease in the percentage of cycling cells (G_1 + S + G_2M) compared to control as the hydralazine concentration approached 10-20 mcg/ml (Figure 20). There was no further decrease in percent cycling cells at hydralazine concentrations above 20 mcg/ml. This suggests an inhibiting of cells from progressing through the cell cycle as the concentration of hydralazine reaches 20 mcg/ml. Also of interest is the observed increase of approximately 10% in the percent S phase cells from 0 to 20 mcg/ml hydralazine concentration. From 20 to 40 mcg/ml, there is a drop in percent S phase cells and return back to control levels, and cells at 80 mcg/ml exhibit no differences from control. At hydralazine concentrations of 0 to 20 mcg/ml there is an apparent slowing down of the cell cycle in S phase with a slight accumulation of cells in S phase. At concentrations greater than 40 mcg/ml there appears to be almost a total inhibition of the cell cycle with G_1 and S phase populations at

flow cytometry, suggest that there was no effect produced by hydralazine, at any concentration, on the percent of cells in G_0, G_1, S and G_2M phases (Figure 24). Results of a duplicate experiment are presented in Table 12.

Flow cytometric measurements of mean red fluorescence revealed a 3 to 8% increase in fluorescent intensity of G_1, S, and G_2M populations over the concentration range 20 to 80 mcg/ml (Figure 25). Since red fluorescence is a measurement of acridine orange binding to single strand nucleic acid, the data suggest a possible dose related increase in RNA/protein synthesis. These conclusions are based upon the idea that as hydralazine concentration increases, the cell may respond with an increased RNA/protein synthesis to compensate for possible damage inflicted.

The effect of hydralazine on the susceptibility of DNA to acid-induced denaturation of human lymphocytes was assessed by FCM methods to determine if hydralazine caused a change in chromatin structure, as a change in chromatin structure may have been responsible for hydralazines effect on population kinetics and may be related to induction of the lupus symptoms in patients treated with hydralazine. In this experiment, human peripheral lymphocytes were isolated, exposed to varying concentrations of hydralazine for 24 hours, washed, fixed in ethanol/acetone and subjected to acid-induced denaturation of DNA. Mean green and mean red fluorescence were analyzed by FCM. The mean green fluorescence reflecting double-strand nucleic acid (primarily DNA) content reveals no dose effect rela-

tionship of hydralazine on acid-induced denaturation of lymphocyte DNA in situ (Figure 25). Samples were measured on 2 different days. Measurements of mean green fluorescence for days 1 and 2 are essentially linear and the relative shift of the different days data reflects differences in photomultiplier tube settings. The results suggest that hydralazine does not compete with acridine orange for intercalation sites in the double strand DNA because no decrease in mean green fluorescence with increasing hydralazine dose was noted. The lack of effect on susceptibility to acid-induced denaturation suggests that hydralazine does not affect chromatin structure as assessed by acridine orange staining and analysis by flow cytometry. Mean red fluorescence values revealed no dose effect relationship of hydralazine on the binding of acridine orange via stacking type interactions to single-strand DNA (Figure 26). Standard deviations of total fluorescence values versus hydralazine dosage shows some variation but no significant dose response effect on total binding sites available to acridine orange (Figure 27). Standard deviation of $_t$ (red fluorescence/red + green fluorescence) plotted against dosage (Figure 28) shows some variability, but no significant effect of hydralazine on susceptibility of DNA to acid-induced denaturation. It is important to remember that this is only one experimental technique to assess the interaction of hydralazine with chromatin structure. The data for duplicate experiments and analysis done on days 1 and 2 are presented in Table 13.

The literature reports conflicting results on the response of

lymphocytes from normal volunteers and systemic lupus erythematosus (SLE) patients to mitogen stimulation. This experiment sought to study the effect of hydralazine on PHA stimulation of lymphocytes from a normal volunteer versus a patient with idiopathic SLE.

Peripheral lymphocytes were isolated from the blood of a normal donor and a SLE patient, stimulated with PHA and exposed to varying concentrations of hydralazine after 72 hours. Population kinetics were studied using FCM on day 1, 2, 3 and 4 (after 72 hours of PHA stimulation). Measurements were also done on day 5 (after 24 hours of hydralazine).

The percent cells in G_0 and G_1 populations, as measured by flow cytometry, for the control and SLE patients are essentially identical (Figures 29, 30). There is no significant effect in percent G_0 cells at the varying hydralazine dosages in control or SLE patients. There is an approximately 5% decrease in the percent G_1 cells at 5 mcg/ml suggesting that cells are slowed in progression through the cell cycle. At 40 mcg/ml there is a 7-15% increase in percent G_1 cells of both donor and SLE patients when compared to the hydralazine-free culture and this may reflect a freezing of cells in various stages of the cell cycle as they were before the hydralazine was added. It should be noted that the cultures were 5 days old at this time and approaching the maximum culture duration for lymphocytes without replacement of media. There is probably some slowing of the cell cycle and/or some cell death due to this fact at four days. This may explain how 40 mcg/ml can result in a greater percent G_1

population on day 5 than the 0 mcg/ml cultures.

The percent cells in S phase were also analyzed. There is about a 5% increase in the percent S phase cells of the lupus patient on day 4 (Figures 31, 32) before the addition of hydralazine. A dose-related effect of hydralazine can be seen on percent cells in S phase. At 5 mcg/ml there is an increase of about 5% in S phase populations of both the control donor and the lupus patient. This suggests a possible slowing of cells in the S phase and a tendency for cells to accumulate in S phase. At 40 mcg/ml there is a 5-10% decrease in S phase cells suggesting that cells may be halted at the point before addition of hydralazine.

Finally, percent cells in G_2M populations do not appear to differ between the two patients (Figures 33, 34). Data are summarized in Table 14.

A viability study using human peripheral lymphocytes was performed to assess the effects of hydralazine on the viability of non-cycling lymphocytes. Human peripheral lymphocytes were isolated, exposed to hydralazine for 24 hours, washed and recultured with PHA. Samples were taken at 24 hours and 96 hours to determine the effect of hydralazine exposure on non-cycling lymphocyte viability. Figure 35 shows that hydralazine has no effect on stationary (G_0) lymphocytes stimulated with PHA for 24 hours as assessed by trypan blue dye exclusion. After 96 hours of PHA stimulation the control culture had a viability of about 79% which decreased to 64% as the dosage of hydralazine increases from 0 to 80 mcg/ml. Table 15 contains the data

for Figure 35.

IV. Spontaneously hypertensive rats (SHR) experiments.

Lymphocyte experiments so far had been short-term exposure of hydralazine to human lymphocytes in vitro. This experiment sought to study the effect of long-term hydralazine exposure on lymphocytes of SHR in vivo. SHR were exposed to hydralazine for 12 weeks, killed, their lymphocytes isolated, stained with acridine orange and analyzed for green and red fluorescence using flow cytometry. This experiment sought to determine if hydralazine had any effect on lymphocyte DNA content, RNA content, and chromatin structure as measured by flow cytometry. The values for mean green fluorescence and mean red fluorescence versus log of hydralazine dosage is shown in Figure 36. The -2.5 log value corresponds to a dose of 0.003 mg/kg/day and the control is plotted at this value on the x-axis. The highest dose of 90 mg/kg/day corresponds to a value of +1.95 on the x-axis. There is no dose-effect relationship of hydralazine on the DNA and RNA content of these lymphocytes. This also suggests hydralazine is not competing with acridine orange for intercalating sites or for electrostatic binding to single strand nucleic acids. The peak green and peak red fluorescence of acridine orange stained lymphocytes yielded the same tentative conclusions as shown in Figure 36. A summary of data is presented in Table 16.

The experiment involving acid-induced denaturation of rat lymphocytes failed because the cell concentration in the fixative solution exceeded the recommended maximum of 10 x 10^6 cells per 10 ml

of fixative solution (70% ethanol/acetone) and cell clumping occurred making it impossible to disperse the cells for exposure to RNase A.

The male reproductive tract provides an almost ideal organ system to study the acute and chronic effects of a chemical on cellular proliferation and differentiation. This experiment was performed to determine the effect of hydralazine on testicular cell differentiation and sperm chromatin structure. Testes were removed from SHR, after 12 weeks of exposure to hydralazine, prepared for staining with acridine orange, and analyzed by flow cytometry.

Population kinetics were used to study the percent of testicular cells in various populations and subpopulations to determine if hydralazine had any dose-effect relationship on these populations. Figure 37A is an example of the raw data as it comes from the flow cytometer. Boxes 6 and 7 are subpopulations of the tetraploid cells which are 1° spermatocytes. Box 3 and 4 are two subpopulations of diploid cells which are 2° spermatocytes and in the lower left hand corner are the haploid cells which are spermatids. Figure 37B is an enhancement of the haploid spermatid population. It contains three subpopulations. Area 3 contains round spermatids that have histones associated with the DNA. Area 2 contains elongating spermatids that are undergoing a replacement of protamines for histones. Area 1 contains elongated spermatids which have protamines associated with their nuclear DNA.

A plot of percent cells in tetraploid subpopulation 1 and 2 and percent tetraploid cells of total cells versus log hydralazine

dosage is seen in Figure 38. The straight line for the percent tetraploids of total cells suggests there was no dose-effect relationship. The symmetry of the lines depicting tetraploid subpopulations 1 and 2 reflects shifts in the positioning of the rectilinear box used to separate the two populations and translates to two straight lines. A plot of percent cells in diploid subpopulation 1 and 2 and percent diploid cells of total versus log hydralazine dosage also reveals no dose-effect relationship (Figure 39). Finally, a plot of percent round, elongating, elongated, and total percent haploids versus log hydralazine dosage again reveals no dose-effect response (Figure 40).

The testes that were frozen were used to perform counts of sonication resistant sperm heads (elongated spermatids) per gram of testicular tissue to determine if hydralazine may have had any effect on the actual number of cells going through the maturation process. Figure 41 shows a plot of sperm head count (x 10^8) per gram of testis tissue. Again, there is no discernible dose-effect relationship. A summary of the data is presented in Table 17.

Caudal epididymal sperm allows analysis of the effect of hydralazine on mature spermatozoa. Mature sperm do not contain significant amounts of RNA, therefore the differential staining of sperm reflects predominantly a ratio of double- to single-strand DNA. This ratio can be expressed by the index α_t. Figure 42 shows a plot of the standard deviation of α_t versus log hydralazine dosage. The data suggests that hydralazine had no dose-effect relationship on the ratio

of double- to single-strand DNA in mature spermatozoa, in other words, no effect on the susceptibility of DNA to acid-induced denaturation. A summary of the data appears in Table 18. There was no effect on the body or testis weight of the SHR (Figure 43, Table 19).

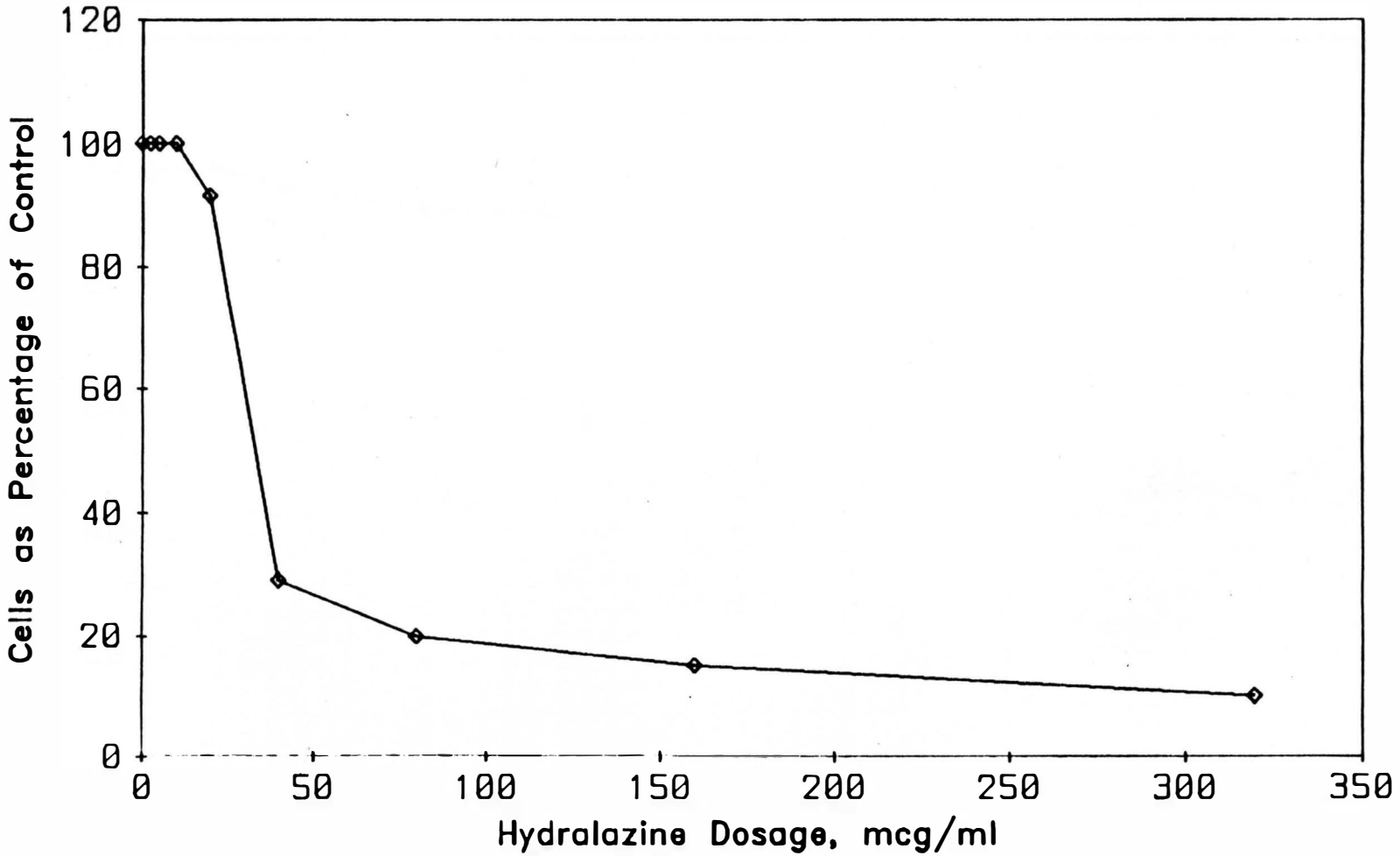

FIGURE 10. FRIEND LEUKEMIA CELL GROWTH VERSUS HYDRALAZINE DOSAGE.

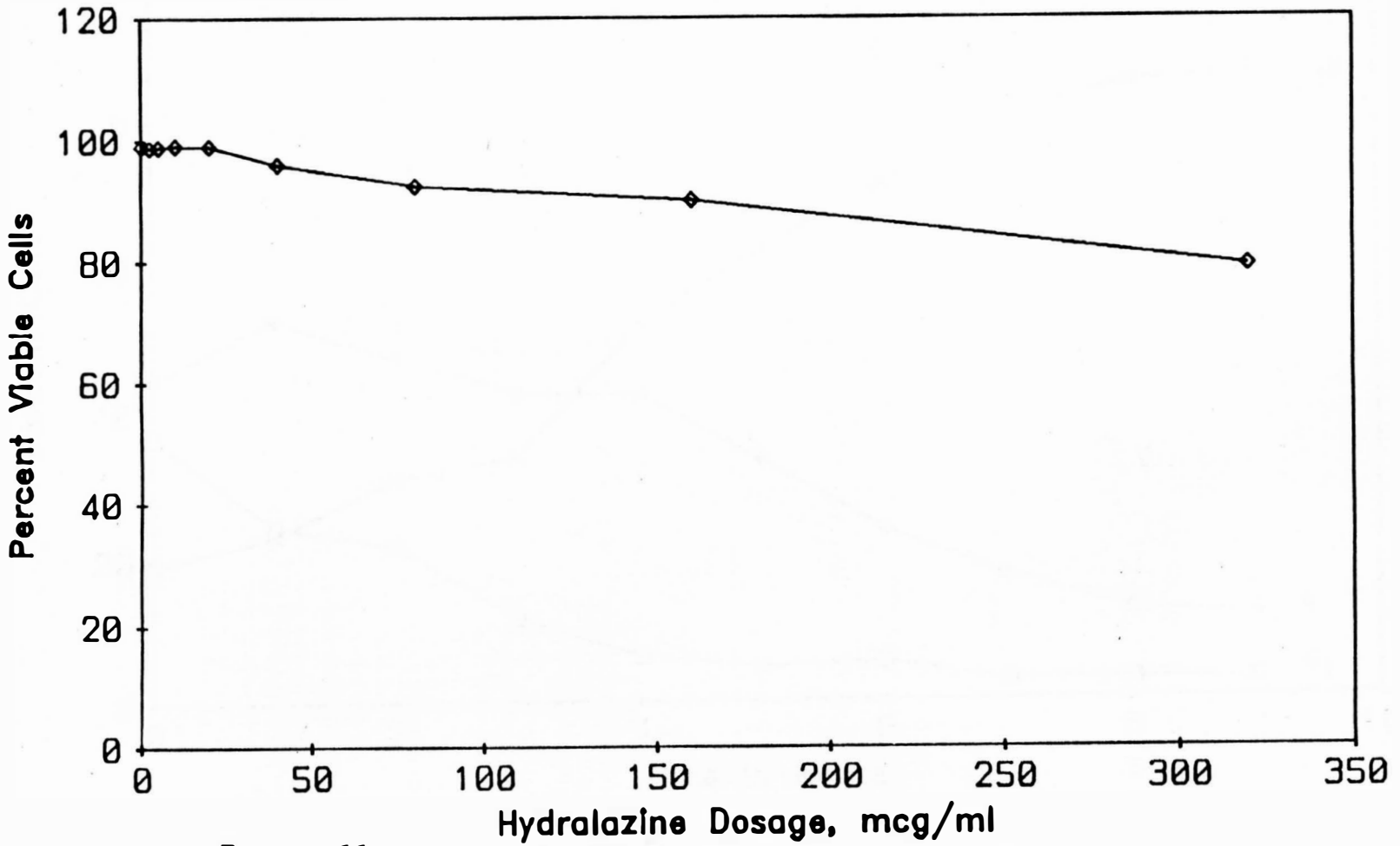

FIGURE 11. FRIEND LEUKEMIA CELL VIABILITY VERSUS HYDRALAZINE DOSAGE AFTER 20 HOURS OF EXPOSURE.

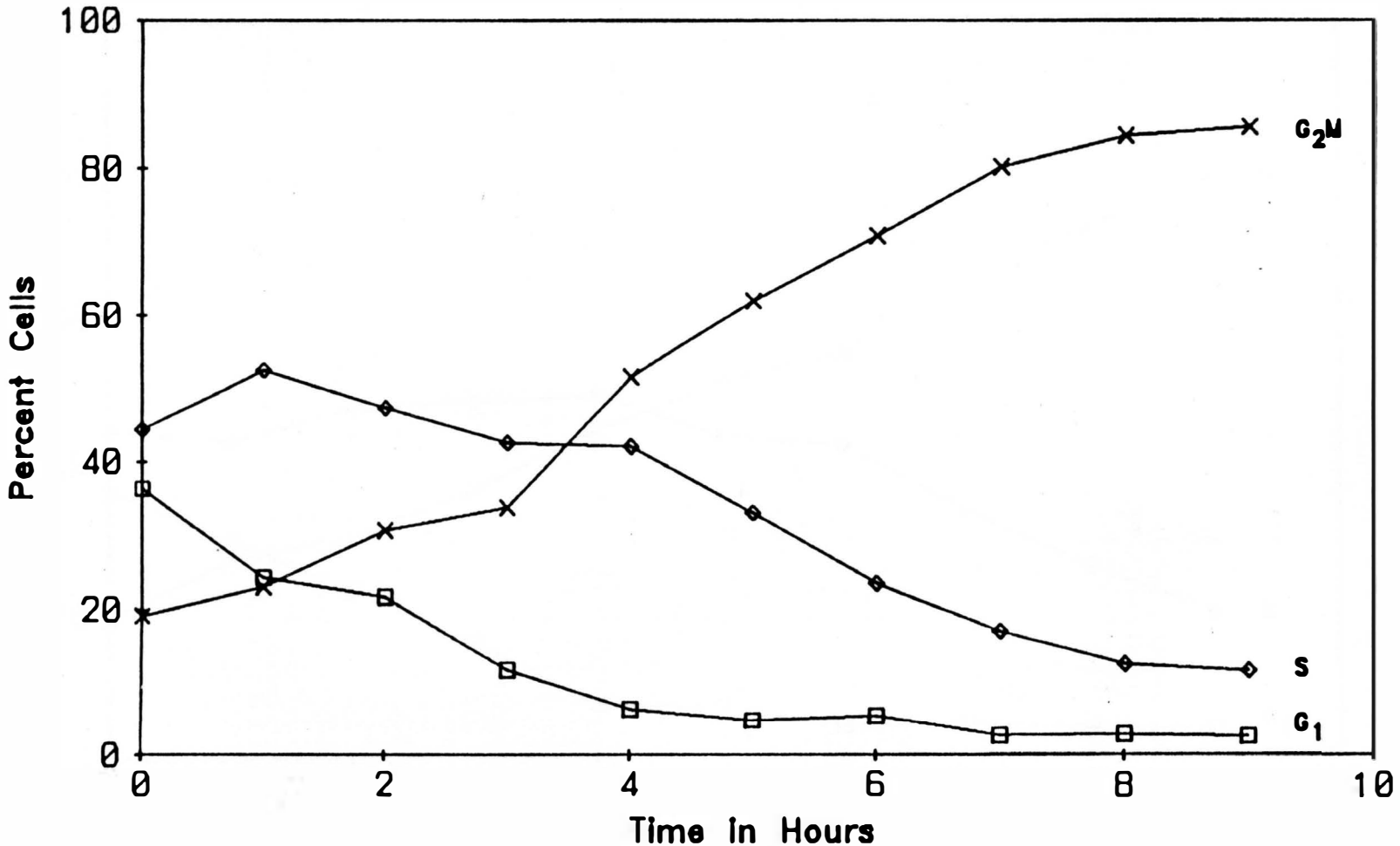

FIGURE 12. POPULATION KINETICS OF FRIEND LEUKEMIA CELLS AFTER VINBLASTINE BLOCK VERSUS TIME. CONTROL CULTURE.

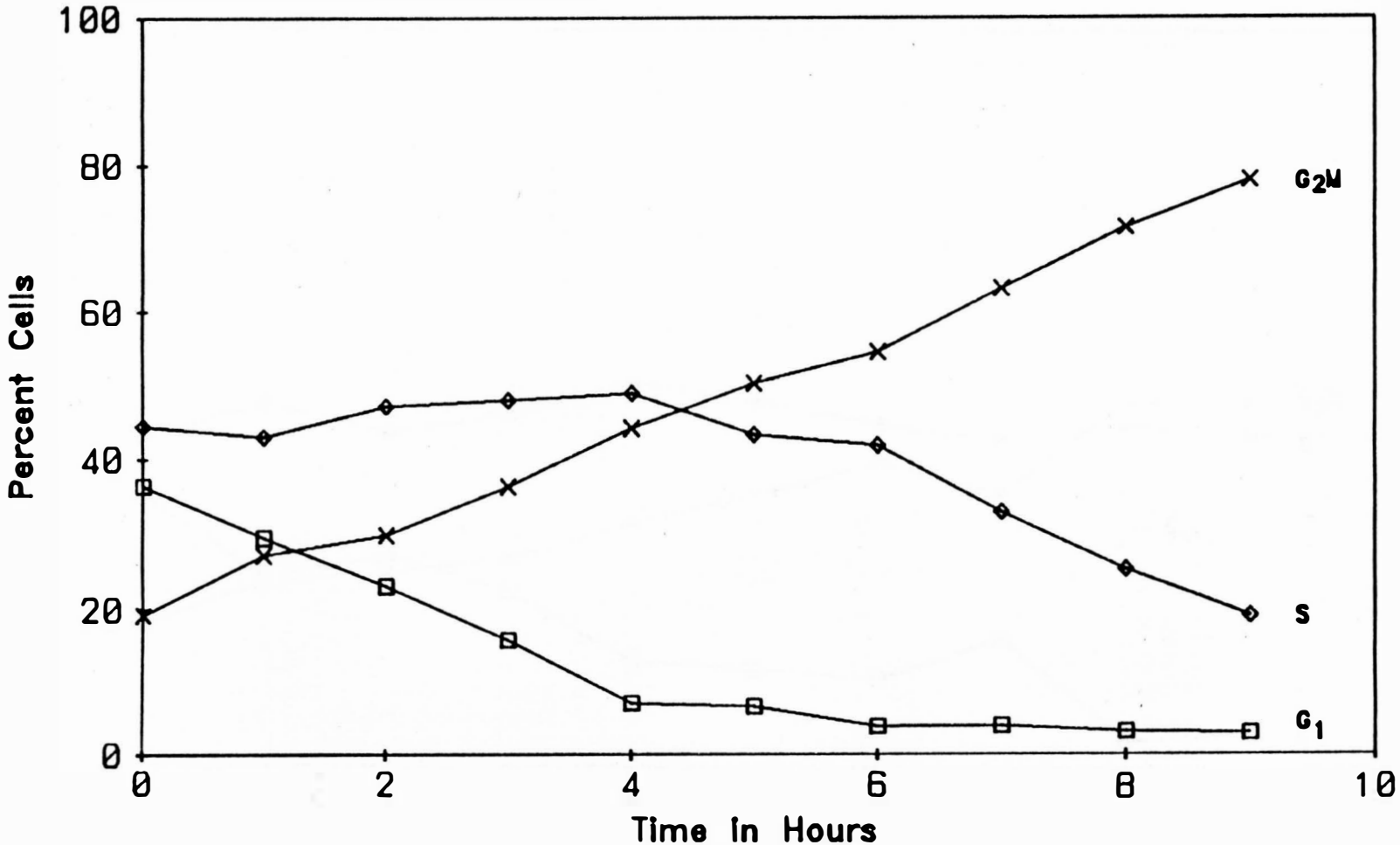

FIGURE 13. POPULATION KINETICS OF FRIEND LEUKEMIA CELLS AFTER VINBLASTINE BLOCK VERSUS TIME. HYDRALAZINE AT 20 UG/ML ADDED 1 HOUR AFTER VINBLASTINE.

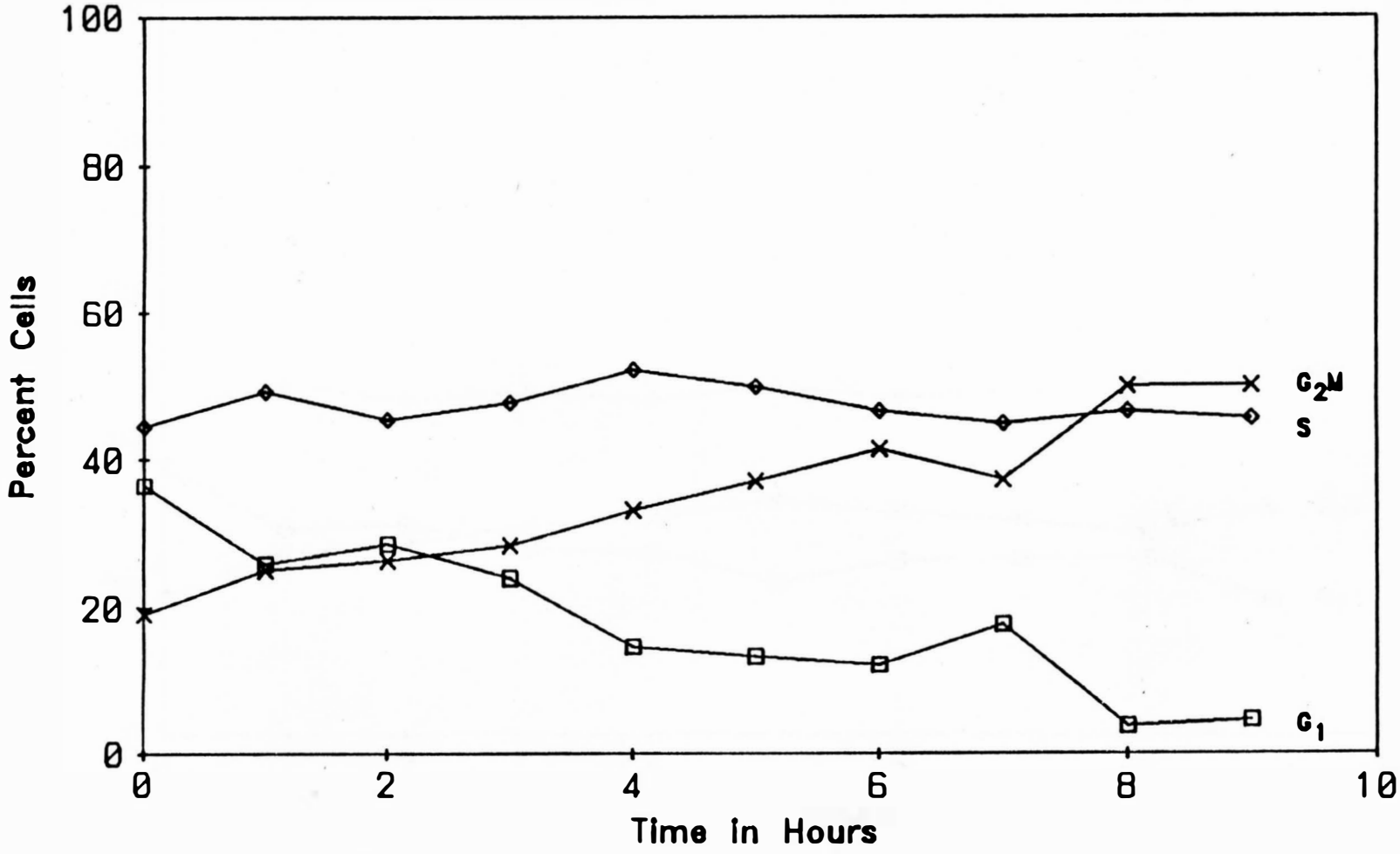

FIGURE 14. POPULATION KINETICS OF FRIEND LEUKEMIA CELLS AFTER VINBLASTINE BLOCK VERSUS TIME. HYDRALAZINE AT 40 UG/ML ADDED 1 HOUR AFTER VINBLASTINE.

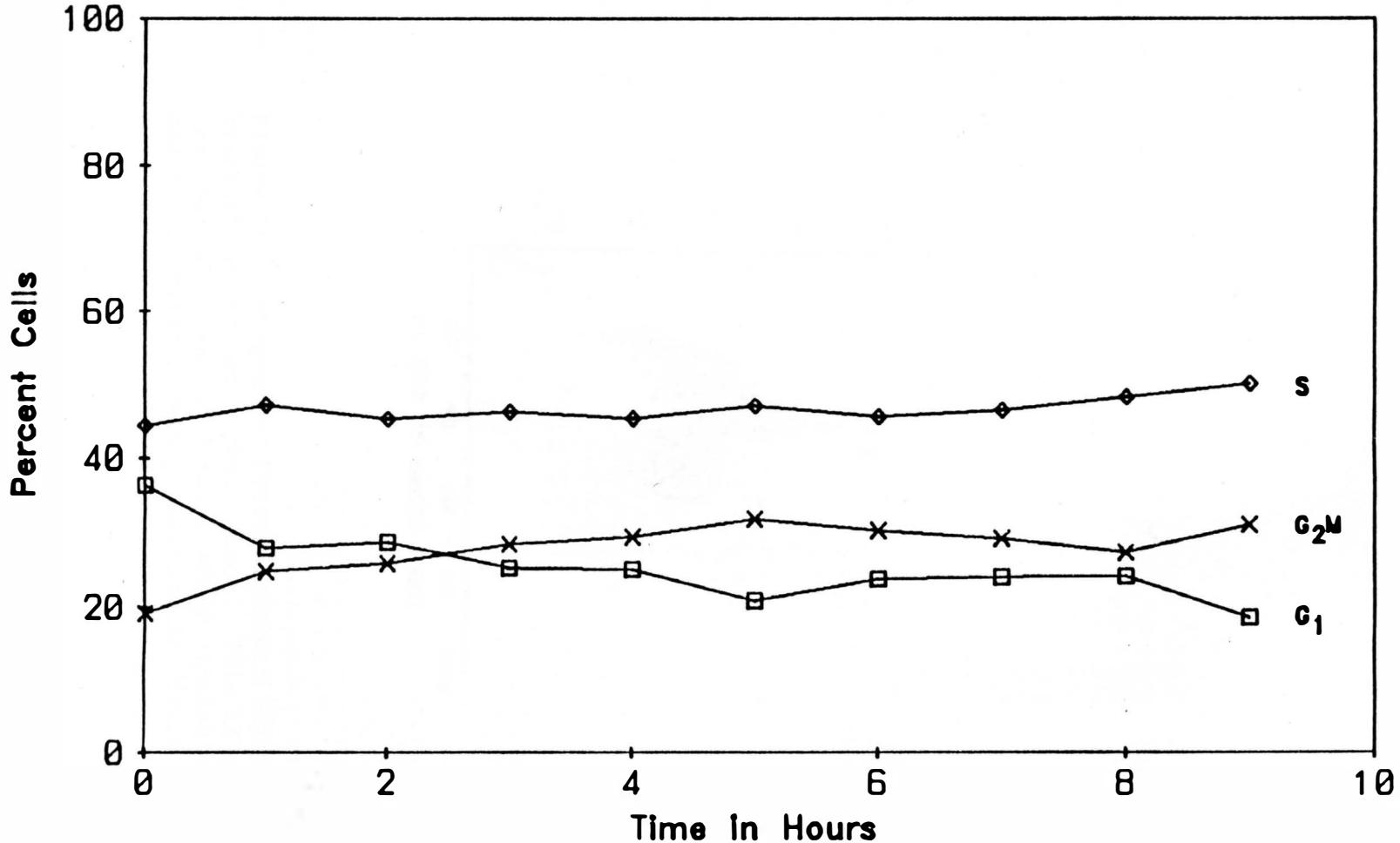

FIGURE 15. POPULATION KINETICS OF FRIEND LEUKEMIA CELLS AFTER VINBLASTINE BLOCK VERSUS TIME. HYDRALAZINE AT 80 UG/ML ADDED 1 HOUR AFTER VINBLASTINE.

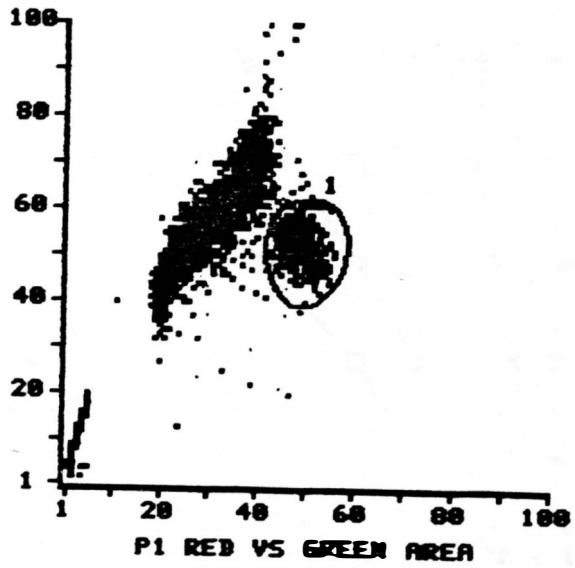

Figure 16. Cytogram of Friend leukemia cells after vinblastine-induced M phase block. This is a control culture measured 3 hours after vinblastine addition. Mitotic cell population in Circle 1.

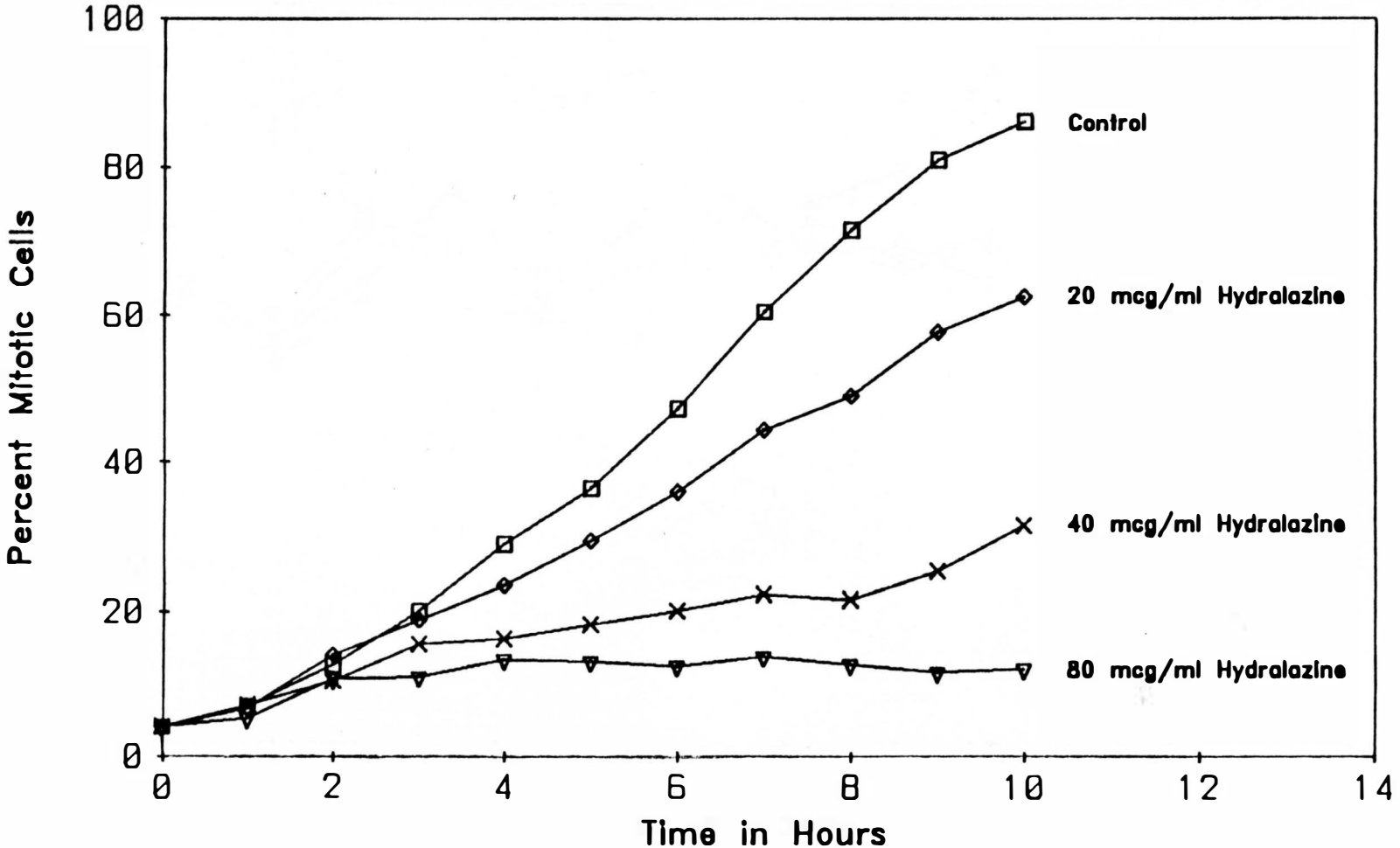

FIGURE 17. PERCENT MITOTIC FRIEND LEUKEMIA CELLS VERSUS TIME AFTER VINBLASTINE BLOCK.

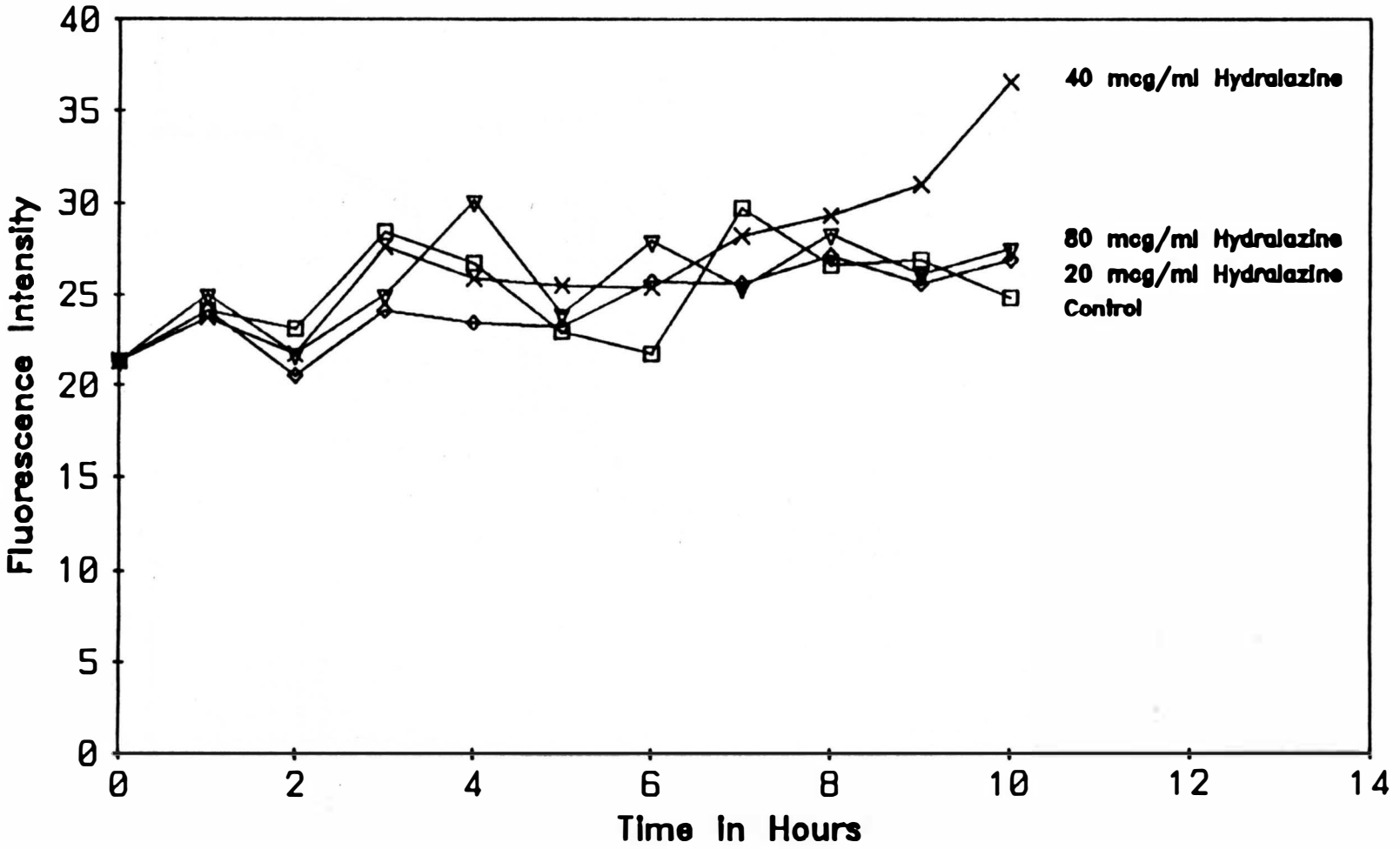

FIGURE 18. STANDARD DEVIATION OF THE MITOTIC POPULATION VERSUS TIME AFTER THE ADDITION OF VINBLASTINE. DATA INCLUDED FOR THE 0, 20, 40 AND 80 UG/ML HYDRALAZINE CULTURES.

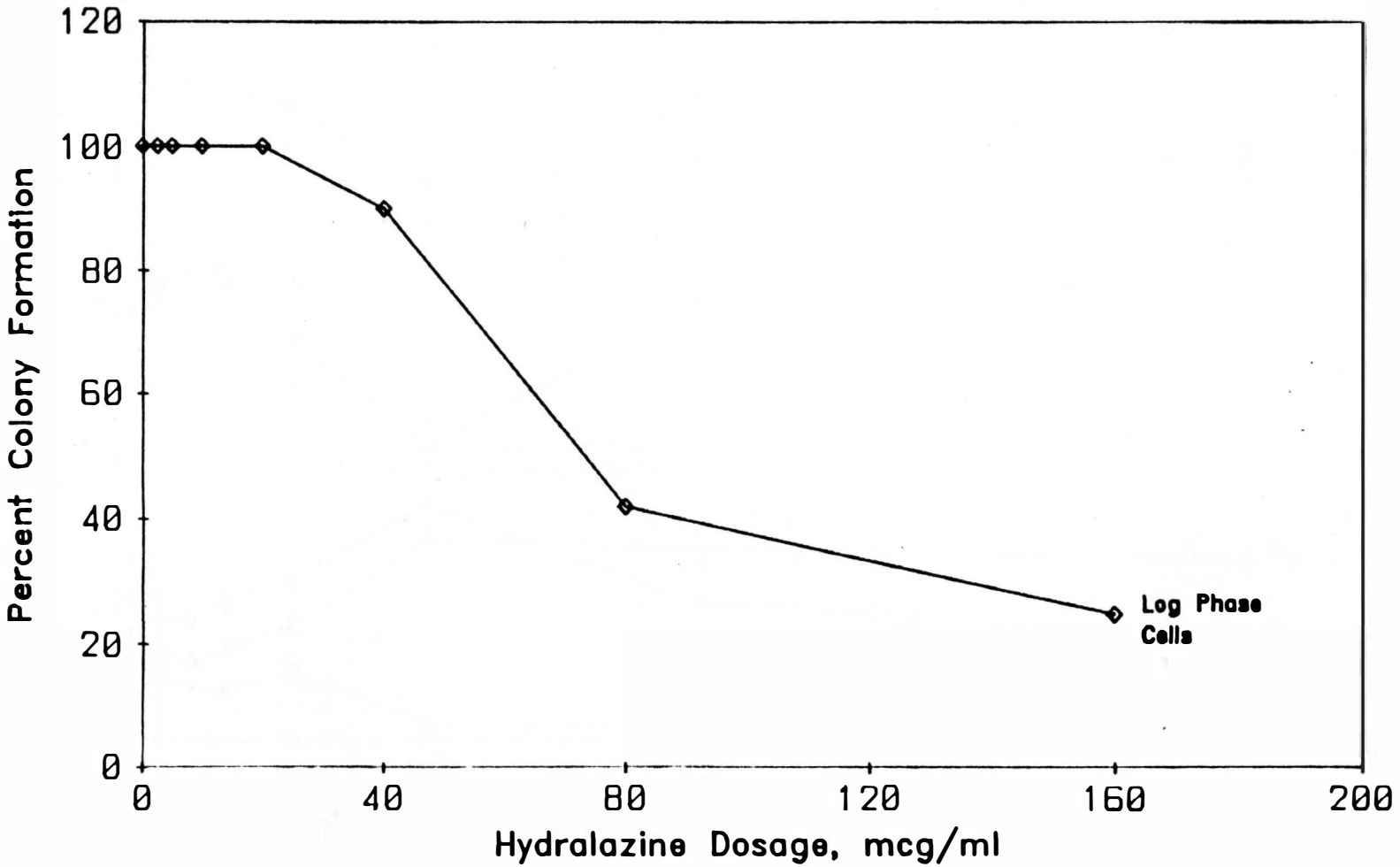

FIGURE 19. PERCENT SURVIVABILITY OF LOG PHASE CHINESE HAMSTER OVARY CELLS (AS ASSESSED BY COLONY FORMATION RELATIVE TO CONTROL) AFTER 20 HOUR EXPOSURE TO HYDRALAZINE.

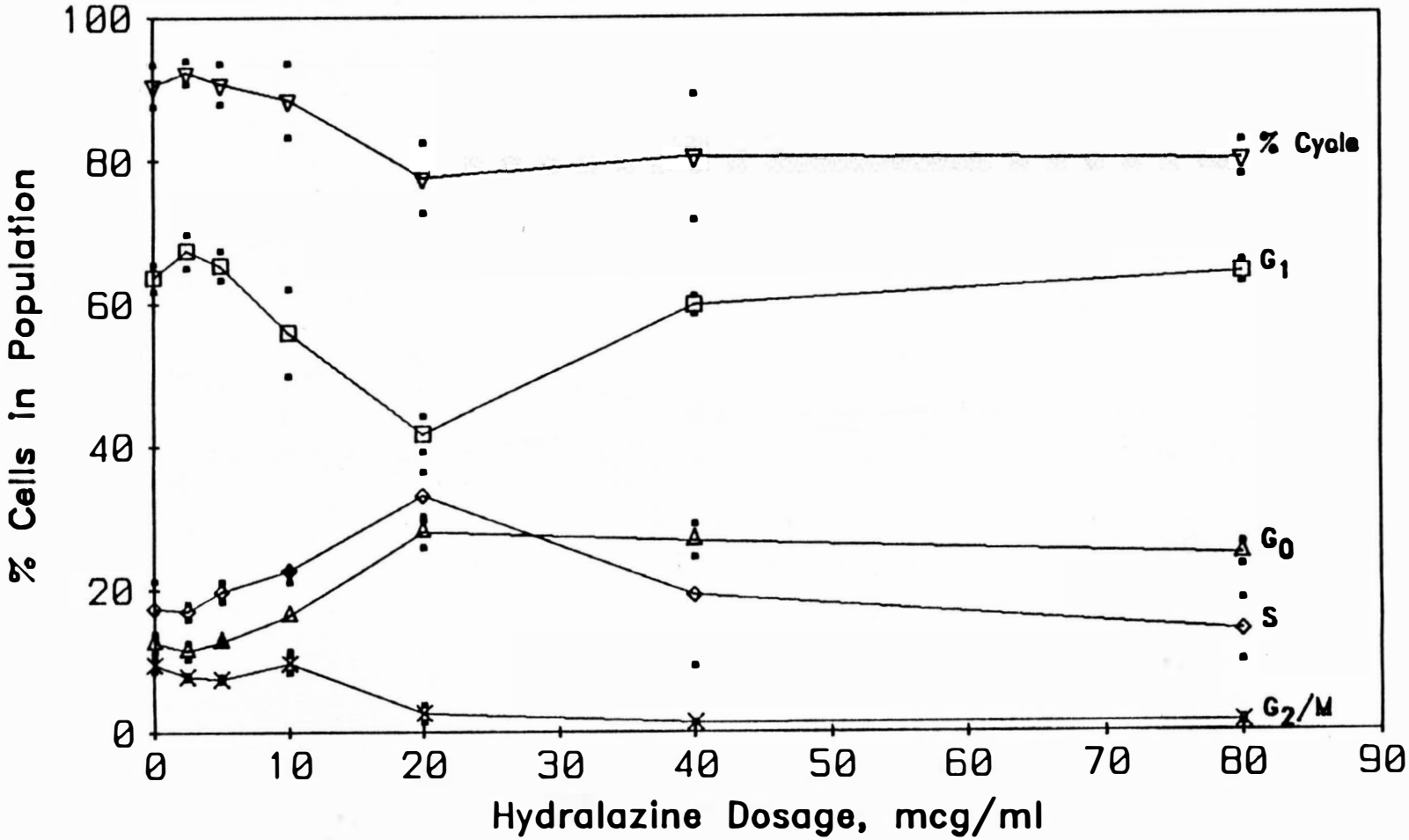

FIGURE 20. PERCENT CELLS IN G_0, G_1, S, G_2M AND CYCLING CELLS VERSUS DOSAGE OF HYDRALAZINE IN PHA-STIMULATED LYMPHOCYTES (72 HOURS) AFTER 24 HOURS HYDRALAZINE EXPOSURE.

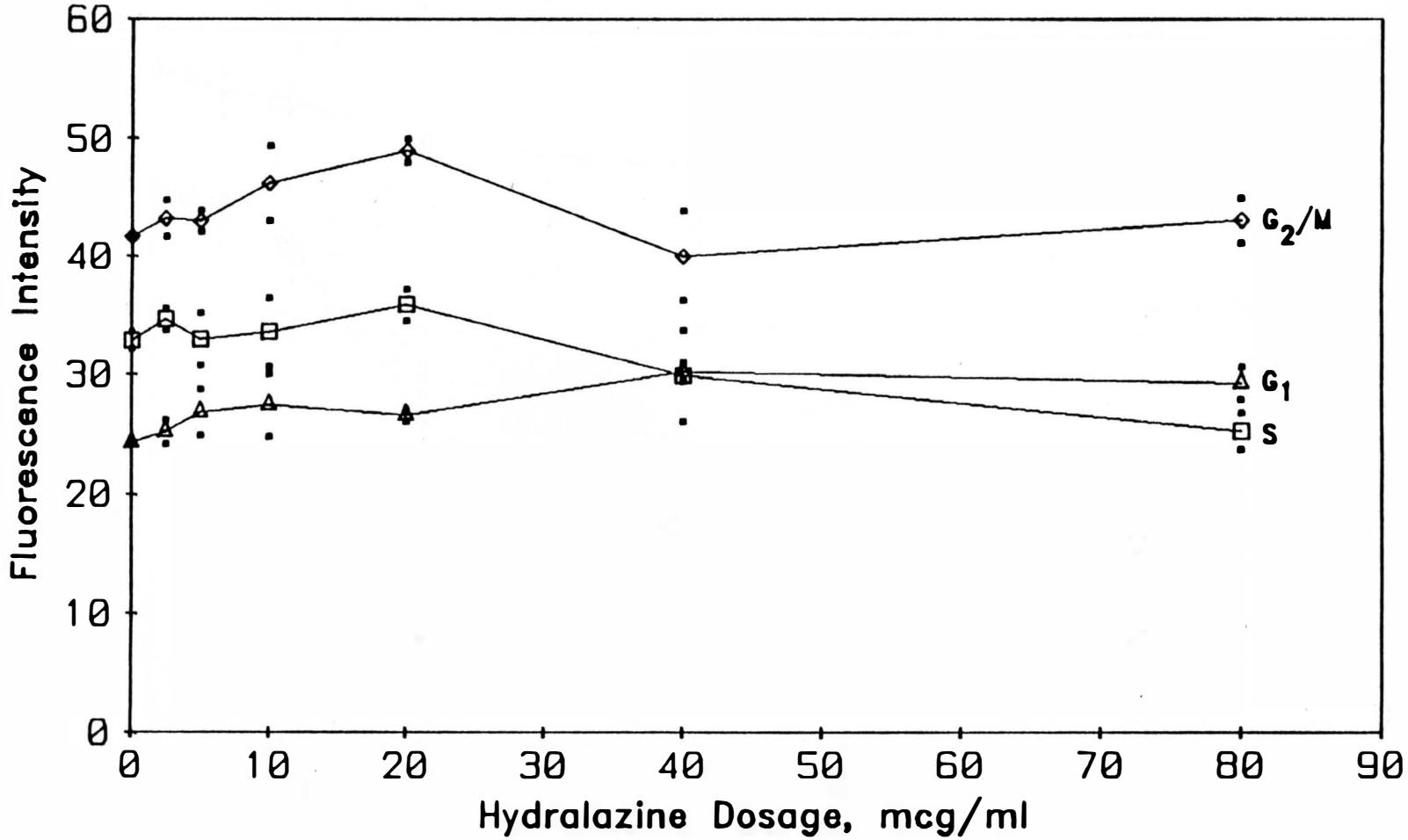

FIGURE 21. RED FLUORESCENCE IN G_1, S AND G_2M VERSUS DOSAGE OF HYDRALAZINE OF LOG PHASE LYMPHOCYTES EXPOSED TO HYDRALAZINE FOR 24 HOURS.

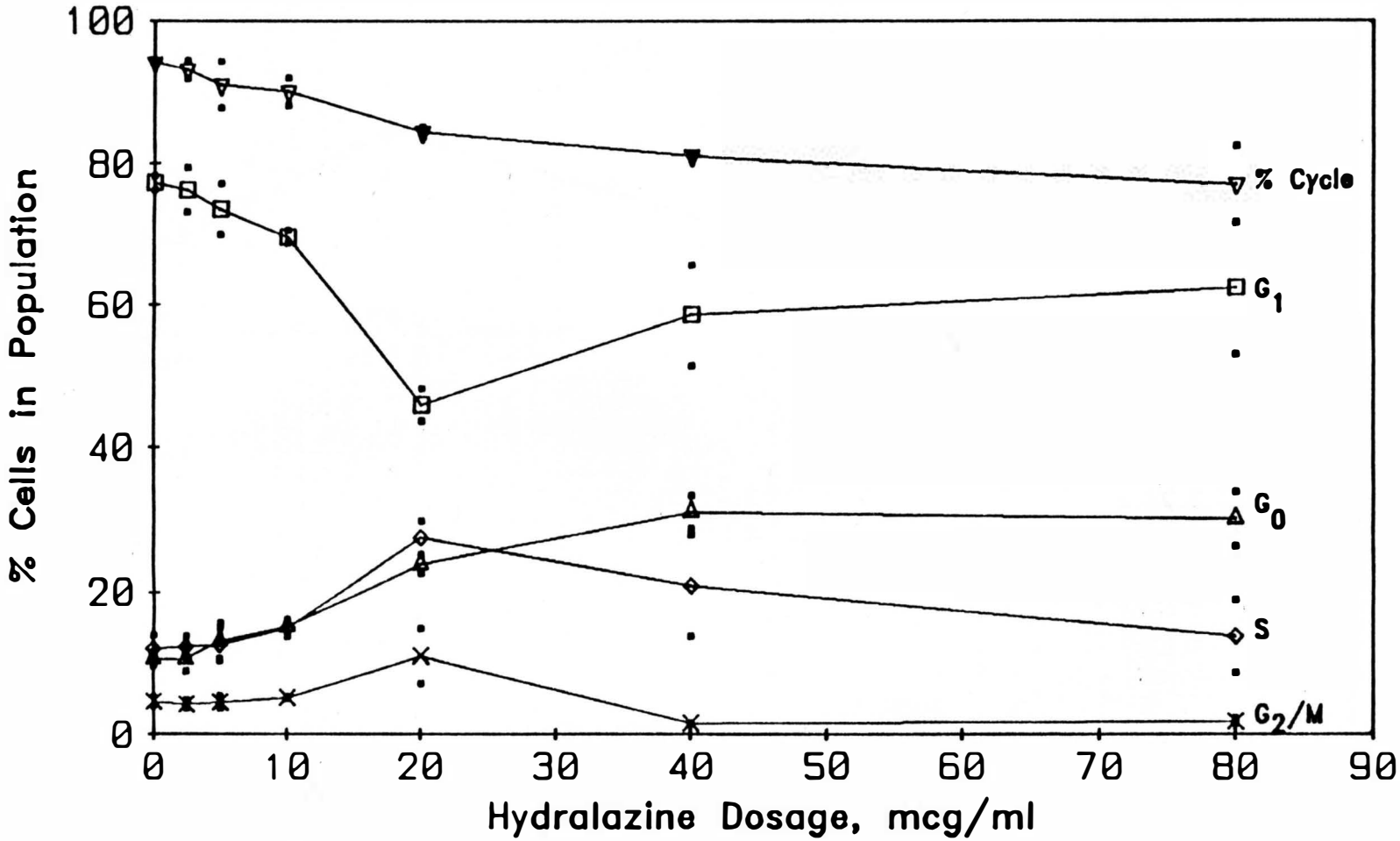

FIGURE 22. PERCENT CELLS IN G_0, G_1, S, G_2M AND CYCLING CELLS VERSUS DOSAGE OF HYDRALAZINE OF LOG PHASE LYMPHOCYTES EXPOSED TO HYDRALAZINE FOR 48 HOURS.

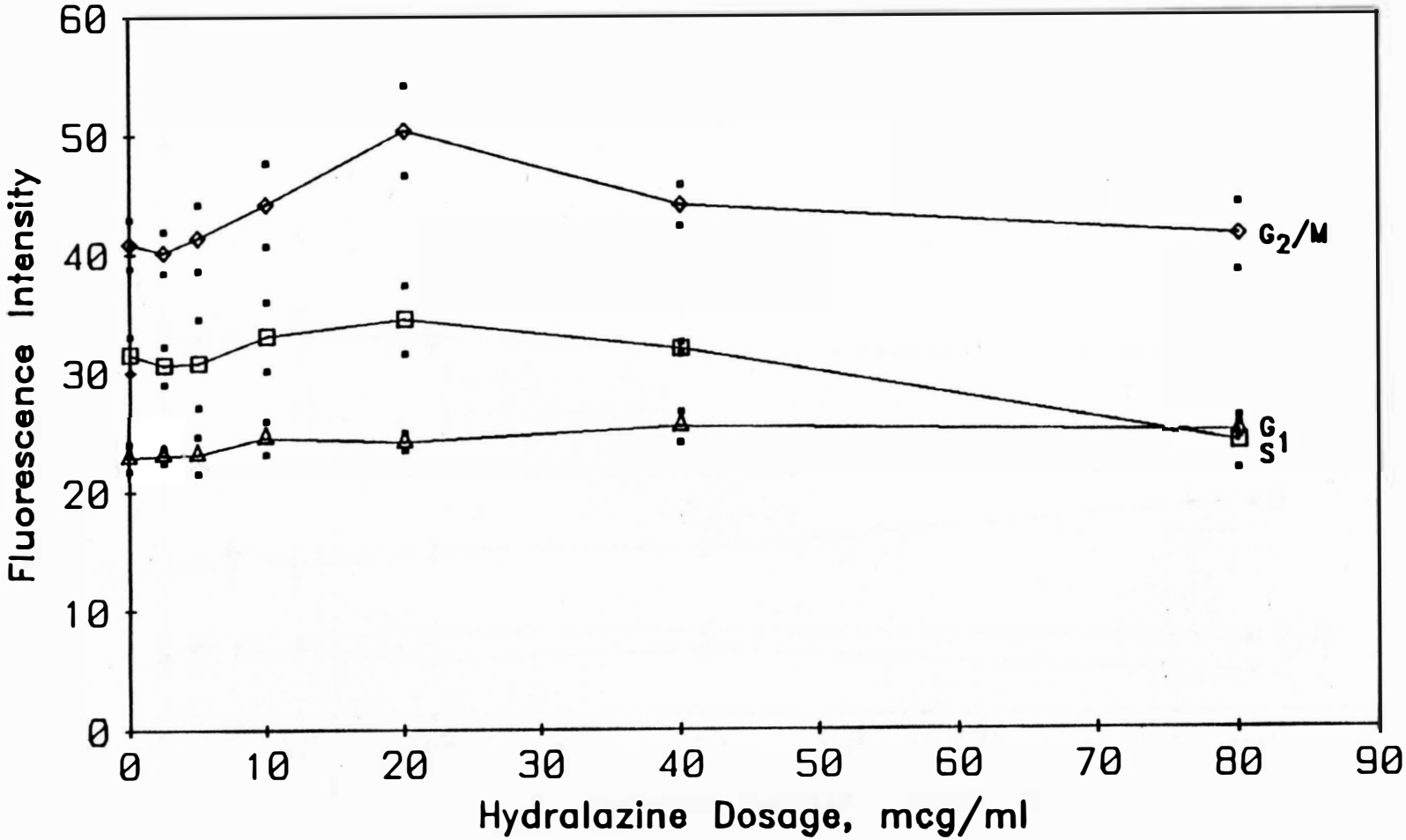

FIGURE 23. RED FLUORESCENCE IN G_1, S AND G_2M VERSUS DOSAGE OF HYDRALAZINE OF LOG PHASE LYMPHOCYTES EXPOSED TO HYDRALAZINE FOR 48 HOURS.

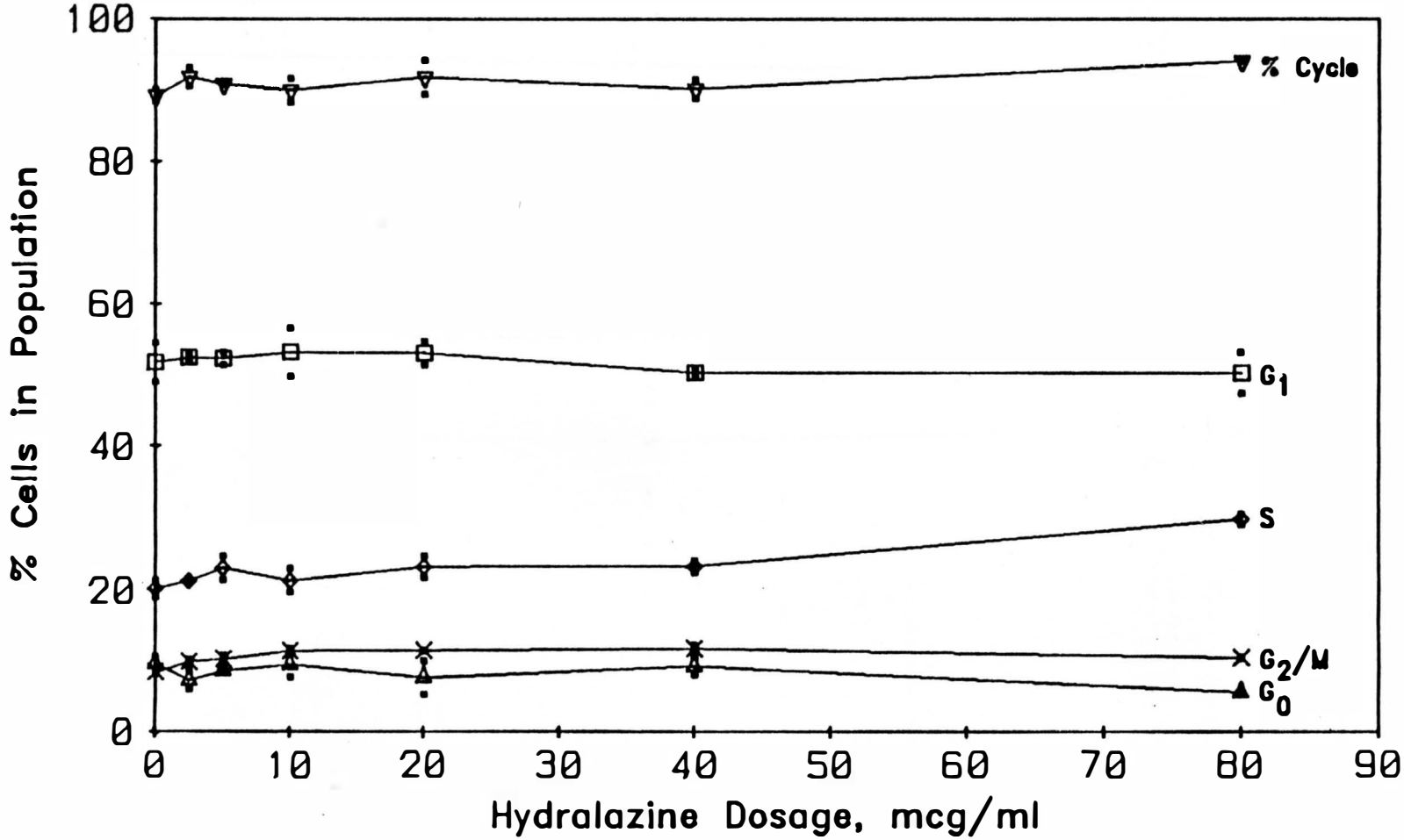

FIGURE 24. PERCENT CELLS IN G_0, G_1, S, G_2M AND CYCLING CELLS VERSUS DOSAGE OF HYDRALAZINE OF STATIONARY (G_0) LYMPHOCYTES EXPOSED TO HYDRALAZINE AND THEN PHA-STIMULATED.

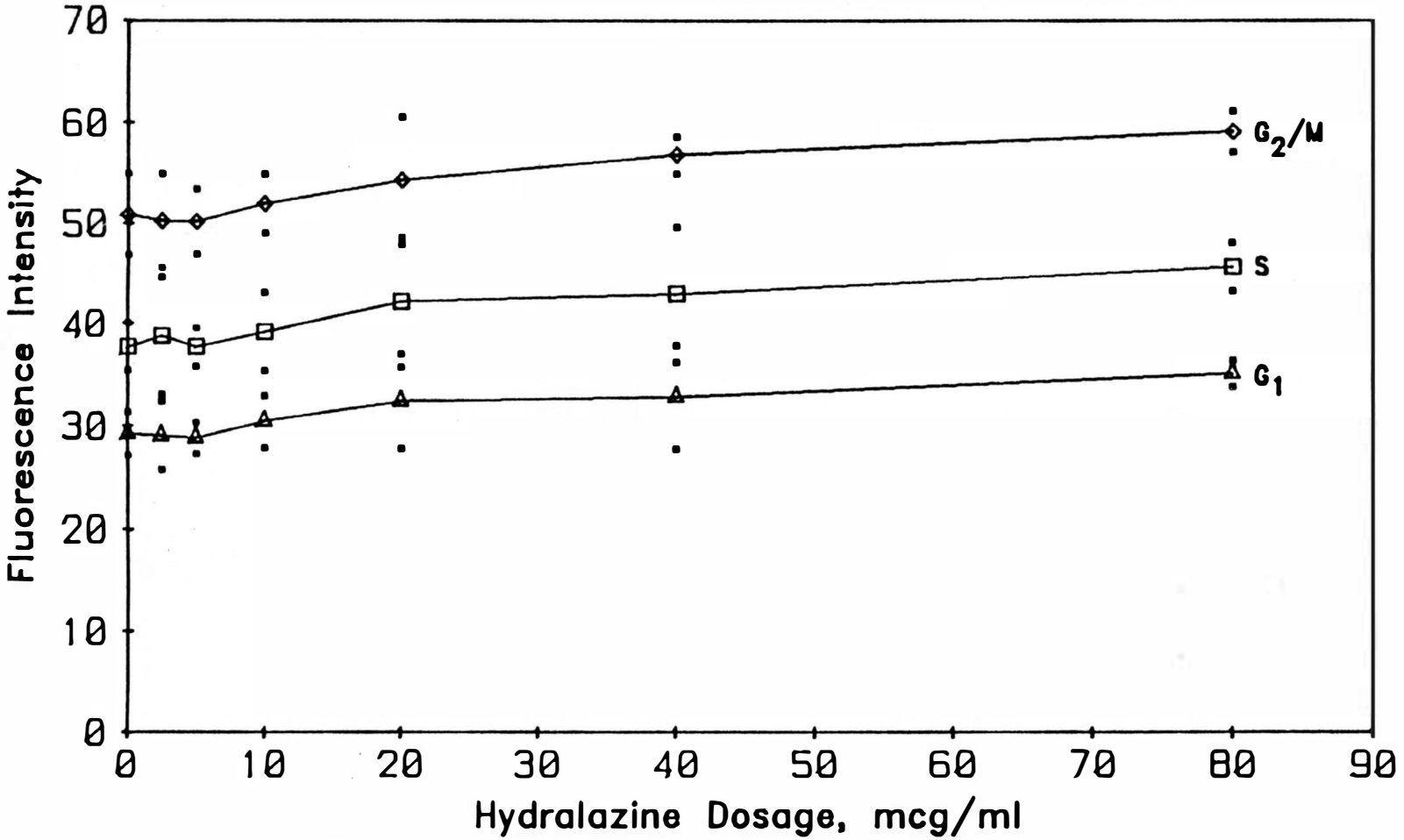

FIGURE 25. RED FLUORESCENCE IN G_1, S AND G_2M VERSUS DOSAGE OF HYDRALAZINE OF STATIONARY (G_0) LYMPHOCYTES EXPOSED TO HYDRALAZINE AND THEN PHA-STIMULATED.

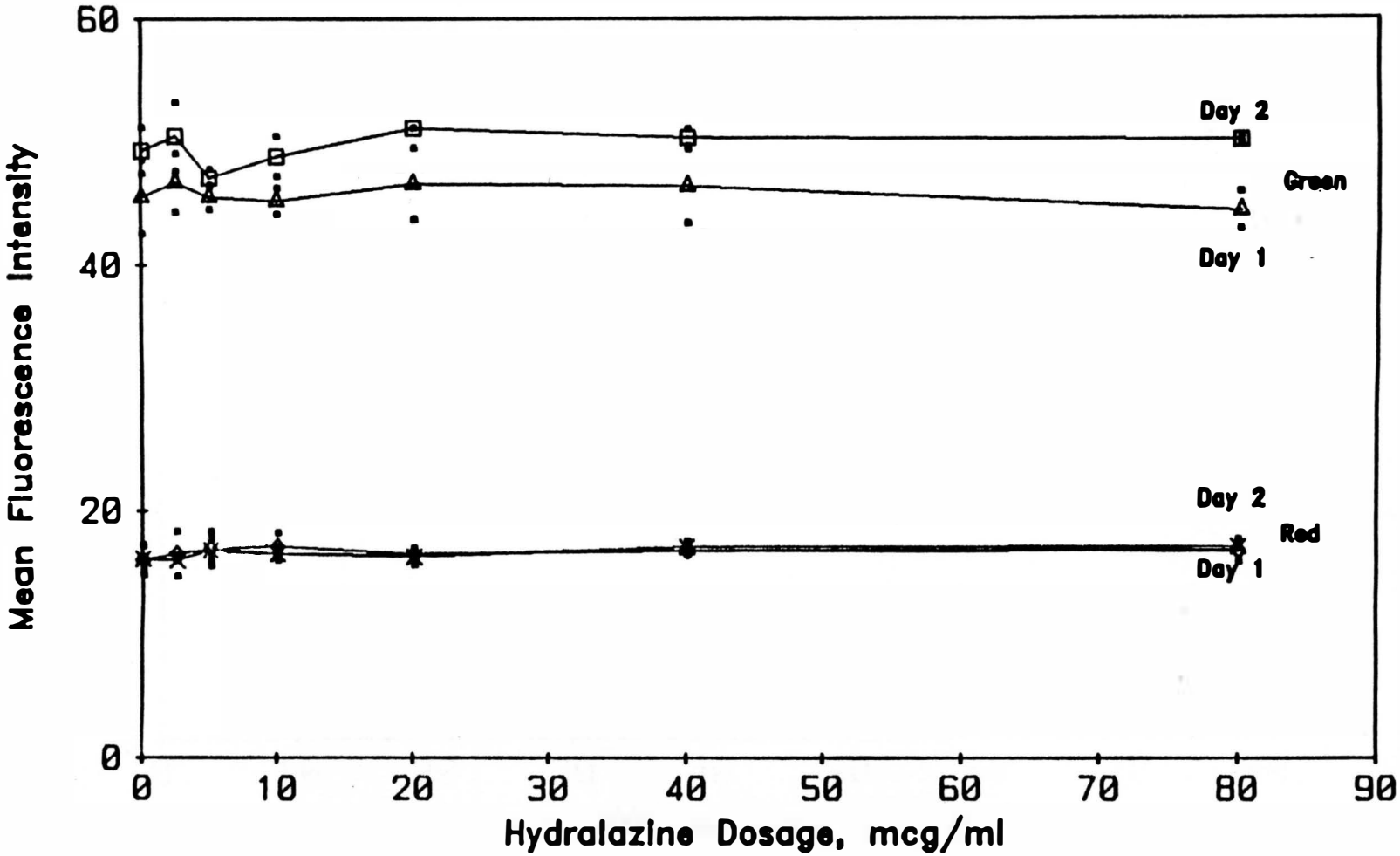

FIGURE 26. RED AND GREEN FLUORESCENCE OF ACID-DENATURED HUMAN LYMPHOCYTES VERSUS DOSAGE OF HYDRALAZINE.

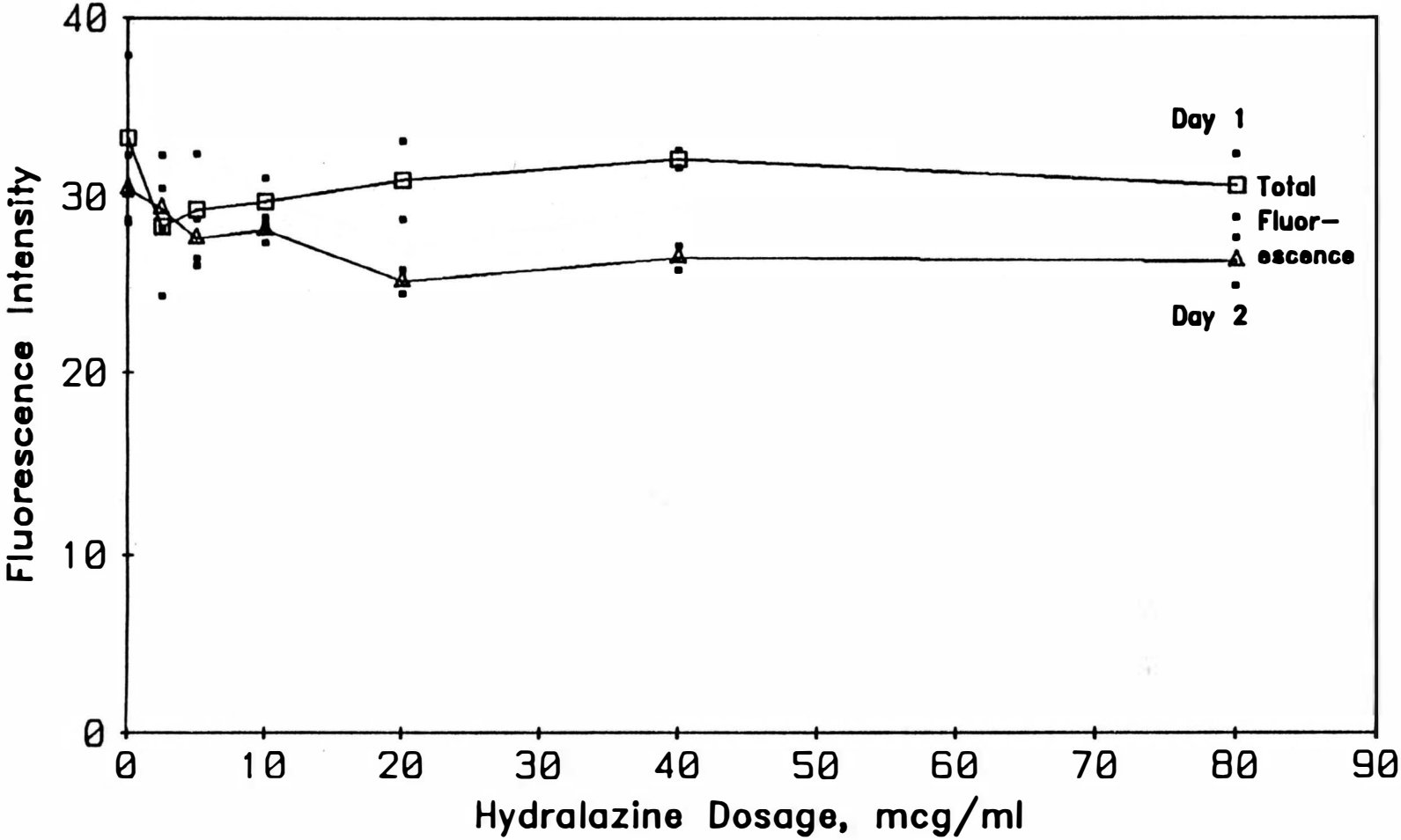

FIGURE 27. STANDARD DEVIATION OF TOTAL FLUORESCENCE VERSUS DOSAGE OF HYDRALAZINE OF ACID-DENATURED HUMAN LYMPHOCYTES.

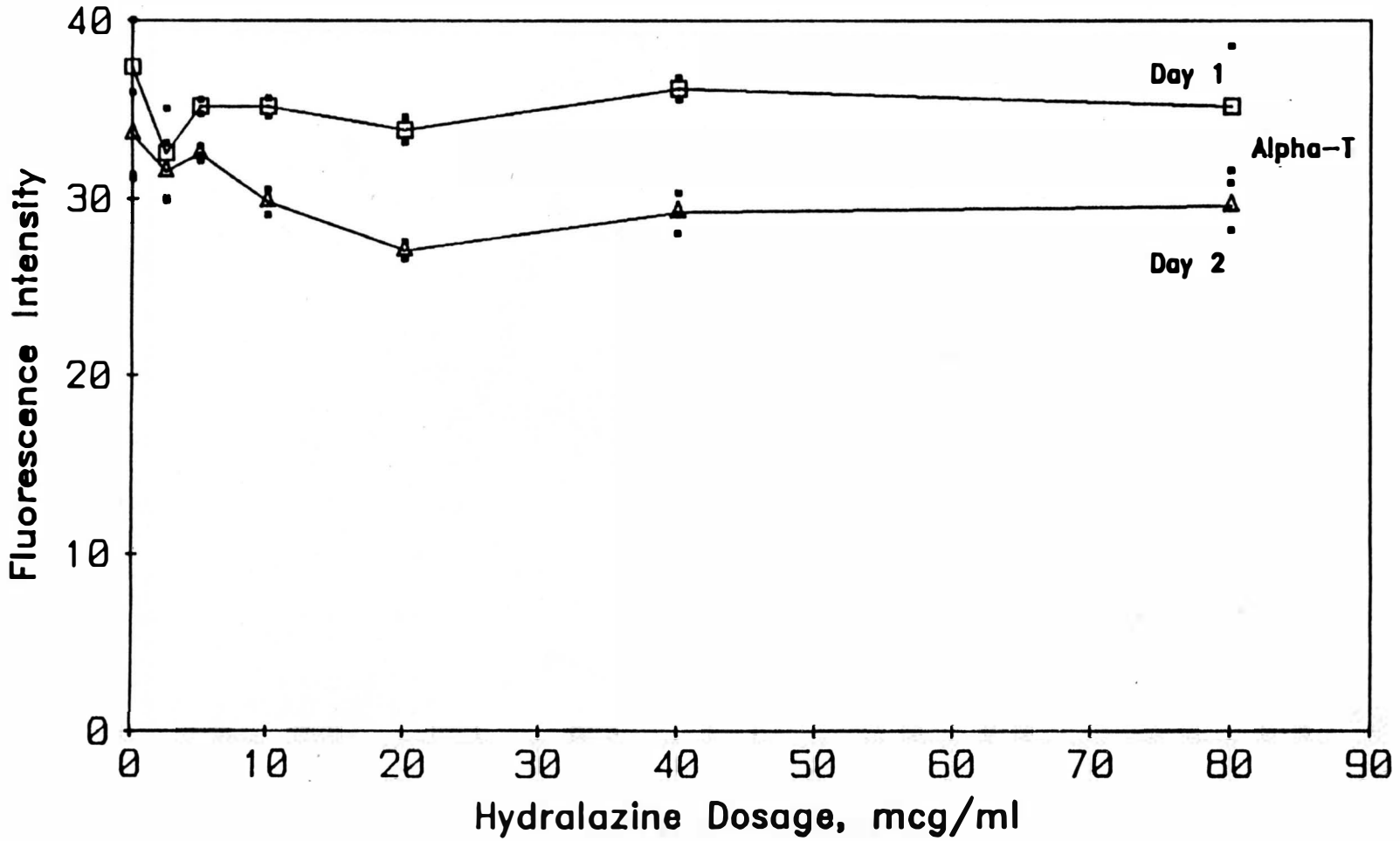

FIGURE 28. STANDARD DEVIATION OF ALPHA-T VERSUS DOSAGE OF HYDRALAZINE OF ACID-DENATURED HUMAN LYMPHOCYTES.

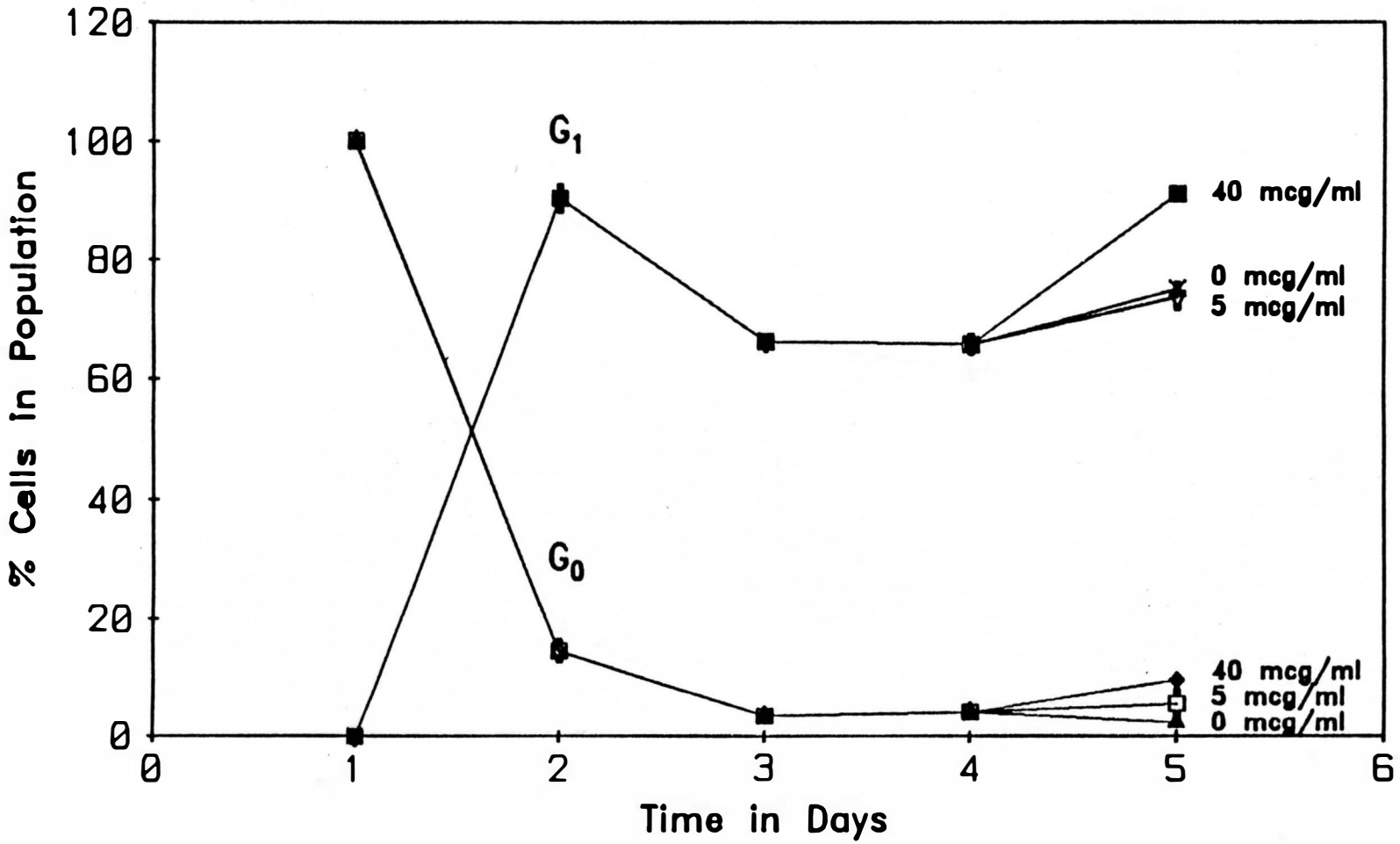

FIGURE 29. PERCENT CELLS IN G_0 AND G_1 VERSUS CULTURE TIME, CONTROL PATIENT. HYDRALAZINE ADDED AFTER DAY 4 MEASUREMENTS TAKEN.

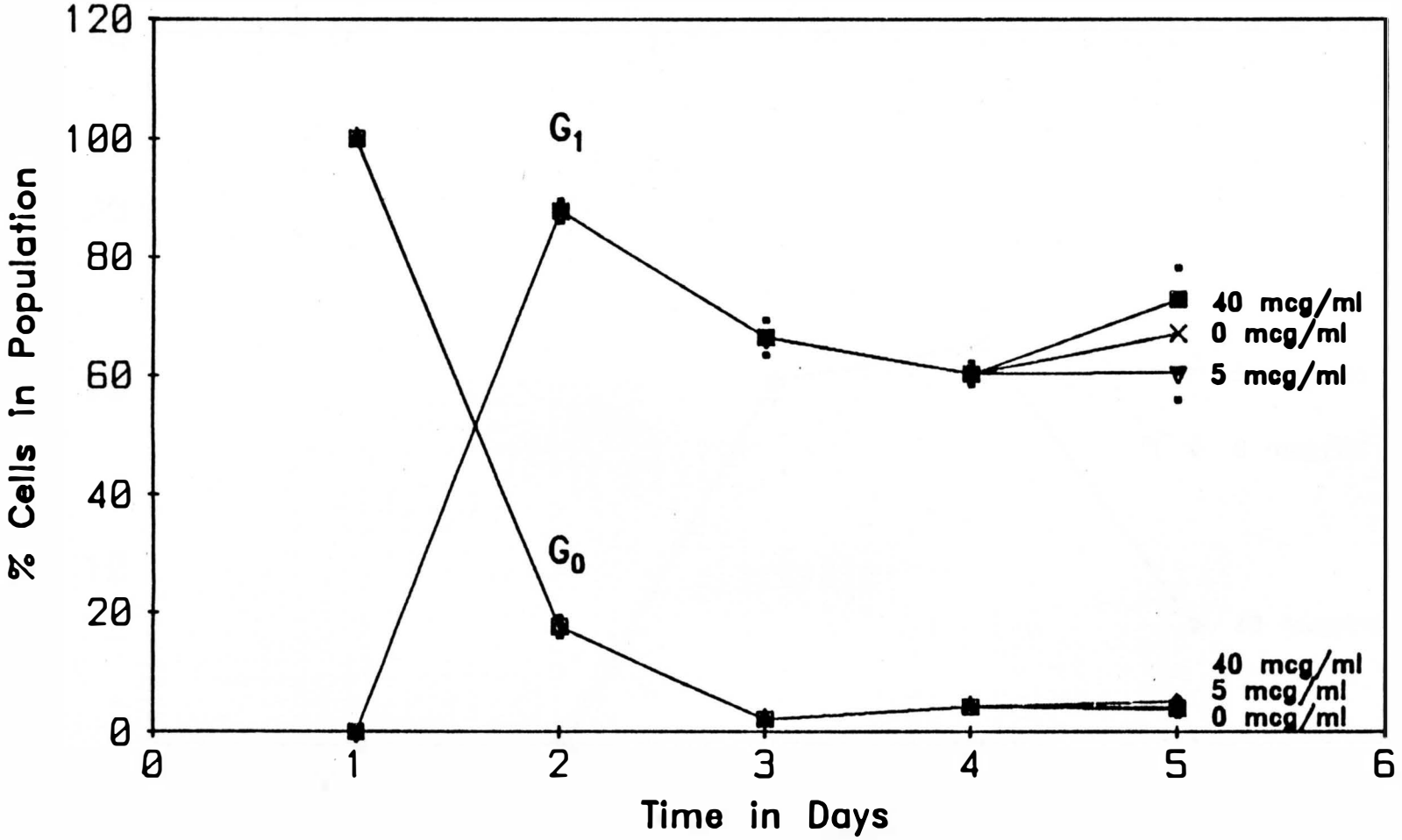

FIGURE 30. PERCENT CELLS IN G_0 AND G_1 VERSUS CULTURE TIME, LUPUS (SLE) PATIENT. HYDRALAZINE ADDED AFTER DAY 4 MEASUREMENTS TAKEN.

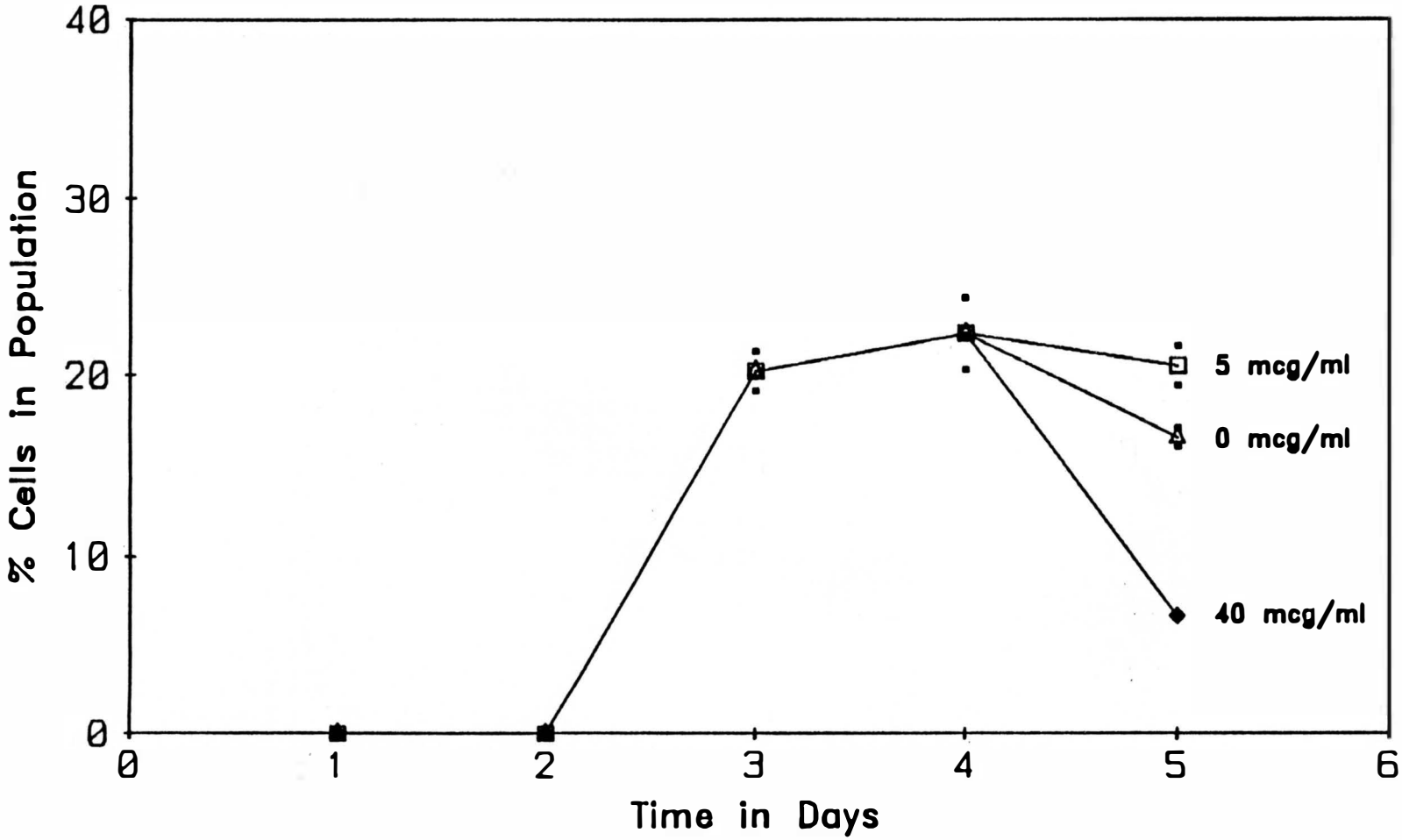

FIGURE 31. PERCENT CELLS IN S VERSUS CULTURE TIME, CONTROL PATIENT. HYDRALAZINE ADDED AFTER DAY 4 MEASUREMENTS TAKEN.

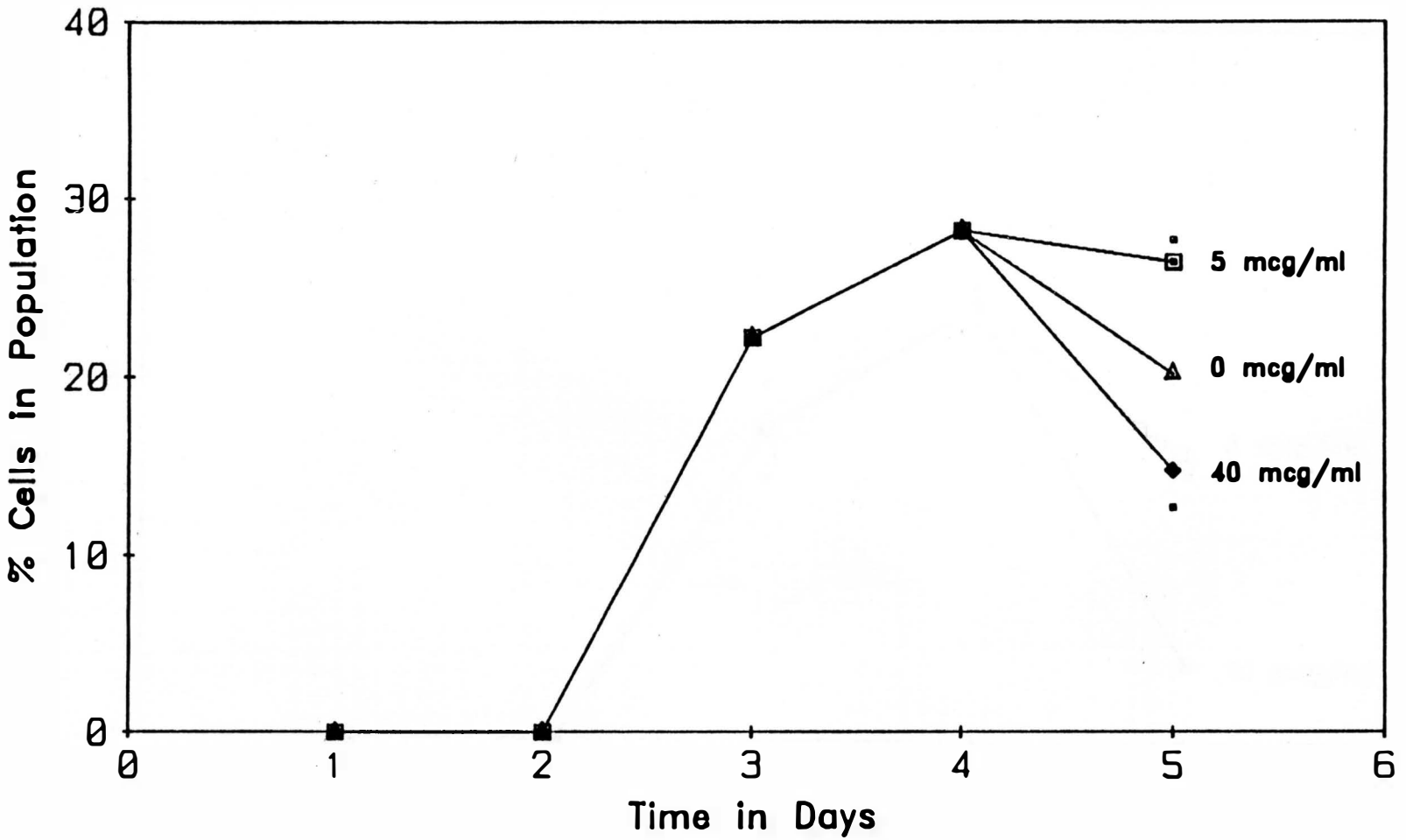

FIGURE 32. PERCENT CELLS IN S VERSUS CULTURE TIME, LUPUS (SLE) PATIENT. HYDRALAZINE ADDED AFTER DAY 4 MEASUREMENTS TAKEN.

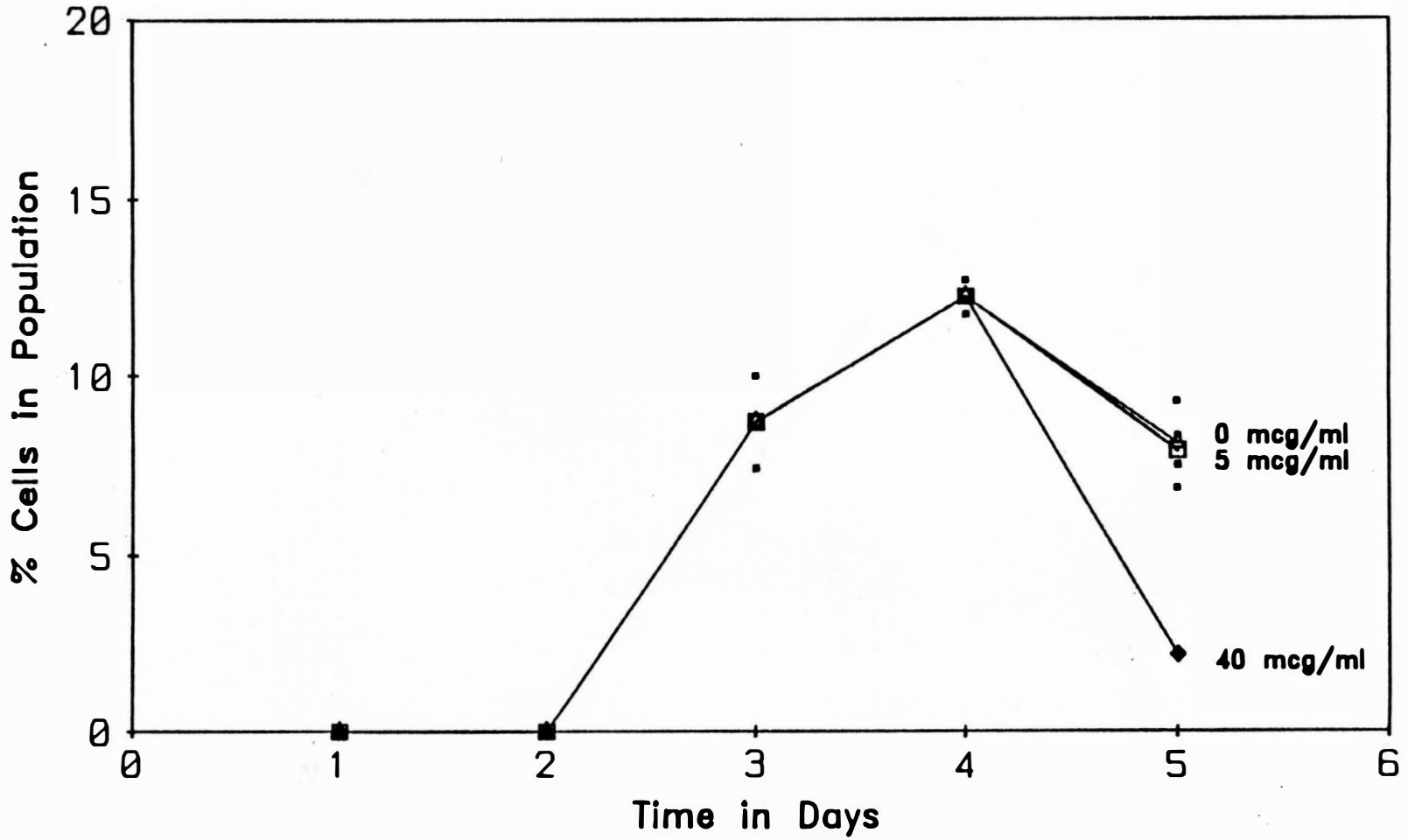

FIGURE 33. PERCENT CELLS IN G_2M VERSUS CULTURE TIME, CONTROL PATIENT. HYDRALAZINE ADDED AFTER DAY 4 MEASUREMENTS TAKEN.

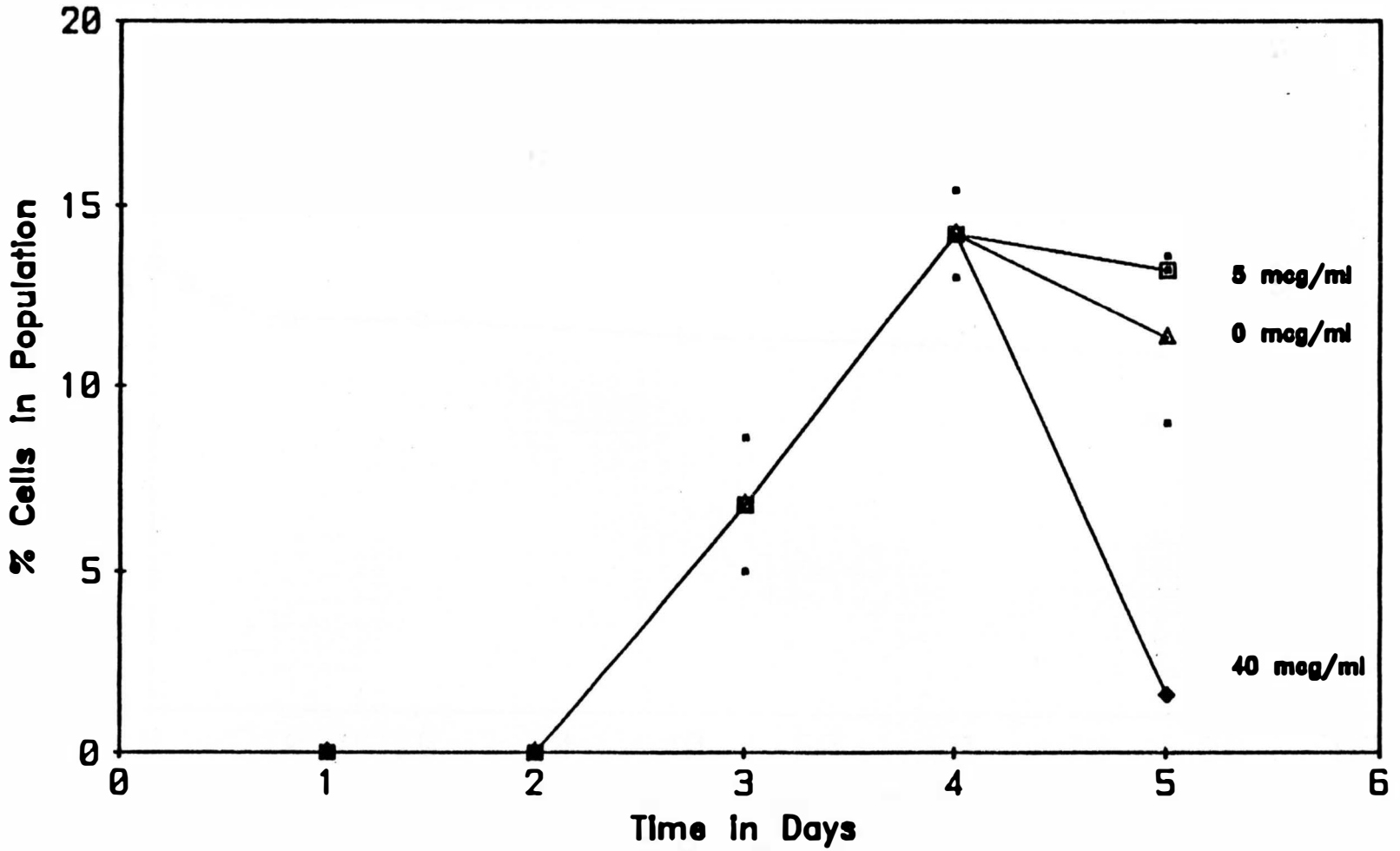

FIGURE 34. PERCENT CELLS IN G_2M VERSUS CULTURE TIME, LUPUS (SLE) PATIENT. HYDRALAZINE ADDED AFTER DAY 4 MEASUREMENTS TAKEN.

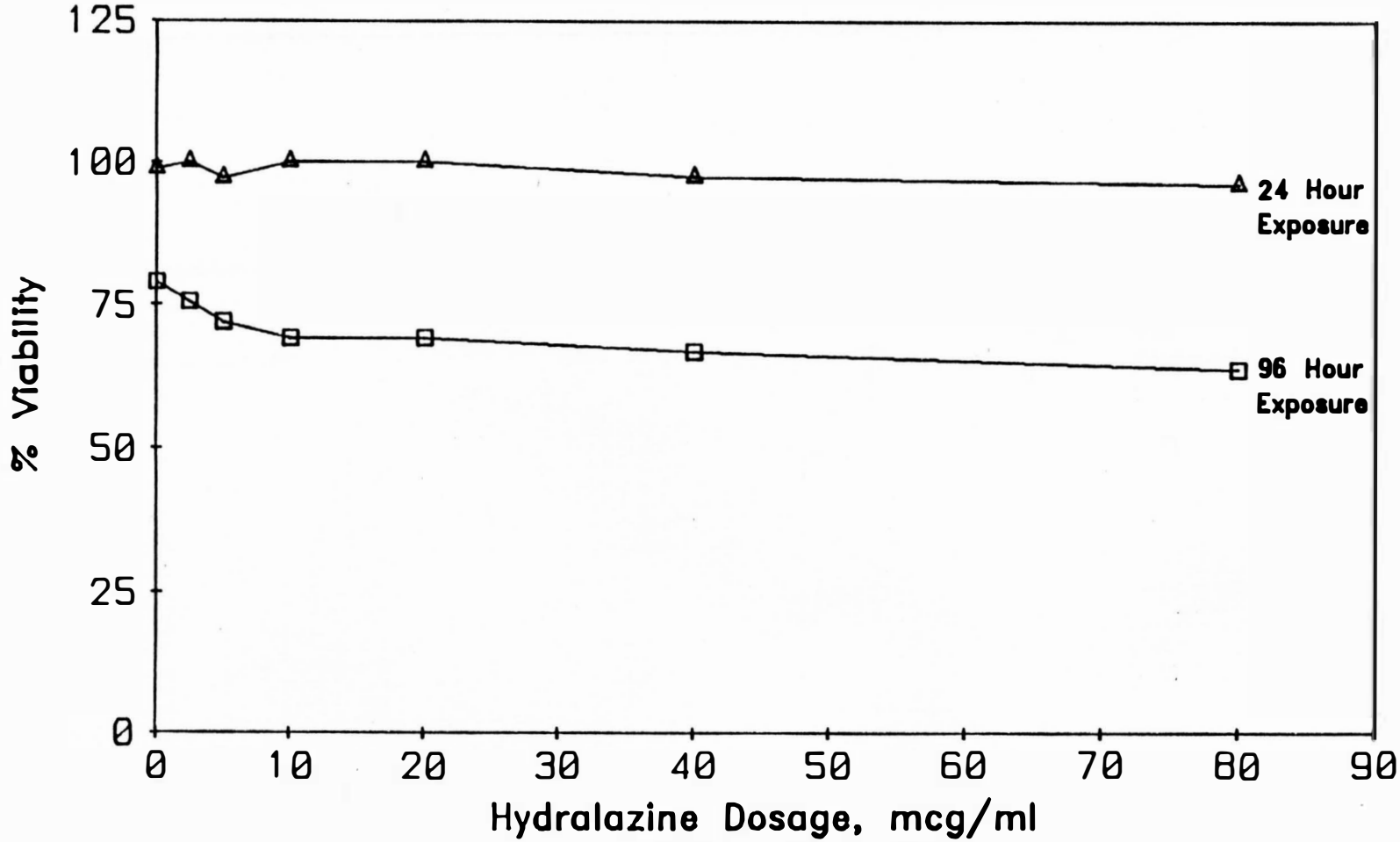

FIGURE 35. VIABILITY OF STATIONARY (G_0) LYMPHOCYTES EXPOSED TO HYDRALAZINE FOR 24 HOURS, THEN PHA-STIMULATED. MEASUREMENTS TAKEN AT 24 AND 96 HOURS AFTER PHA ADDITION.

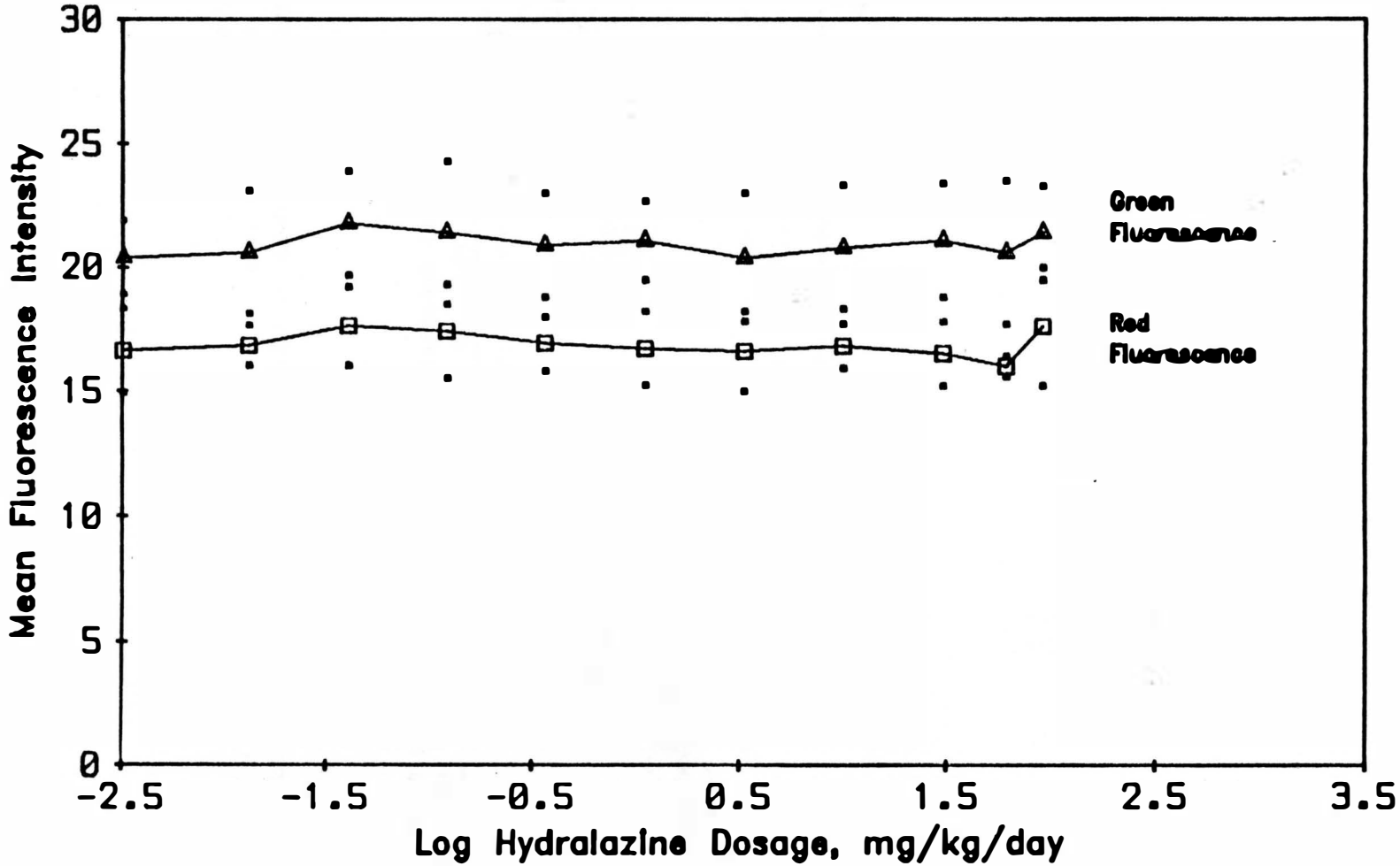

FIGURE 36. RED AND GREEN FLUORESCENCE OF RAT LYMPHOCYTES AFTER 12 WEEKS OF HYDRALAZINE EXPOSURE.

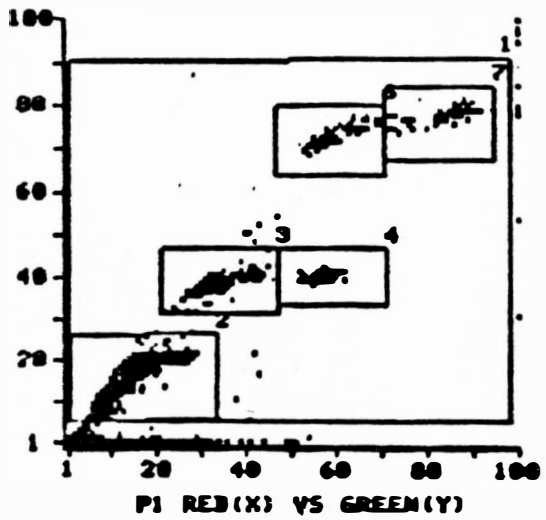

Figure 37A. Cytogram of red versus green fluorescence of rat testicular cells.

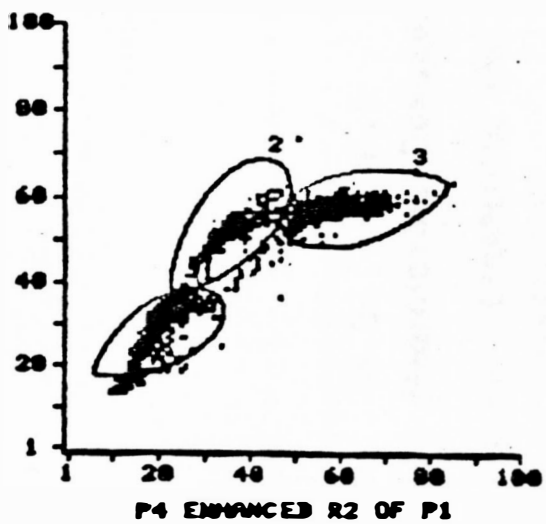

Figure 37B. Cytogram of haploid cell population and subpopulations.

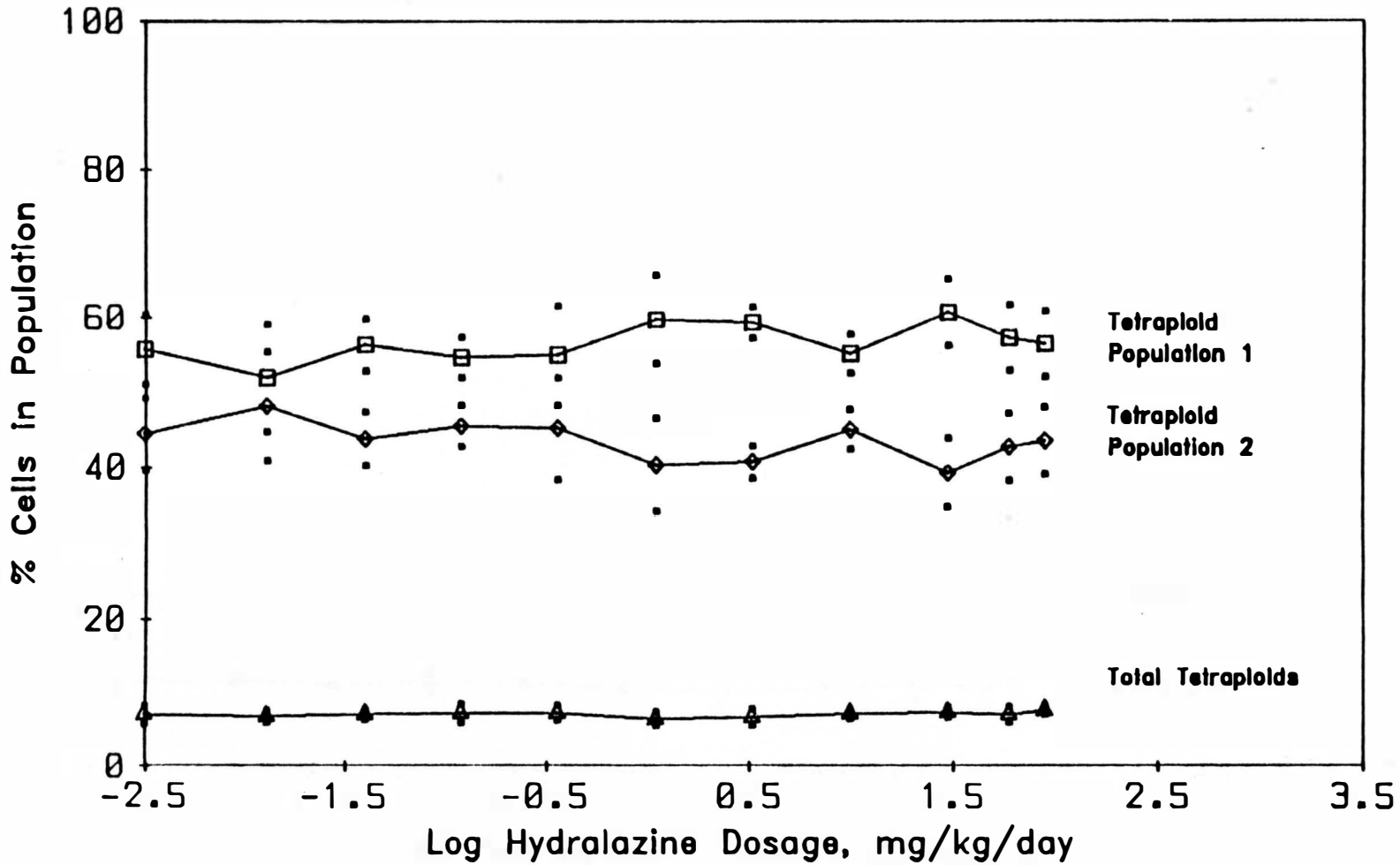

FIGURE 38. PERCENT TETRAPLOIDS AND TETRAPLOID SUBPOPULATION VERSUS DOSAGE OF HYDRALAZINE.

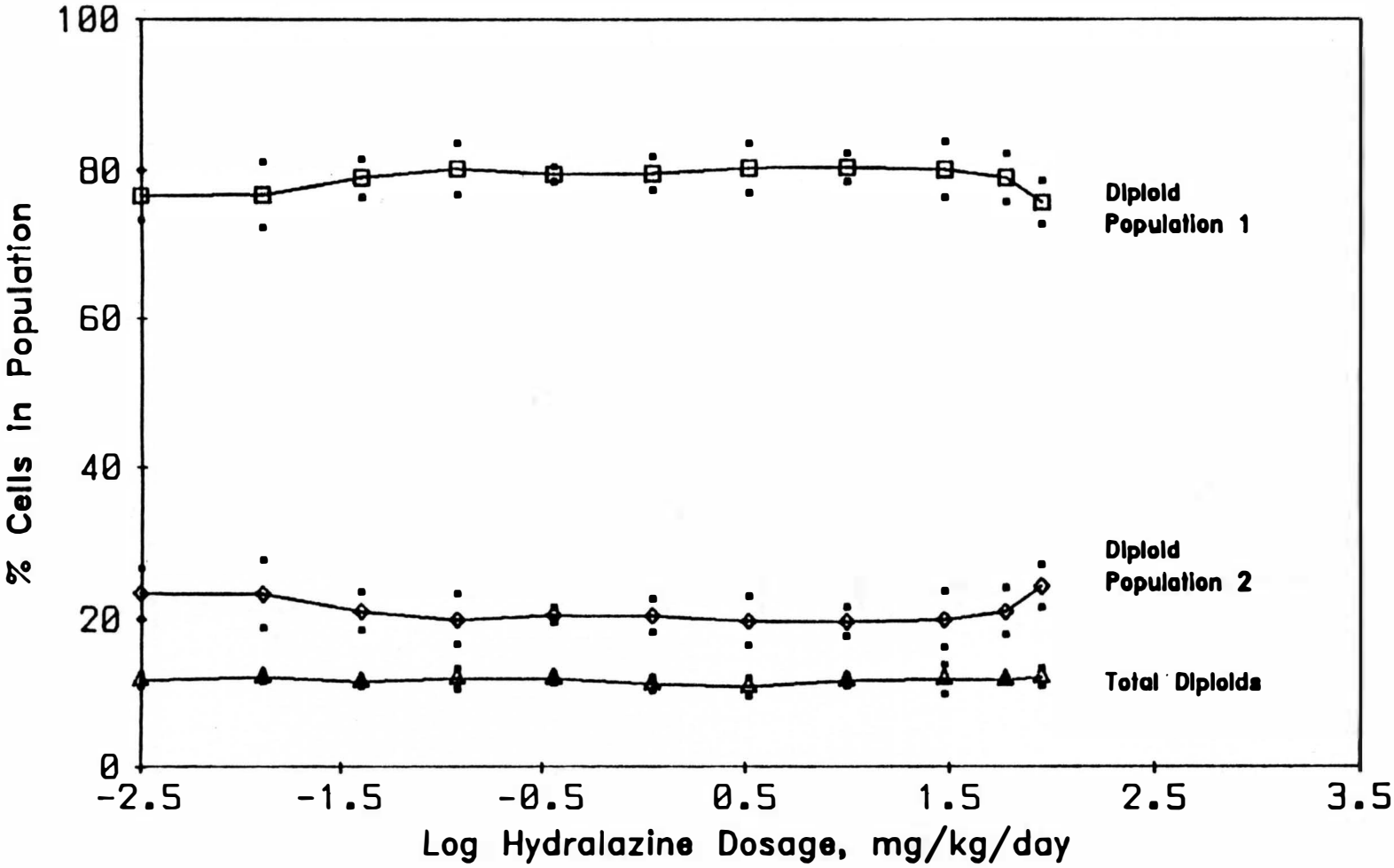

FIGURE 39. PERCENT DIPLOIDS AND DIPLOID SUBPOPULATIONS VERSUS DOSAGE OF HYDRALAZINE.

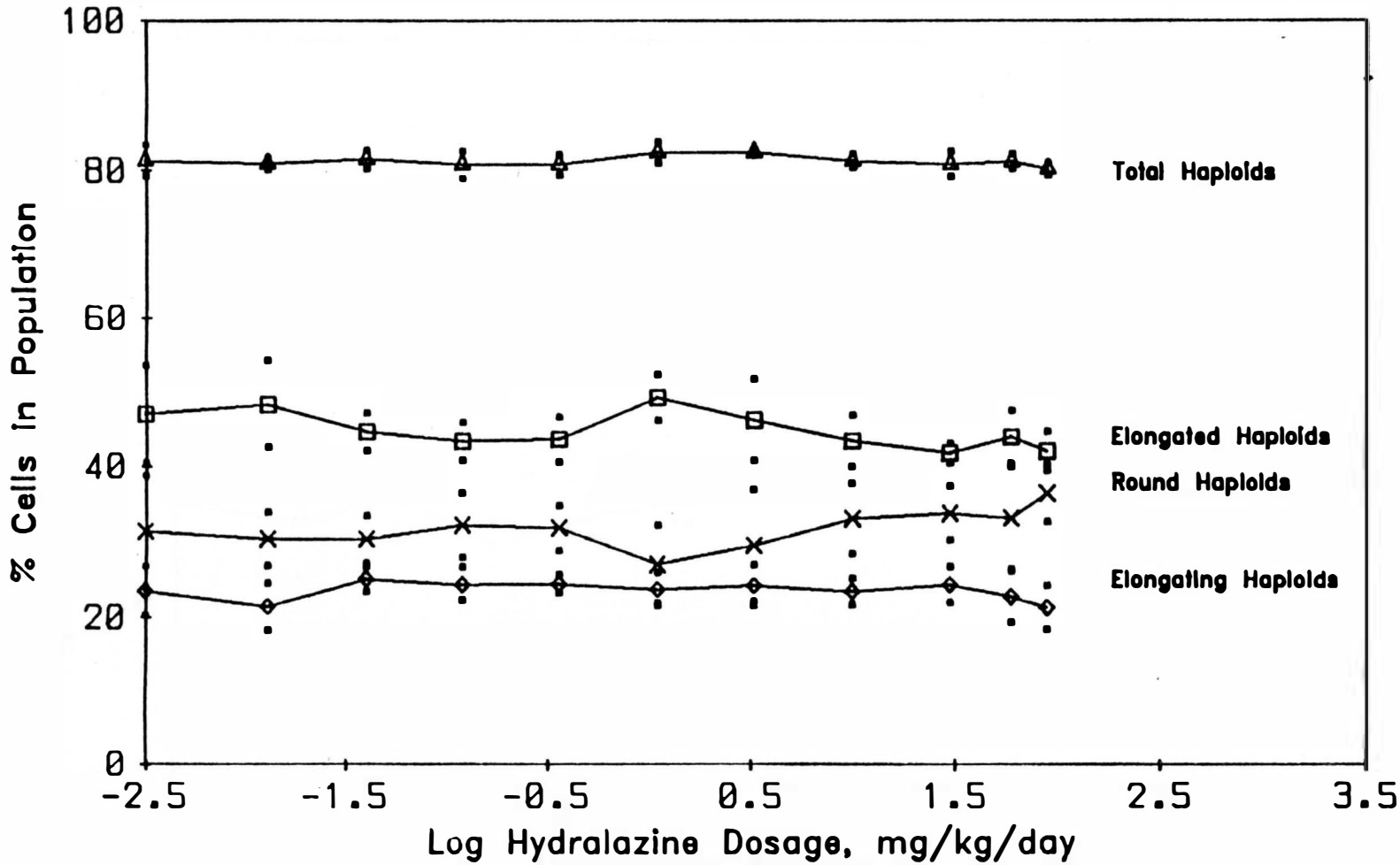

FIGURE 40. PERCENT HAPLOIDS AND HAPLOID SUBPOPULATIONS VERSUS DOSAGE OF HYDRALAZINE.

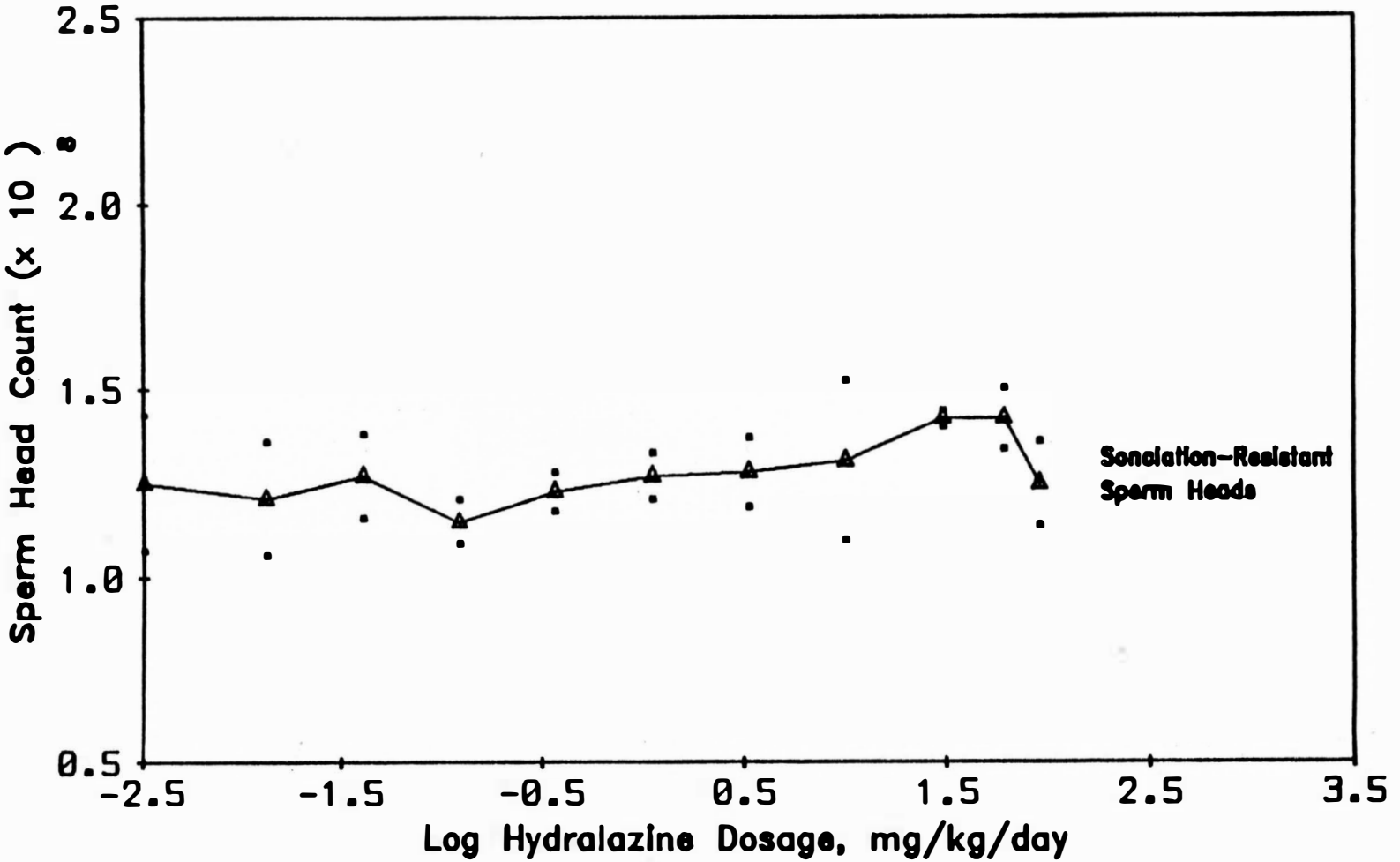

FIGURE 41. SONICATION RESISTANT SPERM HEADS PER GRAM TESTITULAR TISSUE VERSUS DOSAGE OF HYDRALAZINE.

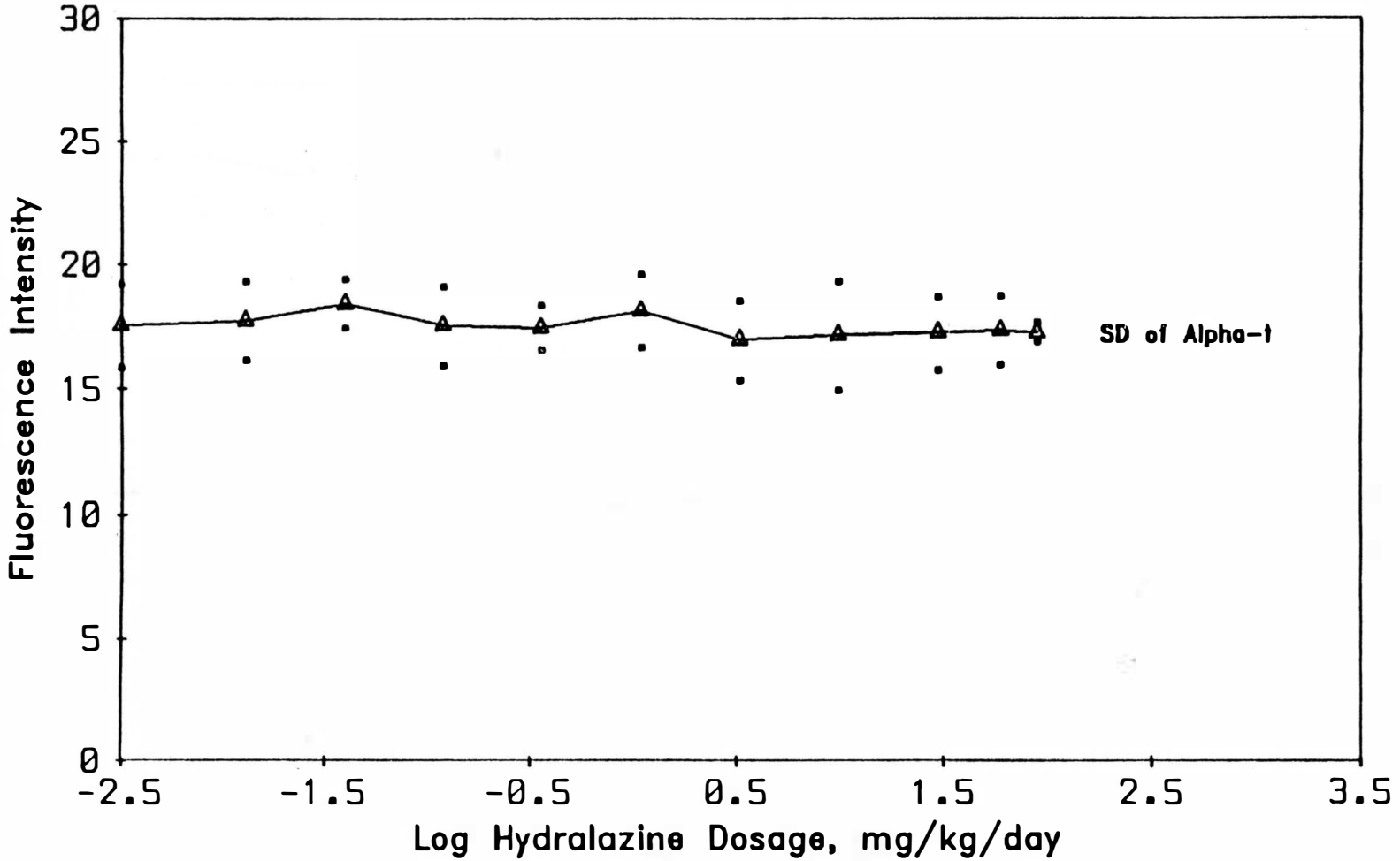

FIGURE 42. STANDARD DEVIATION OF α_T RAT EPIDIDYMAL SPERM VERSUS HYDRALAZINE DOSAGE.

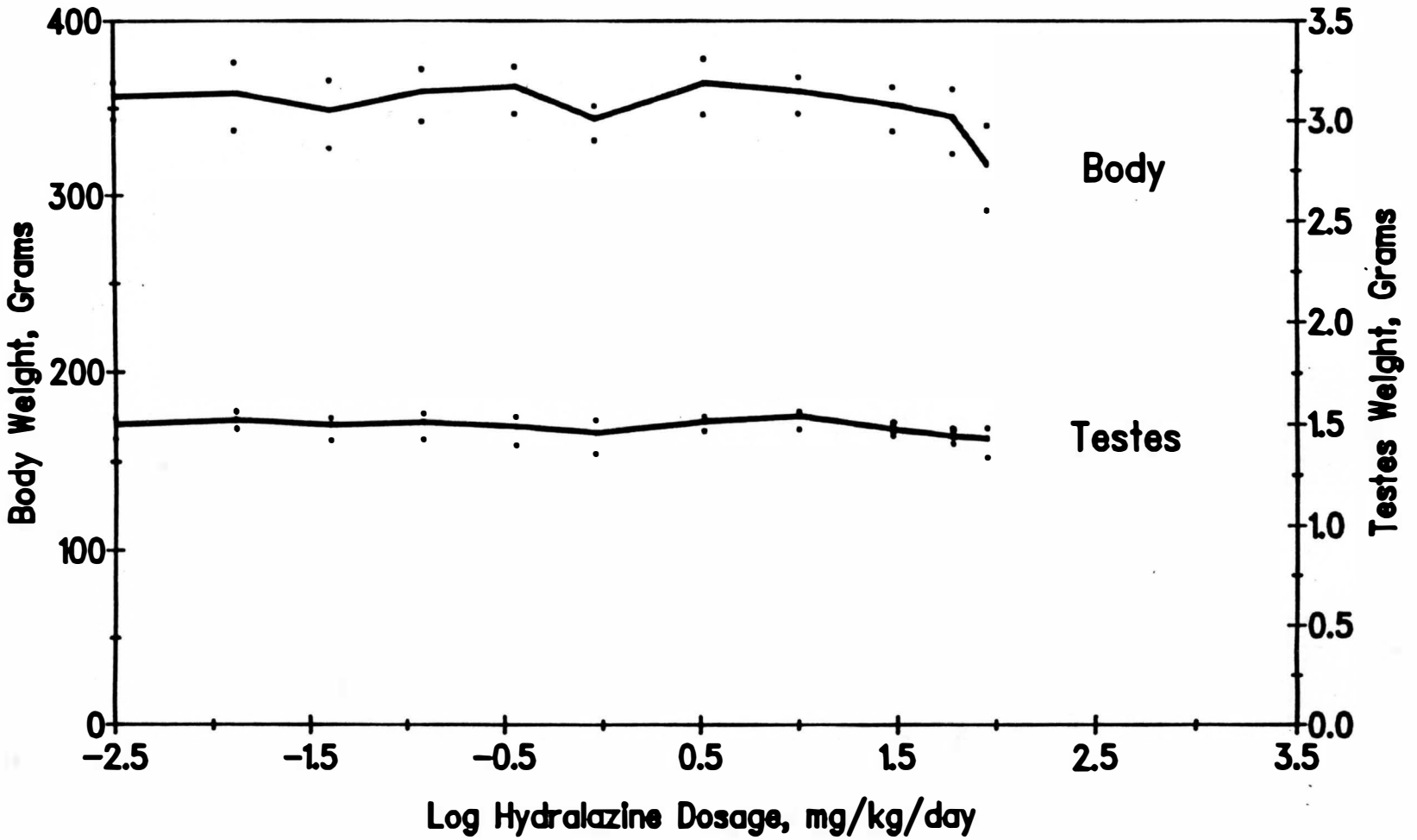

FIGURE 43. EFFECT OF HYDRALAZINE ON RAT BODY AND TESTITULAR WEIGHT.

Table 1. Friend Leukemia Cell Growth Data

Hydralazine Dose	Cell Count/ml	% Growth vs. Control
0	1.2×10^6	100
2.5	1.2×10^6	100
5.0	1.4×10^6	+100
10.0	1.3×10^6	+100
20.0	1.1×10^6	91.6
40.0	3.5×10^5	29.2
80.0	2.4×10^5	20.0
160.0	1.8×10^5	15.0
320.0	1.2×10^5	10.0

Table 2. Friend Leukemia Cell Viability Data

Hydralazine Dosage (mg/ml)	% Viable Cells
0	98.9
2.5	98.7
5.0	98.8
10.0	99.0
20.0	98.9
40.0	95.9
80.0	92.3
160.0	90.0
320.0	79.3

Table 3. Population kinetics of Friend leukemia cells after vinblastine induced M phase block, no hydralazine.

	% Cells in Population		
Time	G_1	S	G_2M
0 hours	36.4	44.3	19.2
1	24.4	52.4	23.1
2	21.8	47.3	30.8
3	11.7	42.5	33.9
4	6.3	42.1	51.5
5	4.8	33.2	61.9
6	5.4	23.7	70.8
7	2.7	17.1	80.2
8	2.9	12.6	84.4
9	2.6	11.7	85.6

Table 4. Population kinetics of Friend leukemia cells after vinblastine induced M phase block. Hydralazine 20 ug/ml added 1 Hour after vinblastine.

	% Cells in Population		
Time	G_1	S	G_2M
0 hours	36.4	44.3	19.2
1	29.5	42.9	27.2
2	23.0	47.0	29.9
3	15.8	47.8	36.3
4	7.1	48.7	44.1
5	6.7	43.2	50.1
6	3.9	41.7	54.3
7	4.0	32.8	63.1
8	3.2	25.2	71.5
9	3.0	19.0	77.9

Table 5. Population kinetics of Friend leukemia cells after vinblastine induced M phase block. Hydralazine 40 µg/ml added 1 hour after vinblastine.

	% Cells in Population		
Time	G_1	S	G_2M
0 hours	36.4	44.3	19.2
1	25.8	49.1	25.0
2	28.5	45.2	26.3
3	23.9	47.6	28.3
4	14.7	52.1	33.1
5	13.3	49.7	37.0
6	12.2	46.4	41.3
7	17.7	44.7	37.1
8	3.8	46.4	49.8
9	4.6	45.4	49.9

Table 6. Population kinetics of Friend leukemia cells after vinblastine-induced M phase block. Hydralazine 80 ug/ml added 1 hour after vinblastine.

	% Cells in Population		
Time	G_1	S	G_2M
0 hours	36.4	44.3	19.2
1	28.0	47.1	24.8
2	28.8	45.2	25.9
3	25.3	46.2	28.5
4	25.1	45.3	29.5
5	20.9	47.0	31.9
6	23.8	45.6	30.4
7	24.1	46.5	29.3
8	24.2	48.3	27.4
9	18.6	50.1	31.2

Table 7. Percent mitotic Friend leukemia cells versus time after vinblastine block.

Hours after Vinblastine	Hydralazine Concentrations (mcg/ml) 0	20	40	80
0	4.1	4.1	4.1	4.1
1	6.9	6.6	7.0	5.2
2	12.6	14.0	10.4	10.6
3	20.1	18.8	15.5	10.9
4	29.0	23.5	16.2	13.3
5	36.4	29.4	18.2	13.1
6	47.1	36.0	20.1	12.4
7	60.3	44.2	22.3	13.8
8	71.4	48.8	21.6	12.7
9	80.9	57.5	25.5	11.6
10	86.1	64.2	31.6	12.1

Table 8. Standard deviation of α_t the mitotic population versus time after the addition of vinblastine.

	Hydralazine Dosage (mcg/ml)			
Time	0	20	40	80
0 hours	21.3	21.3	21.3	21.3
1	24.1	24.1	23.7	25.0
2	23.1	20.5	21.7	21.7
3	28.4	24.1	27.6	25.0
4	26.7	23.4	25.9	30.1
5	22.9	23.2	25.5	23.9
6	21.7	25.7	25.4	27.9
7	29.7	25.6	28.2	25.4
8	26.6	27.1	29.3	28.3
9	26.9	25.6	31.0	26.1
10	24.8	26.9	36.6	27.5

Table 9. Percent survival of CHO cells after 20 hour exposure to hydralazine.

Hydralazine Dosage (mcg/ml)	Log Phase Culture
0	100
2.5	100
5.0	100
10.0	100
20.0	100
40.0	90
80.0	42
160.0	25

Table 10. Cell cycle population kinetics and red fluorescence intensity of log phase lymphocytes exposed to hydralazine for 24 hours.

Hydralazine Concentration	0 mcg/ml	2.5 mcg/ml	5.0 mcg/ml	10 mcg/ml	20 mcg/ml	40 mcg/ml	80 mcg/ml
% Cells in G_0							
Exp 1	12.5 ± 1.3	11.4 ± 1.1	12.6 ± 0.1	16.2 ± 4.8	28.0 ± 2.2	26.8 ± 2.3	24.8 ± 1.6
Exp 2	20.2 ± 1.13	17.4 ± 2.1	21.2 ± 1.6	22.0 ± 5.9	25.0 ± 5.4	32.7 ± 8.2	27.3 ± 2.0
% Cells in G_1							
Exp 1	63.7 ± 1.9	67.5 ± 2.4	65.4 ± 2.1	55.9 ± 6.1	41.7 ± 2.5	59.7 ± 1.3	64.1 ± 1.5
Exp 2	62.6 ± 2.4	64.9 ± 1.6	61.1 ± 0.4	56.6 ± 2.6	47.2 ± 1.0	53.0 ± 8.6	62.3 ± 2.3
% Cells in S							
Exp 1	17.3 ± 3.9	16.9 ± 1.1	19.7 ± 1.4	22.7 ± 0.2	33.1 ± 3.4	19.2 ± 9.9	14.2 ± 4.3
Exp 2	55.5 ± 0.1	14.1 ± 1.4	14.8 ± 2.0	17.9 ± 2.6	27.8 ± 3.0	16.8 ± 0.7	15.4 ± 2.2
% Cells in G_2M							
Exp 1	9.4 ± 0.8	7.8 ± 0.2	7.5 ± 0.3	9.6 ± 1.2	2.7 ± 1.2	1.4 ± 0.1	1.5 ± 0.4
Exp 2	7.3 ± 0.5	7.5 ± 0.3	6.7 ± 0.9	7.3 ± 0.3	5.1 ± 0.5	1.6 ± 0.3	1.7 ± 0
% Cycling Cells							
Exp 1	90.4 ± 2.9	92.2 ± 1.6	90.6 ± 2.8	88.3 ± 5.1	77.6 ± 4.8	80.4 ± 8.7	79.8 ± 2.4
Exp 2	85.5 ± 3.1	86.6 ± 3.1	82.7 ± 2.0	81.9 ± 5.6	80.1 ± 4.5	70.7 ± 9.1	79.5 ± 4.5
Mean Red Fluor G_1							
Exp 1	24.3 ± 0.1	25.2 ± 1.0	26.8 ± 1.9	27.4 ± 2.6	26.6 ± 0.5	30.2 ± 0.8	29.3 ± 1.3
Exp 2	24.2 ± 1.2	24.4 ± 0.2	24.4 ± 0.4	24.4 ± 0.1	24.9 ± 1.3	26.8 ± 0.3	28.3 ± 0.5
Mean Red Fluor S							
Exp 1	32.8 ± 0.7	34.6 ± 0.9	32.9 ± 2.2	33.5 ± 2.9	35.8 ± 1.3	29.9 ± 3.8	25.3 ± 1.5
Exp 2	33.5 ± 0.5	32.7 ± 0.8	33.9 ± 1.1	33.3 ± 1.4	36.4 ± 2.1	26.2 ± 1.9	25.0 ± 2.6
Mean Red Fluor G_2M							
Exp 1	41.7 ± 0.1	43.2 ± 1.5	43.0 ± 0.9	46.2 ± 3.1	48.9 ± 1.0	40.0 ± 3.8	43.1 ± 1.9
Exp 2	43.3 ± 1.7	43.0 ± 1.2	43.8 ± 0.7	43.7 ± 0.5	47.1 ± 0.3	40.2 ± 5.0	38.2 ± 2.7

Table 11. Cell cycle population kinetics and red fluorescence intensity of log phase lymphocytes exposed to hydralazine for 48 hours.

Hydralazine Concentration	0 mcg/ml	2.5 mcg/ml	5.0 mcg/ml	10 mcg/ml	20 mcg/ml	40 mcg/ml	80 mcg/ml
% Cells in G_0							
Exp 1	10.6 ± 1.0	10.6 ± 1.6	13.1 ± 2.5	15.1 ± 0.9	23.8 ± 1.2	31.1 ± 2.3	30.2 ± 3.8
Exp 2	19.3 ± 0.1	20.0 ± 2.6	22.8 ± 5.9	20.3 ± 2.0	27.2 ± 4.9	34.5 ± 4.4	33.9 ± 3.7
% Cells in G_1							
Exp 1	77.3 ± 1.0	76.3 ± 3.1	73.6 ± 3.5	69.7 ± 0.9	45.8 ± 2.2	58.5 ± 7.2	62.4 ± 9.4
Exp 2	69.8 ± 0	72.1 ± 2.1	69.6 ± 3.7	68.3 ± 0.7	53.4 ± 0.3	47.9 ± 1.6	59.1 ± 1.2
% Cells in S							
Exp 1	12 ± 1.9	12.3 ± 1.5	12.6 ± 2.2	14.9 ± 1.2	27.5 ± 2.3	20.9 ± 7.1	13.8 ± 5.1
Exp 2	10.7 ± 0.5	10.9 ± 3.9	9.8 ± 1.3	12.8 ± 1.8	17.5 ± 1.5	23.1 ± 0.2	12.8 ± 4.0
% Cells in G_2M							
Exp 1	4.7 ± 0.7	4.3 ± 0.6	4.6 ± 0.9	5.25 ± 0.2	11.0 ± 3.8	1.6 ± 0.1	1.9 ± 0.4
Exp 2	3.5 ± 0.7	3.5 ± 0.4	3.3 ± 0.2	4.2 ± 0.4	6.7 ± 1.7	1.25 ± 0.3	1.0 ± 0.1
% Cycling Cells							
Exp 1	94 ± 0.3	93.0 ± 1.3	90.9 ± 3.2	89.9 ± 1.9	84.3 ± 0.7	81.1 ± 0.1	77.1 ± 5.4
Exp 2	84.1 ± 1.2	86.6 ± 2.5	81.7 ± 6.5	85.3 ± 3.0	77.7 ± 0.1	72.2 ± 2.2	73.0 ± 2.7
Mean Red Fluor G_1							
Exp 1	22.9 ± 1.1	23.1 ± 0.6	23.1 ± 1.5	24.5 ± 1.4	24.2 ± 0.7	25.4 ± 1.2	24.9 ± 0.5
Exp 2	23.6 ± 0	23.1 ± 0.8	23.2 ± 1.5	24.0 ± 0.6	24.8 ± 1.2	24.4 ± 0.9	25.2 ± 1.2
Mean Red Fluor S							
Exp 1	31.5 ± 1.5	30.6 ± 1.6	30.8 ± 3.7	33.0 ± 2.9	34.4 ± 2.9	31.9 ± 0.5	24.0 ± 2.1
Exp 2	27.9 ± 1.4	27.9 ± 0.4	27.4 ± 2.7	28.8 ± 0.6	29.8 ± 2.9	30.1 ± 1.1	22.1 ± 0.6
Mean Red Fluor G_2M							
Exp 1	40.9 ± 2.1	40.2 ± 1.8	41.4 ± 2.8	44.2 ± 3.5	50.4 ± 3.8	44.1 ± 1.7	41.4 ± 2.9
Exp 2	40.5 ± 0.5	39.6 ± 1.7	40.1 ± 4.3	42.1 ± 2.2	45.5 ± 1.7	39.4 ± 3.0	40.1 ± 0.9

Table 12. Cell cycle population kinetics and red fluorescence of stationary (G_0) lymphocytes exposed to hydralazine and then PHA-stimulated.

Hydralazine Concentration	0 mcg/ml	2.5 mcg/ml	5.0 mcg/ml	10 mcg/ml	20 mcg/ml	40 mcg/ml	80 mcg/ml
% Cells in G_0							
Exp 1	7.8 ± 2.3	9.5 ± 4.3	9.9 ± 1.7	9.2 ± 1.3	8.2 ± 2.5	9.0 ± 0.8	7.7 ± 2.2
Exp 2	9.6 ± 1.0	7.4 ± 1.2	8.7 ± 0.1	9.5 ± 1.7	7.7 ± 2.3	9.3 ± 1.2	5.7 ± 0.1
% Cells in G_1							
Exp 1	46.8 ± 2.3	48.8 ± 0	47.9 ± 0.5	49 ± 2.1	47.2 ± 0.2	46.1 ± 2.4	40.8 ± 7.5
Exp 2	51.7 ± 2.8	52.3 ± 0.5	52.2 ± 0.9	53.1 ± 3.4	53.0 ± 1.7	50.2 ± 0.4	50.2 ± 2.9
% Cells in S							
Exp 1	19.6 ± 2.7	23 ± 2.6	21.1 ± 3.5	23.7 ± 5.6	22.8 ± 5.0	25.2 ± 6.6	29.9 ± 10.4
Exp 2	20.2 ± 1.3	21.4 ± 0.1	23.1 ± 1.6	21.4 ± 1.6	23.3 ± 1.5	23.4 ± 0.8	29.9 ± 0.7
% Cells in G_2M							
Exp 1	8.3 ± 0.3	9.1 ± 1.0	10.1 ± 0.7	11.3 ± 1.0	10.8 ± 2.2	11.0 ± 0.4	7.9 ± 5.8
Exp 2	8.5 ± 0.3	9.9 ± 0.3	10.3 ± 0.5	11.4 ± 0.4	11.5 ± 0.1	11.8 ± 0.5	10.5 ± 0.1
% Cycling Cells							
Exp 1	90.5 ± 2.5	89.5 ± 4.6	88.9 ± 2.2	90.0 ± 1.5	90.6 ± 3.3	90.2 ± 0.3	90.1 ± 7.6
Exp 2	89.2 ± 0.9	91.8 ± 1.3	90.8 ± 0.1	89.9 ± 1.7	91.8 ± 2.4	90.1 ± 1.3	94.0 ± 0
Mean Red Fluor G_1							
Exp 1	29.2 ± 2.1	29.0 ± 3.3	28.8 ± 1.5	30.4 ± 2.5	32.4 ± 4.6	32.8 ± 5.0	35.1 ± 1.3
Exp 2	26.4 ± 3.6	30.1 ± 0.2	30.8 ± 1.0	30.4 ± 0.9	30.9 ± 0.6	30.6 ± 1.5	34.3 ± 1.1
Mean Red Fluor S							
Exp 1	37.7 ± 2.4	38.8 ± 5.8	37.7 ± 1.9	39.2 ± 3.8	42.2 ± 6.5	42.9 ± 6.7	45.7 ± 2.4
Exp 2	37.1 ± 0.3	38.0 ± 1.9	40.0 ± 0.6	39.8 ± 1.7	40.2 ± 0.3	40.5 ± 1.4	47.9 ± 0.1
Mean Red Fluor G_2M							
Exp 1	50.9 ± 4.0	50.3 ± 4.7	50.2 ± 3.2	52.0 ± 2.9	54.3 ± 6.3	56.8 ± 1.8.0	59.1 ± 2.0
Exp 2	47.0 ± 3.4	51.0 ± 1.5	52.8 ± 1.9	52.0 ± 1.0	52.6 ± 1.1	54.2 ± 1.9	60.4 ± 1.3

Table 13. Fluorescent measurements on lymphocytes subjected to acid-induced denaturation of DNA in situ.

Hydralazine Concentration	0 mcg/ml	2.5 mcg/ml	5.0 mcg/ml	10 mcg/ml	20 mcg/ml	40 mcg/ml	80 mcg/ml
Mean Red Fluorescence							
Day 1	16.0 ± 1.2	16.5 ± 1.8	16.9 ± 1.4	17.1 ± 1.1	16.5 ± 0	16.8 ± 0.3	16.9 ± 0.9
Day 2	16.1 ± 1.0	16.0 ± 0.1	16.8 ± 0.9	16.5 ± 0.5	16.3 ± 0.7	17.1 ± 0.5	17.9 ± 0.1
Mean Green Fluorescence							
Day 1	45.5 ± 3.0	46.7 ± 2.4	45.5 ± 1.0	45.2 ± 1.1	46.6 ± 2.9	46.4 ± 3.0	44.4 ± 1.5
Day 2	49.3 ± 1.9	50.5 ± 2.8	47.1 ± 0.7	48.8 ± 1.6	51.1 ± 0	50.3 ± 0.7	50.1 ± 0.3
Standard Deviation of Alpha-t							
Day 1	33.6 ± 2.3	31.5 ± 1.6	32.5 ± 0.4	29.8 ± 0.7	27.1 ± 0.5	29.2 ± 1.1	29.6 ± 1.3
Day 2	37.3 ± 6.2	32.5 ± 2.5	35.1 ± 0.4	35.1 ± 0.5	33.8 ± 0.7	36.1 ± 0.6	35.1 ± 3.5
Standard Deviation of Total Fluorescence							
Day 1	30.4 ± 1.9	29.3 ± 1.1	27.6 ± 1.1	28.1 ± 0.7	25.1 ± 0.7	26.5 ± 0.7	26.3 ± 1.4
Day 2	33.3 ± 4.6	28.3 ± 4.0	29.2 ± 3.2	29.7 ± 1.3	30.9 ± 2.2	32.1 ± 0.5	30.6 ± 1.8

Table 14. Cell cycle population kinetics of PHA stimulated, hydralazine exposed lymphocytes from a control and SLE patients.

		Day 1 PHA added	Day 2	Day 3	Day 4	Day 5 (after 24 h Hydralazine) 0 mcg/ml	5 mcg/ml	40 mcg/ml
G_0	Control	100	14.7 ± 1.5	3.6 ± 0.5	4.3 ± 0.4	2.47 ± 0	5.7 ± 2.0	9.9 ± 0
	SLE	100	17.6 ± 1.5	2.1 ± 0.1	4.2 ± 0.4	3.8 ± 1.0	4.0 ± 0	5.2 ± 0
G_1	Control	0	90.3 ± 2.0	66.3 ± 0.5	65.8 ± 1.2	75.1 ± 0.8	73.8 ± 1.8	91.1 ± 0
	SLE	0	87.8 ± 1.7	66.3 ± 2.9	60.1 ± 1.8	66.9 ± 11.2	60.3 ± 0	72.7 + 0
S	Control	0	0	20.2 ± 1.1	22.3 ± 2.0	16.5 ± 0.5	20.5 ± 1.1	6.7 ± 0
	SLE	0	0	22.2 ± 0.1	28.2 ± 0.3	20.2 ± 7.5	26.4 ± 0	14.8 ± 0
G_2M	Control	0	0	8.7 ± 1.3	12.2 ± 0.5	8.1 ± 1.2	7.9 ± 0.4	2.2 ± 0
	SLE	0	0	6.8 ± 1.8	14.2 ± 1.2	11.3 ± 2.3	13.2 ± 0	1.6 ± 0

Table 15. Percent Viability of Lymphocytes

Dosage of hydralazine mcg/ml	24 h	96 h
0	98.9	78.9
2.5	100	75.4
5.0	97.2	71.9
10.0	100	69.2
20.0	100	69.2
40.0	97.5	66.8
80.0	96.2	63.9

Table 16. Red and green fluorescent measurements of rat lymphocytes exposed to hydralazine for 12 weeks.

	0	0.013	0.04	0.12	0.36	1.1	3.3	10	30	60	90
Mean Green Fluorescence	20.4 ±1.5	20.6 ±2.5	21.8 ±2.1	21.4 ±2.9	20.9 ±2.1	21.1 ±1.6	20.4 ±2.6	20.8 ±2.5	21.1 ±2.3	20.6 ±2.9	21.4 ±1.9
Mean Red Fluorescence	16.6 ±1.7	16.8 ±0.8	17.6 ±1.6	17.4 ±1.9	16.9 ±1.1	16.7 ±1.5	16.6 ±1.6	16.8 ±0.9	16.5 ±1.3	16.0 ±0.4	17.6 ±2.4
Green Peak Fluorescence	204.2 ±15.4	206.2 ±22.8	218.0 ±20.4	212.0 ±30.3	210.0 ±18.7	208.0 ±17.8	204.0 ±26.0	204.0 ±24.0	209.0 ±22.4	207.5 ±28.7	215.0 ±21.8
Red Peak Fluorescence	136.4 ±14.3	135.0 ±5.7	148.0 ±13.0	142.0 ±14.8	138.0 ±8.3	140.0 ±14.1	134.0 ±13.4	140.0 ±12.2	137.0 ±10.9	135.0 ±5.7	147.0 ±19.8

Table 17. Population kinetics of developing spermatocytes and sonication-resistant sperm head count.

	Dose Groups (mg/kg)										
	0	0.013	0.04	0.12	0.36	1.1	3.3	10	30	60	90
Haploids, % of Total	81.2 ±2.1	80.8 ±0.8	81.4 ±1.2	80.7 ±1.8	80.7 ±1.4	82.3 ±1.4	82.3 ±0.4	81.2 ±0.9	80.7 ±1.7	81.1 ±1.0	80.1 ±0.8
% Elongated	46.9 ±6.5	48.2 ±5.8	44.6 ±2.5	43.3 ±2.6	43.6 ±3.0	49.2 ±3.1	46.2 ±5.5	43.4 ±3.4	41.8 ±1.3	44.0 ±3.5	42.1 ±2.6
% Elongating	23.4 ±3.2	21.3 ±3.2	25.0 ±1.6	24.3 ±2.2	24.4 ±1.2	23.7 ±2.2	24.2 ±2.8	23.4 ±1.8	24.3 ±2.4	22.7 ±3.5	21.2 ±3.0
% Round	31.3 ±7.4	30.3 ±3.6	30.3 ±3.2	32.2 ±4.3	31.8 ±3.0	27 ±5.2	29.5 ±7.5	33.1 ±4.7	33.8 ±3.6	33.2 ±6.8	36.5 ±3.8
Diploids, % of Total	11.6 ±0.9	12.1 ±0.7	11.4 ±0.6	11.9 ±1.4	11.9 ±0.6	11.2 ±0.9	10.8 ±1.2	11.6 ±0.7	11.8 ±2.0	11.7 ±0.1	12.1 ±1.2
Pop. 1	76.5 ±3.3	76.7 ±4.4	78.9 ±2.5	80.1 ±3.4	79.4 ±1.0	79.5 ±2.2	80.2 ±3.3	80.3 ±1.9	80.0 ±3.7	78.9 ±3.2	75.6 ±2.9
Pop. 2	23.3 ±3.3	23.2 ±4.4	21.0 ±2.5	19.9 ±3.3	20.5 ±1.0	20.4 ±2.2	19.7 ±3.2	19.6 ±2.0	19.9 ±3.7	21.0 ±3.1	24.3 ±2.8
Tetraploids, % of Total	7.0 ±1.3	6.8 ±0.8	7.0 ±0.7	7.2 1.3	7.2 ±1.0	6.4 ±0.9	6.7 ±1.1	7.1 ±0.7	7.3 ±0.7	7.0 ±1.0	7.6 ±0.6
Pop. 1	55.6 ±4.7	51.8 ±7.2	56.2 ±3.5	54.5 ±2.7	54.8 ±6.7	59.6 ±6.0	59.2 ±2.1	55.0 ±2.6	60.6 ±4.5	57.2 ±4.4	56.4 ±4.4
Pop. 2	44.3 ±4.7	48.0 ±7.2	43.7 ±3.5	45.4 ±2.7	45.1 ±6.7	40.3 ±6.0	40.7 ±2.1	45.0 ±2.6	39.3 ±4.5	42.7 ±4.4	43.5 ±4.4
Sonication-Resistant Sperm head per gram testes (x 10_8)	1.25 ±0.18	1.21 ±0.15	1.27 ±0.11	1.15 ±0.06	1.23 ±0.05	1.27 ±0.06	1.28 ±0.09	1.31 ±0.21	1.42 ±0.02	1.42 ±0.08	1.25 ±0.11

Table 18. Rat Epididymis Data

Dose Groups (mg/kg/day)

	0	0.013	0.04	0.12	0.36	1.1	3.3	10	30	60	90
SD of Alpha-t	17.5 ±1.7	17.7 ±1.6	18.4 ±1.0	17.5 ±1.6	17.4 ±0.9	18.1 ±1.5	16.9 ±1.6	17.1 ±2.2	17.2 ±1.5	17.3 ±1.4	17.2 ±0.4

Table 19. Rat Body and Testis Weights

Dose Group (mg/kg/day)	Body	Teste
Control	357 ± 10.9	1.495 ± 0.050
0.013	359 ± 19.8	1.517 ± 0.024
0.04	349 ± 19.5	1.492 ± 0.055
0.12	360 ± 15.1	1.506 ± 0.065
0.36	363 ± 13.6	1.485 ± 0.071
1.1	344 ± 9.8	1.455 ± 0.083
3.3	365 ± 16.1	1.513 ± 0.026
10	360 ± 10.5	1.539 ± 0.044
30	352 ± 12.8	1.474 ± 0.009
60	345 ± 18.7	1.441 ± 0.015
90	318 ± 24.2	1.430 ± 0.072

DISCUSSION

The objective of this work was to determine the relationship between hydralazine exposure and alterations in cell growth and differentiation both *in vivo* and *in vitro*. Hydralazine-induced alterations of chromatin structure of both histone containing somatic cells and protamine containing sperm cells were analyzed to study mechanisms of these alterations that may provide clues as to why hydralazine treated patients develop antibodies against DNA/chromatin with lupus-like symptoms.

The effect of hydralazine on FL and CHO cell growth, viability, and proliferative potential was determined using two different techniques. One approach based on cell counts and trypan blue dye exclusion measures the immediate effect of the drug on cell growth and viability and was applied to cultures of log phase FL cells (83). A second technique, inhibition of colony formation (83), measures the immediate effects of the drug on cell survival and the effect of the drug on proliferative potential of the cells, because at least four consecutive doublings are required to form a macroscopically visible (50 cell) colony (84). The latter technique was applied to CHO cells, because they grow as a monolayer and generally manifest a high cloning efficiency (84).

After twenty hours of exposure to hydralazine, the viability of exponentially growing FL cells remained greater than 90% for hydralazine concentrations up to 160 mcg/ml whereas growth was reduced to less than 30% of control at hydralazine concentrations of 40 mcg/ml

and greater (Table 1, 2). FL cells tend to differentiate in stationary phase cultures and so a viability study on stationary phase FL cells was not done. One can see that growth of FL cells is affected to a much greater extent than viability with hydralazine concentration of 40 mcg/ml or greater.

The differential inhibition of colony formation of exponentially growing versus stationary CHO cells by hydralazine paralleled the results of the effect of the drug, described above, on log phase FL cells. The growth of log phase CHO cells was inhibited by concentrations greater than 20 mcg/ml of hydralazine (Table 9, Figure 19) with hydralazine concentrations of 160 mcg/ml reducing colony formation to 25% of control.

A preliminary experiment using stationary phase CHO cells suggested that hydralazine had no effect on colony formation except when concentrations reached 160-320 mcg/ml. The data from this experiment is being withheld because the experiment was done only once and the validity was in question. The results of the log phase CHO cells is in agreement with growth study on log phase FL cells, the inhibition of growth beginning when hydralazine concentrations reached 20 mcg/ml. It is anticipated that results from the repeat experiment will show a greater effect of hydralazine on growth inhibition of log phase CHO cells versus stationary phase CHO cells.

In addition to the growth and viability studies carried out on FL cells and CHO cells, the viability of human lymphocytes as affected by hydralazine was also assessed. It was found that hydralazine had

no effect on viability of non-cycling lymphocytes that were treated with 0-80 mcg hydralazine per ml for 24 hours (Table 15). PHA-stimulated cultures incubated for 96 hours following a 24-hour treatment with 0-80 mcg hydralazine per ml showed a decrease in viability of about 15% (Table 15) over control as the hydralazine concentration reached 80 mcg/ml. Therefore, actively cycling lymphocytes (after 96 hours of PHA-stimulation) appear to be more susceptible to the toxic effects of hydralazine than non-stimulated (G_0) lymphocytes. The concentration of hydralazine where inhibition of viability becomes significant is difficult to define but it appears that viability is affected (10-15% decrease) in the concentration range of 10-40 mcg/ml.

A series of experiments utilizing cell cycle population kinetics of human lymphocytes and FL cells were designed in an attempt to learn where hydralazine exerts its effects on the cell cycle.

Two separate series of experiments were performed on human lymphocytes to assay the effect of the drug on various parameters of lymphocyte growth and stimulation. In one set of experiments, lymphocytes were pretreated with hydralazine for 24 hours and then grown in the presence of PHA. Thus, the cytotoxic effect of hydralazine on stationary (G_0) lymphocytes, that were subsequently PHA-stimulated, was assessed at 24 and 96 hours after PHA addition. In the second series of experiments, PHA-stimulated lymphocytes (cycling) were treated with hydralazine at 72 hours of stimulation and cells were stained with acridine orange, and green and red fluorescent measurements were taken at 24 and 48 hours after the addition of hydralazine.

This experiment was to assess the effect of the drug on the midway proliferative phases of stimulation (64).

Lymphocyte stimulation was studied by flow cytometry. As described previously in detail (64), acridine orange stained lymphocytes could be classified into subpopulations which include unstimulated (G_0) lymphocytes and, upon mitogen stimulation, G_1, S and G_2M stimulated lymphocytes based upon their increase in RNA or RNA and DNA content (84). Since the cell cycle stage of a large number (5×10^3) of individual cells can be characterized by this technique, the analysis of PHA stimulation by flow cytometry is much more precise and informative than results obtained either by determining the incorporation of radioactive thymidine or by morphological identification of blast formation.

If lymphocytes were first stimulated with PHA and then incubated with the drug starting at 72 hours of culture (midway through the proliferative stage of stimulation), there was a decrease of 10% in percent cycling cells at 80 mcg/ml hydralazine. There was also an increase (10-12%) in S-phase population cells as hydralazine concentration approached 20 mcg/ml. These values began to return toward control levels at 40 mcg/ml hydralazine concentrations. Populations of G_1, S and G_2M were essentially unchanged from control at a hydralazine concentration of 80 mcg/ml (Figure 20). The data suggest a possible slowing of cell progression through S phase and a delay or inhibiting of cells from re-entering G_1.

As a result of the ability to simultaneously stain both DNA and RNA in individual cells, it was found that the RNA content of G_2M phase cells increased by about 15% at the 20 mcg/ml hydralazine concentration, then returned to control level at 40 and 80 mcg/ml (Table 10). Similarly, at 48 hours after treatment with hydralazine results were similar (Figure 22, Table 11). The increase in RNA in G_2M phase cells at 20 mcg/ml hydralazine concentrations may be related to the increase in S phase population at the same hydralazine concentration. It is possible that cells inhibited in S phase may be damaged to the point where increased RNA/protein synthesis is necessary to compensate or repair cellular constituents.

When non-cycling (G_0) lymphocytes were treated with hydralazine concentrations of 0-80 mcg/ml for 24 hours, then PHA-stimulated, no effect on population kinetics was noted (Figure 24), however, a 15-20% increase in RNA content, as reflected by mean red fluorescence, was noted in G_1, S and G_2M populations as the hydralazine concentration approached 80 mcg/ml (Figure 25, Table 12). Again, it is possible that hydralazine causes the need for increased RNA/protein synthesis to compensate for cell damage.

An experiment using PHA-stimulated lymphocytes from a control donor and a systemic lupus erythematosus patient, treated with 0, 5, and 40 mcg/ml of hydralazine after 72 hours of stimulation showed no effect in the population kinetics analyzed by flow cytometry daily (Table 5).

The data suggests that hydralazine causes an inhibition of cell progression through S phase of the cell cycle that may be associated with hydralazines effect on growth and viability (59, 66). The effects of a drug on chromatin structure can be assessed by acid-induced denaturation of DNA studies (67) This experiment was of interest because hydralazine is known to cause alteration in the physical properties of nucleic acids (32). Lymphocytes treated with hydralazine for 24 hours, then later subjected to acid-induced denaturation of DNA, in situ, showed no effect of hydralazine concentrations from 0-80 mcg/ml on the mean green and mean red fluorescence as determined by flow cytometry (Figure 26). Similarly, the standard deviation of total cellular fluorescence and $_t$ (Figures 27, 28) showed no dose-effect of hydralazine on non-cycling (G_0) lymphocytes subjected to acid-induced denaturation of DNA, in situ. These findings would suggest that hydralazine does not alter DNA or RNA content of lymphocytes as there was no concentration-related difference in mean red or mean green fluoresce values of cells exposed to varying concentrations of hydralazine. Furthermore, hydralazine does not appear to interfere with acridine orange staining as total fluorescence was unaffected by varying hydralazine concentrations. It appears that hydralazine does not compete with acridine orange for intercalation or electrostatic binding sites. These results suggest that hydralazine does not affect chromatin structure, at least, as reflected by susceptibility to acid-induced denaturation.

A stathmokinetic experiment, using vinblastine to create an M phase block in log phase FL cells was designed to gain more insight into where in the cell cycle hydralazine may be exerting its inhibitory effects. Log phase cells progress through the cell cycle at a characteristic rate. If a drug like vinblastine is added to cultures of log phase growing cells, there is a linear increase in the percent mitotic cells with respect to time. A drug that causes inhibition of progression of cells through the cell cycle will cause a change in the rate of accumulation of mitotic cells (84, 87). The time it takes between the point of hydralazine addition and the change in rate of mitotic cell accumulation can be subtracted from the M phase point in the cell cycle where the block is present to determine the point in the cell cycle where inhibition is occurring. This is called the "terminal point of drug action."

It was therefore possible to assess the effect of hydralazine on the rate of increase in mitotic cells (Figure 17). Data are presented in Table 7. The results of this experiment suggest that the terminal point of action of hydralazine is at the S-G_2 phase transition in FL cells. This is in agreement with results of cell cycle population kinetics of human lymphocytes, which suggested a slowing of cells through the S phase of the cell cycle.

The studies up to this point had been short term (less than 5 days exposure) *in vitro* cell culture studies. The SHR provided an *in vivo* model for determining the effects on lymphocytes after 12 weeks of hydralazine exposure.

Red and green fluorescence of non-cycling rat lymphocytes, as measured by flow cytometry, also failed to show a dose-effect relationship to hydralazine dose (Figure 36). Data are presented in Table 16. These findings would suggest that DNA and RNA content of rat lymphocytes is unaltered by hydralazine after long-term exposure (12 weeks). In addition, it appears that hydralazine does not affect the stainability of single-strand or double-strand nucleic acid by competing with acridine orange for binding sites. This was also noted in the acid-induced denaturation of lymphocyte DNA experiment.

The male rodent reproductive tract provides a nearly ideal organ system to study acute and chronic effects of drugs and environmental chemicals on cell proliferation and differentiation (86). The ability of dual-parameter flow cytometry to rapidly and simultaneously measure seven or more testicular cell types and extratesticular sperm (91) at several stages of maturation makes it a powerful system for evaluating in vivo toxic effects on cellular systems. In this study, seven testicular cell types (Figures 37A, 37B) and epididymal sperm were evaluated after 12 weeks of hydralazine administration to spontaneously hypertensive rats (91). Figures 38, 39 and 40 reveal there was no effect of hydralazine on testicular cell population kinetics as measured by flow cytometry. This would imply no effect on differentiation of testicular cell types. Data are presented in Table 17. In addition, mature sperm from the caudal epididymus show no effect on the standard deviation of α_t as related to the dose of hydralazine (Figure 42). Mature sperm exhibits a difference in sperm chromatin

structure that shifts the acridine orange fluorescence from green to red and is most likely related to an increased sensitivity for double-strand DNA to denature to single-strand DNA under the acid stress and staining condition (80). The nature of the chemically induced changes that produce this sensitivity is not understood. The lack of effect of hydralazine on differentiating testicular cells and mature spermatozoa may suggest hydralazine exhibited poor penetration into testes tissues or that hydralazine simply exhibited no measurable effect on these cells.

The effects of hydralazine on proliferation of testicular cells was assessed by determining the count of sonication-resistant sperm heads per gram of testis tissue. This technique (85) has been used to assess the toxic properties of chemicals on the development of sperm cells. Figure 41 shows there was no dose-related effect on the sonication resistant sperm heads per gram of testis tissue. The data are included in Table 17. Again, hydralazine does not appear to interfere with the proliferation or differentiation of testicular cells nor affect the susceptibility of DNA to denature when exposed to acid in mature sperm.

CONCLUSION

On the basis of the work presented here, several conclusions can be deduced.

1) Log phase growing cells are more sensitive to the toxic effects of hydralazine than stationary phase cells.

2) The growth of log phase cells is inhibited before the viability is affected.

3) Hydralazine seems to exert a slowing of cell progression through S phase and the terminal point of action is approximately at the S-G_2 phase transition.

4) Hydralazine does not appear to exert any effect on the susceptibility to acid-induced DNA denaturation of somatic cells or mature spermatozoa.

5) The proliferation and differentiation of male rat germ cells is unaffected by hydralazine exposure.

6) Hydralazine does not appear to compete with acridine orange for binding sites (intercalation or stacking).

LITERATURE CITED

1. Reidenberg, MM. The chemical induction of systemic lupus erythematosus and lupus-like illnesses. Arthritis and Rheum, 24(8):1004-1010, 1981.

2. Lee, SL., and Chase, PH. Drug-induced systemic lupus erythematosus: a critical review. Semin Arthritis Rheum, 5:83-103, 1975.

3. Totoritis, MC, and Rubin, RL. Drug-induced lupus. Post-graduate Medicine, 78(3):149-160, 1975.

4. Hess, EV. Introduction to drug-related lupus. Arthritis and Rheum, 24(8):vi-ix, 1981.

5. Harmon, C. Antinuclear antibodies in autoimmune disease. Medical Clinics of North America, 69(3):547-563, 1985.

6. Drayer, DE, Reidenberg, MM. Clinical consequences of polymorphic acetylation of basic drugs. Clin Pharmacol Ther, 22:251-258, 1977.

7. Weber, WW, Tannen, RH. Pharmacogenetic studies on drug-related lupus syndrome. Arthritis and Rheum, 24(8):979-985, 1981.

8. Perry, HM. Late toxicity to hydralazine resembling systemic lupus erythematosus on rheumatoid arthritis. Am J Med, 54:58-72, 1973.

9. Doerge, RF, Wilson and Gisvold's Textbook of Organic Medicinal and Pharmaceutical Chemistry, 8th ed. Lippincott Co. Philadelphia, PA, 1982.

10. Blair, IA. et al. Plasma hydrazine concentrations in man after isoniazid and hydralazine administration. Human Toxicology, 4:195-202, 1985.

11. Perry, HM. Possible mechanisms of the hydralazine-related lupus-like syndrome. Arthritis & Rheum, 24(8):1093-1104, 1981.

12. Perry, HM, Schroeder, HA. Studies on the control of hypertension by hyphex III. Pharmacological and chemical observations on 1-hydrazinophthalazine. Am J Med Sci, 244:82, 1962.

13. Stollar, D. The antigenic potential and specificity of nucleic acids, nucleoproteins, and their modified derivatives. Arthritis and Rheum, 24(8):1010-1017, 1981.

14. Koffler, D. Immunopathogenesis of systemic lupus erythematosus. Ann Rev Med, 25:149-164, 1974.

15. Stollar, BD. Nucleic acid antigens. In: The Antigens. Vol I. (M Sela, ed). Academic Press, New York, NY, p 1-85, 1973.

16. Stollar, BD. The specificity and application of antibodies to helical nucleic acids. Crit Rev Biochem, 3:45-69, 1975.

17. Shishido, K, Ando, T. Estimation of the double-helical content in various single-stranded nucleic acids by treatment with a single strand-specific nuclease. Biochim Biophys Acta, 287:477-484, 1972.

18. McGhee, JD and Felsenfeld, G. Nucleosome structure. Ann Rev Biochem, 49:1115-1156, 1980.

19. Isenberg, I. Histones Ann Rev Biochem, 48:159-191, 1979.

20. Goldblatt, D. and Bustin, M. Exposure of histone antigenic determinants in chromatin. Biochemistry, 14:1689-1695, 1975.

21. Hannestad, K. and Stollar, BD. Certain rheumatoid factors react with nucleosomes. Nature, 275:671-673, 1978.

22. Rekvig, OP and Hannestad, K. The specificity of human autoantibodies that react with both cell nuclei and plasma membranes: the nuclear antigen is present on core mononucleosomes. J Immunol, 123:2673-2681, 1979.

23. Stollar, B.D., Reactions of systemic lupus erythematosus sera with histone fractions and histone-DNA complexes. Arthritis and Rheum, 14:485-492, 1971.

24. Martin, T et al. Substructure of nuclear ribonucleoprotein complexes. Cold Spring Harbor Symp, Quant Biol, 42:899-909, 1978.

25. Douvas, AS, Stumph, WE, Keyes, P, and Tan, EM. Isolation and characterization of nuclear ribonucleoprotein complexes using human anti-nuclear ribonucleoprotein antibodies. J Biol Chem, 254:3608-3616, 1979.

26. Carpenter, JR et al. Prospective study of immune response to hydralazine and development of anti-deoxyribonucleoprotein in patients receiving hydralazine. Am J Med, 69:395-400, 1980.

27. Cameron, DJ, and Erlanger, BF. Nucleic acid-reactive antibodies of restricted heterogeneity. Immunochemistry, 13:263-269, 1976.

28. Yamauch, Y et al. Induction of antibodies to nuclear antigens in rabbits by immunization with hydralazine-human serum albumin conjugates. J Clin Invest, 56:958-969, 1975.

29. Ellman, L, Inman, J, and Green, I. Strain difference in the immune response to hydralazine in inbred guinea pigs. Clin Exp Immunol, 9:927-937, 1971.

30. Klajman, A, et al., Ocurrence, immunoglobulin pattern and specificity of antinuclear antibodies in sera of procainamide treated patients. Clin Exp Immunol, 7:641-649, 1970.

31. Alarcon-Segovia, D, Fishbein, E, and Betancourt, VM. Antibodies to nucleoprotein and to hydrazide-altered soluble nucleoprotein in tuberculous patients receiving isoniazid. Clin Exp Immunol, 5:429-437, 1969.

32. Eldredge, NT, Robertson, WB, and Miller, JJ. The interaction of lupus-inducing drugs with deoxyribonucleic acid. Clin Immunol Immunopathol, 3:263-271, 1974.

33. Dubroff, LM, and Reid, RJ. Hydralazine-pyrimidine interactions may explain hydralazine-induced lupus erythematosus. Science, 208:404-406, 1980.

34. Alhan, S et al. Antigen recognition and the immune response: humoral and cellular responses to small mono- and bifunctional antigen molecules. J Exp Med, 135:1228-1246, 1972.

35. Murahami, WT et al. Immunochemical studies on bacteriophage deoxyribonucleic acid. III Specificity of the Antibodies. J Immunol, 89:116-123, 1962.

36. Leng, M, Sage, E, Fuchs, R, and Daun, MP. Antibodies to DNA modified by the carcinogen N-acetosy-N-2-acetylaminofluorene. FEBS Letters, 92:207-210, 1978.

37. Levine, L et al. Antibodies to photoproducts of deoxyribonucleic acids irradiated with ultraviolet light. Science, 153:1666-1667, 1967.

38. Shaw, S, and Shearer, GM. Cytotoxic T Cell Interaction with Antigen. Arthritis and Rheum, 24(8):1037-1042, 1981.

39. Doherty, PC and Zinkernagel, RM. T cell-mediated immunopathology in viral infection. Transplant Review 19:89-120, 1974.

40. Yap, KL, Ada, GL and McKenzie, I. Transfer of specific cytotoxic T lymphocytes protects mice inoculated with influenza virus. Nature 273:238-239, 1978.

41. Instrumentation for the Environmental and Life Sciences by D.C. Hilderbrand, Departmental Publication of Chemistry Department, SDSU, Brookings, SD. 1979.

42. Gray, JW, Dean, PN and Mendelsohn, ML. Quantitative cell-cycle analysis. In: Flow Cytometry and Sorting. (MR Melamed, PF Mullaney and ML Mendelsohn, eds). John Wiley & Sons, New York. p 383-407, 1979.

43. Darzynkiewicz, Z. Acridine orange as a molecular probe in studies of nucleic acids in situ. In: Flow Cytometry and Sorting. (MR Melamed, PF Mullaney and ML Mendelsohn, eds). John Wiley & Sons, New York, NY, p 285-316, 1979.

44. Change of a sequence of amino acids in phage T_4 lysosyme by acridine orange induced mutations. Proc Natl Acad Sci USA, 56:500, 1966.

45. Lerman, LS. The structure of the DNA-acridine complex. Proc Natl Acad Sci USA, 49:94, 1963.

46. Blake, A et al. The interaction of amino acridines with nucleic acids. Biopolymers, 6:1225, 1968.

47. Li, HJ and Crothers, DM. Studies of the optical properties of the proflavine-DNA complex. Biopolymers, 8:217, 1969.

48. Lerman, LS. Structural considerations in the interaction of DNA and acridines. J Mol Biol, 3:18, 1961.

49. Bauer, W and Vinograd, J. The interaction of closed circular DNA with intercalative dyes. I. The superhelix density of SV40 DNA in the presence and absence of the dye. J Mol Biol, 33:141, 1968.

50. Steiner, RF and Biers, RF. Spectral changes accompanying binding of acridine orange to polyadenylic acid. Science, 127:335, 1957.

51. Boyle, RE et al. The interaction of deoxyribonucleic acid and acridine orange. Arch Biochem Biophys, 96:47,1962.

52. Gersch, NR et al. Interaction of DNA with aminoacridines. J Mol Biol, 13:138, 1965.

53. Bradley, DF. Molecular biophysics of dye-polymer complexes. Trans. NY Acad Sci, 24:64, 1961.

54. Bradley, DF and Wolf, MK. Aggregation of dyes bound to polyanions. Proc Natl Acad Sci, 45:944, 1959.

55. Ichimura, S, Zama, M and Fujita, H. Quantitation determination of single-stranded sections in DNA using the fluorescent probe acridine orange. Biochim Biophys Acta, 240:485, 1971.

56. Bradley, DF and Felsenfeld, G. Aggregation of an acridine dye on native and denatured deoxyribonucleates. Nature, 184:1920, 1959.

57. Darzynkiewicz, Z, Traganos, F, Sharpless, T and Melamed, MR. Thermal denaturation of DNA in situ as studied by acridine orange staining and automated cytofluorometry. Exp Cell Res, 90:411, 1975.

58. Darzynkiewcz, Z, Traganos, F, Sharpless, T and Melamed, MR. Conformation of RNA in situ as studied by acridine orange staining and automated cytofluorometry. Exp Cell Res, 95:142, 1975.

59. Darzynkiewicz, Z, Traganos, F, Sharpless, T and Melamed, MR. Lymphocyte Stimulation: A rapid multiparameter analysis. Proc Natl Acad Sci USA, 73:2881, 1976.

60. Traganos, F, Darzynkiewicz, Z, Sharpless, T and Melamed, MR. Simultaneous staining of ribonucleic and deoxyribonucleic acids in unfixed cells using acridine orange in a flow cytofluoremetric system. J Histochem Cytochem, 25:431, 1977.

61. Doty, P, Goedtken, H, and Fresco, JR. Secondary structure in ribonucleic acids. Proc Natl Acad Sci USA, 45:482, 1959.

62. Howard, A and Pelc, SR. Synthesis of deoxyribonucleic acid in normal and irradiated cells and its relation to chromosome breakage. Heredity, 6 (Suppl):261, 1953.

63. Baserga, R. The biology of cell reproduction. Howard University Press, Cambridge, MA, 1985.

64. Ling, HR et al. Lymphocyte Stimulation. North Holland-American Elsevier, New York, NY, 1975.

65. Evenson, DP. Flow cytometric analysis of male germ cell quality. In: Flow Cytometry Procedures Manual (Darzynkiewicz, Z, Muirhead, K and Cron, S, eds). Academic Press, New York (in press).

66. Darzynkiewicz, Z, Traganos, F, Sharpless, T, and Melamed, MR. Cell cycle-related changes in nuclear chromatin of stimulated lymphocytes as measured by flow cytometry. Cancer Res, 37:4635-4640, 1977.

67. Darzynkiewicz, A, Traganos, F, Andreeff, M, Sharpless, T and Melamed, M.R. Different sensitivity of chromatin to acid denaturation in quiescent and cycling cells as revealed by flow cytometry. J Histochem Cytochem, 27:478-485, 1979.

68. Shapiro, HM. Practical Flow Cytometry, ARL Publishers, New York, 1985.

69. Van Dilla, MA, and Mendelsohn, ML. Introduction and resume of flow cytometry and sorting. In: Flow Cytometry and Sorting. (MR Melamed, PF Mullaney and ML Mendelsohn, eds). John Wiley & Sons, New York, NY pp 383-407, 1979.

70. Flow Cytometry. JA Stainkamp, Los Alamos National Laboratory Publications, 1987.

71. Cytoflorograf Flow Cytometer Modular Flow Cytometry/Cell Sorting Systems Operators Manual, Ortho Diagnostic Systems, Inc., 1982.

72. Bryant, J, Guseman, LF, Egl, DL. Analysis of FCM-derived DNA histograms. In: Flow Cytometry IV. (Laerum, OD, Lindmo, T and Thorud, E, eds). Columbia University Press, New York, NY. p 138-143, 1980.

73. Hulett, HR, Bonner, WH, Barrett, J and Herzenberg, LA. Cell sorting: automatic separation of mammalian cells as a function of intracellular fluorescence. Science, 166:747, 1969.

74. Lehren, MR and Stall, AM. Flow cytometry as an analytical and preparative tool in immunology. J Immunol Meth, 50:R85-R112, 1982.

75. Herzenberg, LA, Sweet, TG and Herzenberg, LA. Fluorescence-activated cell sorting. Sci American, 234(3):108, 1976.

76. Model 75 Ion Laser Operators Manual. Lexel Corporation, Palo Alto, CA.

77. Model 2150 Computer System Operator Reference Manual. Ortho Diagnostic Systems, Inc., 1982.

78. Juchau, MR, and Horita, A. Metabolism of hydrazine derivatives of pharmocalogic interest. Drug Metabolism Reviews, 1:71-100, 1972.

79. Colvin, LB. Metabolic fate of hydrazine and hydrazides. J Pharm Sci, 58(12):1433-1443, 1969.

80. Evenson, DP, Higgins, PJ, Grueneberg, D, and Ballachey, BE. Flow cytometric analysis of mouse spermatogenic function following exposure to ethylnitrosourea. Cytometry 6:2381-253, 1985.

81. Balhorn, R. A model for the structure of chromatin in mammalian sperm. J of Cell Biology, 93:298-305, 1982.

82. Janca, FC, Jost, LK, and Evenson, DP. Mouse testicular and sperm cell development characterized from birth to adulthood by dual parameter flow cytometry. Biol Reprod, 34:613-623, 1986.

83. Evenson, DP, Darzynkiewicz, Z, Staiano-Coico, L, Traganos, F, Melamed, MR. Effects of 9,10-Anthracenedione, 1,4-Bis[(2-[(2hydroxyethyl)amino]-ethyl)amino]-diacetate on Cell survival and cell cycle progression in cultured mammalian cells. Cancer Research, 39:2574-2581, 1979.

84. Traganos, F, Evenson, DP, Staiano-Coico, L, Darzynkiewicz, A, and Melamed, MR. Action of dihydroxyanthraquinone on cell cycle progression and survival of a variety of cultured mammalian cells. Cancer Research, 40:671-681, 1980.

85. Cassidy, SL, Dix, KM and Jenkins, T. Evaluation of a testicular sperm head counting technique using rats exposed to dimethoxyethyl phthalate (DMEP), glycerol -monochlorohydrin (GMCH), epichlorohydrin (ECH), formaldehyde (FA), or methyl methanesulphonate (MMS). Arch Toxicol, 53:71-78, 1983.

86. Evenson, DP, Baer, RK, Jost, LK and Gesch, RW. Toxicity of thiotepa on mouse spermatogenesis as determined by dual-parameter flow cytometry. Tox and Appl Pharm, 82:151-163, 1986.

87. Traganos, F, Darzynkiewicz, Z, Staiano-Coico, L, Evenson, D and Melamed, M. Rapid, automatic analysis of the cell cycle point of action of cytostatic drugs. In: Flow Cytometry IV. (Laerum, OD, Lindmo, T and Thorud, E, eds). Columbia University Press, New York, NY. p 511-515, 1980.

88. Evenson, DP, Darzynkiewicz, Z, Jost, L, Janca, F, Ballachey, B. Changes in accessibility of DNA to various fluorochromes during spermatogenesis. Cytometry, 7:45-53, 1986.

89. Darzynkiewicz, A, Traganos, F, Sharpless, T and Melamed, MR. Interphase and metaphase chromatin. Different Stainability of DNA with acridine orange after treatment at low pH. Exptl Cell Res, 110:201-214, 1977.

90. Darzynkiewicz, A, Traganos, F, Sharpless, T and Melamed, MR. Recognition of cells in mitosis by flow cytofluorometry. J Histochem Cytochem, 25:875-880, 1977.